Scuola Internazionale Superiore di Studi Avanzati

Information processing in dissociated neuronal cultures of rat hippocampal neurons

Thesis submitted for the degree of Doctor Philosophiae

Neurobiology sector

October 2005

Candidate

Paolo Bonifazi

Supervisor

Prof. Vincent Torre

SISSA – Via Beirut 2-4 –34014 TRIESTE – ITALY

... a mio padre ...

INDEX

List of publications

The results presented in the first two chapters of my thesis have been published in the following papers. The third chapter of my thesis represents an article in preparation.

Ruaro M. E., **Bonifazi P.**, Torre V.,

Toward the Neurocomputer: Image Processing and Pattern Recognition With Neuronal Cultures,

IEEE Transactions on Biomedical Engineering, 52 (3): 371-383 (2005).

Bonifazi P., Ruaro M.E., Torre V.,

Statistical properties of information processing in neuronal networks,

European Journal of Neuroscience (in press)

Abbreviations

MEA: multielectrode array

AP: action potential

IP: information processing

AMPA: α-amino-3-hydroxy-5-methylisoxazole-4-propionic acid

NMDA: N-methyl-d-aspartate

GABA: γ-aminobutyric acid

$GABA_A$: γ-aminobutyric acid type A

APV: 2-Aminophosphonovaleric acid

CNQX: 6-cyano-7-nitroquinoxaline-2,3-dione

ANN: artificial neural network

1. Abstract

One of the major aims of Systems Neuroscience is to understand how the nervous system transforms sensory inputs into appropriate motor reactions. In very simple cases sensory neurons are immediately coupled to motoneurons and the entire transformation becomes a simple reflex, in which a noxious signal is immediately transformed into an escape reaction. However, in the most complex behaviours, the nervous system seems to analyse in detail the sensory inputs and is performing some kind of information processing (IP). IP takes place at many different levels of the nervous system: from the peripheral nervous system, where sensory stimuli are detected and converted into electrical pulses, to the central nervous system, where features of sensory stimuli are extracted, perception takes place and actions and motions are coordinated. Moreover, understanding the basic computational properties of the nervous system, besides being at the core of Neuroscience, also arouses great interest even in the field of Neuroengineering and in the field of Computer Science. In fact, being able to decode the neural activity can lead to the development of a new generation of neuroprosthetic devices aimed, for example, at restoring motor functions in severely paralysed patients (Chapin, 2004). On the other side, the development of Artificial Neural Networks (ANNs) (Marr, 1982; Rumelhart & McClelland, 1988; Herz et al., 1981; Hopfield, 1982; Minsky & Papert, 1988) has already proved that the study of biological neural networks may lead to the development and to the design of new computing algorithms and devices. All nervous systems are based on the same elements, the neurons, which are computing devices which, compared to silicon components, are much slower and much less reliable. How are nervous systems of all living species able to survive being based on slow and poorly reliable components? This obvious and naïve question is equivalent to characterizing IP in a more quantitative way.

In order to study IP and to capture the basic computational properties of the nervous system, two major questions seem to arise. Firstly, which is the fundamental unit of information processing:

single neurons or neuronal ensembles? Secondly, how is information encoded in the neuronal firing? These questions – in my view - summarize the problem of the neural code.

The subject of my PhD research was to study information processing in dissociated neuronal cultures of rat hippocampal neurons. These cultures, with random connections, provide a more general view of neuronal networks and assemblies, not depending on the circuitry of a neuronal network *in vivo*, and allow a more detailed and careful experimental investigation. In order to record the activity of a large ensemble of neurons, these neurons were cultured on multielectrode arrays (MEAs) and multi-site stimulation was used to activate different neurons and pathways of the network. In this way, it was possible to vary the properties of the stimulus applied under a controlled extracellular environment. Given this experimental system, my investigation had two major approaches. On one side, I focused my studies on the problem of the neural code, where I studied in particular information processing at the single neuron level and at an ensemble level, investigating also putative neural coding mechanisms. On the other side, I tried to explore the possibility of using biological neurons as computing elements in a task commonly solved by conventional silicon devices: image processing and pattern recognition.

The results reported in the first two chapters of my thesis have been published in two separate articles. The third chapter of my thesis represents an article in preparation.

2. Introduction

2.1 Understanding neural coding

2.1.1 Single neurons: computation and encoding of information

Understanding the neural code requires the identification of the role of single neurons and neuronal ensembles in the neural computation. One of the central questions in neuroscience is how particular tasks or computations, are implemented by neuronal networks in order to generate behavior. Although, according to the dominant view, information processing in neuronal networks results primarily from the properties of synapses and the connectivity of neurons within the network (Hopfield, 1982; Rumelhart & McClelland, 1988; DeCharms & Merzenich, 1996; Georgopoulos et al., 1986; Gray et al., 1989; Nicolelis et al., 1998; Thorpe et al., 2001), several studies support the idea that single neurons are indeed able to perform very precise computations (Koch, 1999; Koch & Segev, 2000; Koch et al., 1983). Starting from the initiation and the dynamics of action potentials (APs), the timing of the generation of AP can be controlled very precisely, with a submillisecond precision, by fast membrane fluctuations (Mainen & Sejnowski, 1995). Action potential waveforms can be highly variable so that they can reliably signal the history of the input for some dozens of ms before the spike (De Polavieja et al., 2005).

There are several proofs that computation, at a single neuron level, can take place in the dendrites, for example in direction-selective neurons, to analyse motion and in coincidence-detector neurons for the auditory system (which are performing the equivalent of the Boolean operation AND).

Direction-selective neurons respond to image motion in a preferential direction but not in the opposite direction (Barlow & Levick, 1965). They can be found in many species from fly eyes to mammalian cortex, and in all these cases, a role for dendritic computation has been proposed. The direction-selective retinal ganglion cells described by Barlow & Levick (Barlow et al., 1964,

Barlow & Levick, 1965) are a classical example of a complex nonlinear operation that appears to use synaptic logic (Koch et al., 1982). A popular model for the biophysical basis of directional selectivity is nonlinear synaptic interaction between cholinergic excitation and GABAergic inhibition mediated by $GABA_A$ receptors in the dendritic tree of ganglion cells (Koch et al., 1982; Koch et al., 1983; Koch et al., 1985; Torre & Poggio, 1978). Intracellular recordings from turtle and frog direction-selective ganglion cells support activation of shunting inhibition in the null direction (Marchiafava, 1979; Watanabe & Murakami, 1984). Nonlinear interaction between excitation and shunting inhibition on small dendritic branches can implement logical operations. The result of the combined operation of a neighboring pair of excitatory and inhibitory inputs will cause somatic depolarization if and only if excitatory input and not inhibitory input is active. This AND-NOT function is a Boolean logical operation, of exactly the same kind as implemented in modern computers and studied in mathematical computational theory.

Analogously, the contribution of the dendrites to computation has been proposed in the sound localization system, where neurons act as coincidence-detectors. Agmon-Snir et al. (1998) proposed that in the auditory system of chicks a special type of neuron is responsible for computing the time difference between sounds arriving to the two ears. Each neuron responds only to a very precise time difference, which corresponds to a specific location in space. The neurons contain only two major dendrites, and each dendrite receives inputs only from one ear. The inputs are supposedly arranged in such a way that there is a constant delay between the inputs arriving from one ear and the inputs arriving from the second ear. Coincident inputs from both ears arriving to the two dendrites are summed up at the soma and cause the neuron to emit action potentials. In this way the neuron would just behave as an AND Boolean operator.

Moreover, passive dendrites can act as passive filters and this property may be exploited to perform simple computations (Koch, 1999). First, for single inputs, by acting as a delay line, the dendrites can “label” particular inputs on distinct regions of the dendritic tree by the latency of the resulting output spikes. In fact, EPSPs with different somatic shape are likely to affect the somatic

output spike trains in different ways (Fetz & Gustafsson, 1983). Second, for multiple inputs, the time course of the somatic voltage response depends on the temporal order of activation of the dendritic synapses (in contrast with the scenario where they are all located on the soma).

Single neurons, apart from being potentially capable of precise relevant computations, can encode in their firing a large amount of information. In fact, since the discovery of face and hand selective cells in the inferior temporal cortex (Gross et al., 1969; Gross et al., 1972), a strict link between single neurons and perception has been proposed. It has been shown that neurons in the human medial temporal lobe (MTL) fire selectively to images of faces, animals, objects or scenes (Fried et al., 1997; Kreiman et al., 2000) and, more surprisingly, a remarkable subset of MTL neurons are selectively activated by strikingly different pictures of given individuals, landmarks or objects and in some cases even by letter strings with their names (Quiroga et al., 2005). These results support the idea of an invariant and sparse neural code. This is an extreme hypothesis based on the explicit representations by highly selective neurons or "grandmother cells", a hypothetical neuron that responds only to a highly complex, specific, and meaningful stimulus, such as the image of one's grandmother (Barlow, 1972). Indeed, how such a robust, fast (it takes a fraction of a second to recognize a person or an object even when seen under strikingly different conditions (Konorski, 1967; Gross et al., 1969; Barlow, 1972; Logothetis & Sheinberg, 1996; Young & Yamane, 1992)), high-level representation is achieved by neurons in the human brain is still unclear. In general, how neurons can encode different percepts is one of the most intriguing questions in neuroscience which has still no answer.

2.1.2 Neuronal networks: computation and encoding of information

As already mentioned above, according to the dominant view information processing in the nervous system results primarily from the properties of synapses and the connectivity of neurons

within the network (Hopfield, 1982; Rumelhart & McClelland, 1988; DeCharms & Merzenich, 1996; Georgopoulos et al., 1986; Gray et al., 1989; Nicolelis et al., 1998; Thorpe et al., 2001).

In the past 60 years, many studies have shown how networks are capable of any basic mathematical computation, like those implemented on digital computers, even though not as rapidly or as conveniently, and, more relevantly, they can perform complex computations like those required for learning and for pattern recognition (Marr, 1982; Rumelhart & McClelland, 1988; Herz et al., 1981; Hopfield, 1982; Minsky & Papert, 1988).

First, in 1943, McCullough and Pitts showed how a collection of simple, interconnected neuron-like units could process information. Their view of neuronal processing was a very simple one. All synaptic inputs converge onto a single compartment (‘point neuron’). Each synapse is modeled by a positive number, its synaptic weight. The activity of each presynaptic fiber (originally assumed to be either on or off) is multiplied by its associated synaptic weight and summed over all inputs. This sum is then compared against a threshold. If the threshold is exceeded, and if no inhibitory unit is active, the neuron generates a spike and sends it on to its postsynaptic targets. Otherwise, the cell remains quiet. McCullough and Pitts proved that a sufficiently large number of these simple logical devices, wired together in an appropriate manner, are capable of universal computation.

Later, in 1982 Hopfield showed how the ability of large collections of neurons to perform "computational" tasks might in part be a spontaneous collective consequence of having a large number of interacting simple neurons.

By passing from the work of McCullough and Pitts through the studies of Hopfield, the field of Artificial Neural Networks (ANNs) grew up and models of networks with more sophisticated neuron-like units and connections were proposed (Anderson & Rosenfield, 1988; Caudill & Butler, 1990). The major aim of ANNs was to capture basic computational properties of biological neuronal networks, such as learning, adaptation and parallelism and to implement these features on new computational devices. In fact, image recognition, movement coordination or other problems

of artificial intelligence, computer vision and robotics require a more sophisticated computation in respect to the standard serial computation implemented on typical computers. Although ANNs can be trained to recognize features and patterns, presently it is still impossible to think of developing a computational device able to process information and to extract features of INPUT in such a fast and reliable way, just like the nervous system can. A strikingly clear example is the ability of the nervous system to extract and classify features of images in just a few hundreds of ms (Konorski, 1967; Gross et al., 1969; Barlow, 1972; Logothetis & Sheinberg, 1996; Young & Yamane, 1992). From a technological point of view, there is even an obvious difficulty in forming large numbers of interconnections in two dimensional silicon devices, which though is a fundamental prerequisite for implementing massive parallel processing. On the other hand, biological neurons form connections and synapses between themselves very naturally.

Besides, apart from these clear technological problems of building hardware capable of parallel computation, there are still many questions, that still remain open, about how neuronal networks work in the nervous system to process information.

In this context, the study of neural coding is a central issue for the investigation of nervous system function. In fact, before being able to understand how neural circuits process information, we must understand how they represent it.

Information is conveyed to and processed within the brain primarily in the form of action potentials. In the great majority of invertebrate species and in almost all vertebrates, sensory signals are coded in trains of evoked action potentials (APs). In the central nervous systems (CNSs) of all vertebrates messages and signals are exchanged and processed as APs trains. How does the sequence of action potentials fired by neurons represent the information that is encoded and conveyed to other neurons?

The neural code is particularly complex because both the properties of the stimulus (light, touch or sound intensity), and the way that the stimulus changes over time are encoded in the temporal pattern of neural spiking. Information about the stimulus value and about changes in the

stimulus are both represented in the time domain by the neural code. As a result, it is important to distinguish between the structure imposed on the code by the nature of the stimulus, and the structure that arises from the nature of encoding itself.

Although there are many open questions about the neural code, it is now widely accepted that in most nervous systems information about a stimulus is encoded in the activity of a large number of responding neurons (population coding) (Pouget et al., 2000).

Earlier studies, owing to technological limitations, were based on the recording of single neurons or of very few neurons and, as a consequence, they mainly contributed to revealing the role of firing rates in the neural coding (Barlow, 1972, Hubel & Wiesel, 1959). In fact, due to the very limited number of cells simultaneously recorded, it was very difficult to detect any different coding strategy based, for example, or the relative timing of firing in ensembles of cells. In the last two decades, the diffusion and application of new experimental techniques that allowed the simultaneous recordings of more than 100 neurons (Nicolelis et al., 1997; Rousche & Normann, 1988; Meister et al., 1996) gave the possibility to study neural coding mechanisms and distributed representations in different part of the brain. In this way, although the response of most neurons even when the same stimulus is presented repeatedly show a high degree of variability (Shadlen & Newsome, 1998), it was shown how precise information can be encoded in different features of the firing pattern of neural ensembles like: the firing rate, the timing of firing, the synchrony of firing, or the order of the first evoked spikes (Nicolelis et al., 1998; Gray et al., 1989; Singer & Gray, 1995, DeCharms & Merzenich, 1996; O'Keefe & Recce, 1993; Hopfield, 1995; Thorpe et al., 2001; Johansson & Birznieks, 2004).

So, only in the last decade synergistic neural coding based on the precise or on the relative timing of spiking between neurons could be experimentally studied and their relevance demonstrated.

A very clear example of how information is distributed and can be differently encoded in neural ensembles was given by Nicolelis et al. (1998). By using multielectrode recordings, they

showed how sensory information is distributed and differently encoded in the activity of different ensembles of neurons situated in distinct cortical regions. In their experiment, using simultaneous multi-site neural ensemble recordings, they compared the representation of tactile information in three areas of the primate somatosensory cortex. They observed how small neural ensembles of 30-40 neurons were simultaneously able to identify the location of a single tactile stimulus in a very precise way. Moreover, they showed how each of those cortical regions could use different encoding schemes, based on the average firing rates or on the precise temporal firing pattern, to retrieve the stimulus correctly. In summarizing their work, they were able to show at the same time how information is distributed in the response of neurons and how different coding mechanisms (rate and temporal) can be used.

Their work, in common with most works dealing with the problem of neural coding, focused on how the information encoded in the activity of a population of neurons can be read out or decoded. In this approach, decoding is an effective way of determining the accuracy, efficiency, and information carrying capacity of a neural code. Information theory and classification analysis are the methodologies generally used to evaluate the coding/decoding schemes (Panzeri et al., 2001; Petersen et al., 2001; Foffani & Moxon, 2004; Nicolelis et al., 1998; Rolls et al., 1997). In particular, information theory (Shannon & Weaver, 1949), a branch of the mathematical theory of probability and mathematical statistics, allows quantifying precisely the concept of information. Entropy is the fundamental measure of information theory and it is used to measure the uncertainty of a random variable. In the field of neuroscience, entropy is generally taken as a measure of the information contained in a stimulus and as a measure of the variability of the neuronal response.

In other experiments (Panzeri et al., 2001; Petersen et al., 2001) similarly performed on the somatosensory cortex (in this case rats were used), it was shown how temporal precision (on the order of 2 ms) of firing in an ensemble of neurons encoded a larger amount of information with respect to the mean firing rate. In particular, an important role was attributed to the first evoked

APs, which could carry more than 80% of the total spike train information, excluding synergy in cross neuronal spike patterns.

As in the case of somatosensory stimuli, for auditory stimuli an important role in information coding was attributed to the temporal firing patterns and to the first evoked APs by Furakawa et al. (2002). They showed how the activity of an ensemble of cortical neurons encoded the sound-source location of the stimulus. The recognition of spike patterns, based on ANNs, used a rate coding scheme (relative spike count) and temporal schemes (relative spike timing). They found that the proportion of information about source location transmitted by first spike latency averaged 89% of that of full spike patterns.

The role of first spike latencies in the neural code can be extremely important. In fact, recognition of complex scenes and images occurring in just few hundreds ms (Thorpe et al., 2001) requires several steps of processing and a very fast processing. Therefore, a neural code based on the first evoked APs in an ensemble of neurons would be the fastest coding mechanisms which can be implemented by neurons.

The study done by Johansson et al. (2004) represents a possible proof for the existence of coding mechanisms based on the first spikes. They demonstrated that the rank order of first spikes in individual units of ensembles of tactile afferents from the human fingertip conveys sufficient information to discriminate four directions of fingertip force and three different shapes of the surfaces contacting the tip. The information is available more promptly than would be possible by the fastest rate code and quick enough to account for the speed observed in natural object manipulations.

First spike codes can be considered for recognition of sudden stimuli as in the cases discussed above, but cannot be easily extended to the dynamical stimuli cases, steady stimuli or movement control.

In this last context, Georgopoulos et al. (1986) showed first in a pioneering paper how, although individual neurons in the arm area of the primate motor cortex are only broadly tuned to a

particular direction in three-dimensional space, the animal can control very precisely the movement of its arm. He found that the direction of movement could be uniquely predicted by the action of a population of motor cortical neurons. When the firing rates of individual neurons were represented as vectors that make weighted contributions along the axis of their preferred direction, the resulting vector sum of all cell vectors (population vector) had a direction which was congruent with the direction of the movement.

Similarly, Wessberg et al. (2000) were able to predict with high accuracy the arm movement of a monkey. They recorded the simultaneous activity of large populations of neurons, distributed in the pre-motor, primary motor and posterior parietal cortical areas, as monkeys performed two distinct motor tasks. Accurate real-time predictions of one- and three-dimensional arm movement trajectories were obtained based on the activity (spike count) of the cortical neuronal ensemble. In this experiment a dynamical description of the movement was described by the population activity represented in time series.

Only in the last decade clear experimental evidence of the important role played by the correlation of firing in neural ensembles has been given. Correlated firing between single neurons in the frontal cortex of monkeys was detected while the animal was performing a behavioural task (Vaadia et. al., 1995). The temporal dynamic of correlation evolved in systematic relation to the behavioural tasks. Their findings were a first demonstration of how neurons can synchronize rapidly their activity to form functional groups performing a computational task.

In a different experiment (DeCharms & Merzenich, 1996), it was shown how correlation can signal the presence of a continuous steady stimulus while the firing rate could encode the transients like the onset of the stimulus. The authors of the experiment reported that the relative firing of a population of neurons in the primary auditory cortex displayed a coordination (synchrony) while a continuous stimulus was present. In this way, although the firing rates did not change, the correlated activity of the cortical neurons was signalling the presence of the stimuli. Interestingly, the firing rate changes were observed at the onset of the stimulus. Their conclusion was that population codes

based on synchronization across neurons can encode features of the stimulus and can follow the time course of the stimulus without provoking a change in the firing rate.

2.2 Investigation of *in-vitro* neuronal networks: dissociated neuronal cultures grown on MEAs

In order to understand neural coding and to investigate how the nervous system performs parallel computation, it is essential to measure simultaneously the activity of large ensembles of neurons (massive parallel recordings). In the previous section of the introduction, I tried to give a large overview of network studies performed *in-vivo*, whereas here I will focus on the studies of *in-vitro* neuronal networks. In the last two decades, great efforts were spent in developing planar multielectrode arrays (MEAs), i.e. dishes with embedded electrodes able to record and stimulate the electrical activity of neuronal preparations like brain slices and dissociated cultures (Pine, 1980; Novak & Wheeler, 1986; Regehr et al., 1989; Jimbo & Kawana, 1992; Martinoia et al., 1993; Nisch et al., 1994). The experimental work I present in my thesis is entirely based on the study of hippocampal dissociated neuronal cultures grown on MEAs. Therefore in this introductory part, I will present previous works describing the electrical activity of dissociated cultures, with particular attention to experiments performed with the use of MEAs. A large literature is especially focused on the study of cortical neurons.

Mammalian neurons can be mechanically and enzymatically dissociated from brain tissue and plated on a dish. In a typical cortical network developing in a 20-mm diameter culture dish, 100000 neurons can be present (Marom & Shahaf, 2002) and they can grow in culture for months. In particular Potter and DeMarse (2001) showed that cortical dissociated cultures can survive for over a year when sterility, temperature, pH, osmolarity, oxygenation are opportunely controlled and when nutrients and growth factors are appropriately provided. Their investigation was particularly relevant for my thesis, since they described in detail what procedures have to be used and to what

points special attention must be paid in order to be able to monitor the electrical activity of neurons over months. In particular, the application of their protocols allowed us to prolong our measurements for hours and to repeat further experiments on the same preparations over a period of several weeks or few months.

After plating the cells, neurons begin to extend arborizations within hours (Huettner & Baughman, 1986). During the first week in culture, the neurons extend many neurites, form synapses, and begin to develop spontaneous activity (Habets et al., 1987; Comer & Ramakers, 1991; Basarsky et al., 1994). The glial cells, if present in the dish, continue to divide and proliferate until limited by contact inhibition or exogenous inhibitors of cell division (Banker & Goslin, 1998). Glial cells provide necessary trophic factors for cultured neurons (Banker & Goslin, 1998), and there is evidence that direct contact between neurons and glia is also crucial for neuronal survival (Pfrieger & Barres, 1997).

Once mature, the network forms a monolayer, with axodendritic branches that extend over 1 mm, and an immense number of functional synapses are present (Marom & Shahaf, 2002; Potter, 2001). A typical cortical preparation contains all the types of cells that are present in the cortex at the time of extraction, including glial cells and the distribution of types of cells in in-vitro networks can be similar to that found in vivo (Neale et al., 1983; Huettner & Baughman, 1986; Nakanishi & Kukita, 2000).

By using planar MEAs, Jimbo, Kawana and their team have carefully studied the development of the spontaneous activity in dissociated rat cortical cultures during maturation (Jimbo and Kawana, 1992; Robinson et al., 1993a,b; Maeda et al., 1995, 1998; Kamioka et al., 1996). They showed (Kamioka et al., 1996) that after a few days of culture, the networks first exhibited uncorrelated spontaneous firing which was progressively transformed into synchronized bursting in approximately 1 week. After a few weeks in culture, the networks showed non-periodic synchronous patterns of electrical activity and this behaviour did not change for more than 2 months, representing in this way the mature state of the network. These phenomena are observed in

most of cultured networks, regardless of the exact source from which cells are extracted, or the means of measurement (Morin et al., 2005; Shahaf & Marom, 2002; Potter, 2001). Regardless of their origin, they all develop some sort of synchronous bursting activity when they mature (Morin et al., 2005; Shahaf & Marom, 2002; Potter, 2001). During the maturation of the network (Maeda et al., 1995) the frequency and propagation velocity of synchronized clustered activity increase remarkably. The origin of spontaneous bursts can vary randomly with each burst and the activity does not necessarily spread across the network in a wave-like fashion. In fact, electrodes that are far away from an initiation site can be recruited into a burst before some others that appear to be physically closer.

The bursting activity is regulated by the balance of inhibition and excitation (Streit et al., 2001) and is temporally concomitant with the increase of intracellular calcium in the neurons (Robinson et al., 1993a). Transitions from asynchronous firing dynamics to synchronous firing dynamics can be induced by increasing the extracellular Ca^{2+} concentration (Canepari et al., 1997). Periodic synchronized bursting with concomitant intracellular calcium transients is induced by low magnesium in the extracellular medium (Robinson et al., 1993a).

Addition of extracellular Mg^{2+} can reduce the spontaneous activity at any Ca^{2+} concentration, and an increase in the extracellular K^{+} concentration can enhance the frequency of periodical synchronous bursts (Canepari et al., 1997). Blockage of N-methyl-D-aspartate (NMDA) and non-NMDA glutamate receptor inhibits synchronous activity (Canepari et al., 1997).

Bursting activity i*n-vivo* is present during development when it contributes to establishing appropriate connections (Meister et al., 1991; Ben-Ari, 2001; Zhang and Poo, 2001) but it is present i*n-vitro* during the entire life (up to 1 year) of the culture. This observation suggests that the bursting could be related to a lack of input which is present in an *in-vivo* system. Starting form this hypothesis, Wagenaar et al. (2005) showed how appropriate stimulation of a cortical dissociated network can lead to a controlled bursting activity. By using a closed loop system, they were able to control over a period of time the electrical discharge of the network through an appropriate

stimulation. The stimulation was distributed through several electrodes of the MEA with an amplitude adjusted in real time depending on the level of network activity. While when applied at lower frequencies the stimulation enhanced the bursting regime, at higher frequencies the bursts were reduced and the electrical activity in the network was more sparse and distributed over the time period, displaying similarity with the mature activity of networks *in-vivo*.

A detailed characterization of the pattern of activity evoked by electrical stimulation through the MEA was presented by Jimbo et al. (2000). They showed that a brief voltage pulse applied to one extracellular electrode can evoke a clear electrical response over almost the entire network. In particular, a strong voltage induces an early phase in the response of a few dozens of ms, and a late phase of several hundreds of milliseconds. The early phase is characterized by precisely-timed firing and by a spread (wave-like) of the electrical activity over the network. By contrast, the late phase is characterized by the occurrence of fluctuating patterns of electrical activity, similar to the dynamics of the spontaneous activity. The late phase of the response could be suppressed by blocking the NMDA-mediated excitatory pathways by adding small amounts of APV to the extracellular medium or by increasing the amount of extracellular Mg^{2+}. On the contrary, the spontaneous activity and the late phase were enhanced by blocking the inhibitory GABA-ergic pathways by adding bicuculline. According to the authors, the neuronal network exhibits two different dynamical states: a state typical of non-chaotic deterministic systems and another state typical of stochastic or chaotic systems.

In-vitro networks have been studied in depth to investigate synaptic plasticity. By using the double-patch technique, the group of Poo investigated synaptic plasticity in pairs of neurons in dissociated rat hippocampal cultures. Their researches contributed greatly to the study of activity-induced synaptic modifications (Dan & Poo, 2004).

Moreover, the use of MEAs has allowed scientists to carry out studies on plasticity in the network at larger scale. A very recent paper (Arnold et al., 2005) showed how exposure of the hippocampal network to bicuculline (the $GABA_A$ receptor antagonist), induces a change in network

activity from uncoordinated firing (lacking any recognizable pattern) to a highly organized, periodic and synchronized bursting firing. Once induced, the burst pattern persists for several days in normal conditions and the maintenance phase is dependent on gene transcription taking place in the critical period of some hours following induction. Thus, cultured hippocampal neurons showed a simple form of plasticity dependent on transcription and protein synthesis.

Very interesting results in terms of plasticity were obtained when using the electrodes of the MEA as source for delivering external stimuli to the network.

Several works published by the group of Jimbo and Kawana pioneered the study of synaptic plasticity in neuronal cultures. In a first work (Maeda et al., 1998), using MEAs, they investigated how intrinsic synchronized activity in cortical cultures was modified with the application of an external stimulation. In particular, they observed that a strong high frequency stimulation (tetanus) was capable of potentiating the response of a weak and low frequency test stimulation, increasing the probability of eliciting bursts and increasing the frequency of spontaneous bursts. A detailed analysis showed that the essential mechanism for inducing plastic modifications was the capability of the tetanus to elicit a propagating burst. In a later paper (Jimbo et al., 1999), they demonstrated that a tetanic stimulation was able to induce simultaneously in the network long-term potentiation and depression. In their experiments control stimuli were delivered separately through each single electrode of the array, in order to measure the network response elicited by the activation of many distinct pathways. Once the tetanus was delivered, tests on the different pathways revealed a potentiated transmission in some cases and depressed transmission in others. These variations could be accounted for by considering the correlation of firing before the tetanus between tetanized pathways and tested pathways. High correlation resulted in potentiation and poor correlation determined depression. In another similar work (Tateno & Jimbo, 1999) it was shown that a tetanic stimulation can affect the reliability and reproducibility of spike trains evoked by a stimulus and can vary the fine temporal structure of evoked spike trains.

Further studies of learning and adaptation in cortical cultures have been carried out by the group of Prof. Marom. In a first investigation, (Shahaf & Marom, 2001) they showed how selective learning could be induced in a network. In particular, given a fixed stimulus, the network could learn to respond to the stimulation in the desired way, i.e. in a predefined time window following the stimulus. The training consisted of repeating the stimulus till the desired response was observed, i.e. stopping the stimulation represented a sort of reward for the network. In repeating this training protocol, the authors observed that the network learned to respond in the desired way in progressively shorter times. This effect was not observed in the absence of training. The authors suggested that presumably the stimulation could induce changes in the network. Stopping the stimulation could allow selection of changes consistent with the desired response.

In a second investigation (Eytan et al., 2003), it has been shown how the network can selectively adapt to frequent stimuli while becoming more sensitive to rare stimuli. In fact, repetitive stimulation with two distinct stimuli (a rare one and a frequent one) delivered through two distinct electrodes, caused a progressively decreasing response to the frequent stimulus whereas, by contrast, the rare stimulus slightly increased its response. The increasing response to the rare stimuli required the presence of the frequent stimuli, but the opposite effect was not observed. By using synaptic blockers, they showed how this effect of selective amplification depended on the balance between inhibition and excitation in the network.

2.3 Neuroengineering, neuroprosthetics and neuroimplants

Being able to decode the neural activity can lead to the development of a new generation of neuroprosthetic devices aimed, for example, at restoring motor functions in severely paralysed patients. In this context, the field of research commonly referred to as neuroengineering tries to combine parallel advances in nanotecnologies, electronics and neuroscience for powerful clinical and technological applications. While benefits from neuroengineering to information technology

still seems premature, implementations of direct brain–machine interfaces (BMIs) have already shown promising results in clinical applications. Recent experimental demonstrations in rodents, primates and patients (Nicolelis, 2003) let one realistically suppose that neuroprosthetic devices could be used for example to restore basic motor functions in patients suffering from severe body paralysis. Moreover, direct brain–machine interfaces can become the core of a new experimental approach with which to investigate the operation of neural systems in behaving animals. This approach assumes that voluntary motor commands can be extracted in real time from the electrical activity of populations of cortical or subcortical neurons spared by the underlying illness (Wessberg et al., 2000), and then used to enact motor function either by directly stimulating the patient's musculature or by controlling the movements of artificial actuators, such as robot arms (Nicolelis, 2001). Over the years, different sources of neuronal signals, ranging from electroencephalograms (EEGs) to intracranial single-unit recordings have been proposed as potential sources of control signals to drive various neuroprostheses (Chapin, 2004). Significant technological problems have yet to be overcome. Great efforts must be spent in the areas of microelectrode array, biocompatibility of brain implants, microelectronics for miniaturization of hardwares, power management, real-time computational modelling and robotics. These engineering bottlenecks must be overcome in order to move from demonstrations to clinical implementations. A few examples of what the future might bring are already present in the literature.

Tangible success has been obtained implanting brain stimulators, such as cochlear implants for restoring auditory function, deep brain stimulators for pain management and control of motor disorders (such as Parkinson's disease), and vagal nerve stimulators for treating chronic epilepsy (Aziz & Yianni, 2003; Siderowf & Stern, 2003; Henry, 2002).

In particular cochlear implants are an evident example of a successful neural prosthesis (Wilson et al., 2003). The cochlear implant is a quite simple microelectrode array that directly stimulates the auditory nerve. Auditory prostheses work by converting features of acoustic signals, such as speech, into patterns of electrical stimuli that are then delivered through an array of

chronically implanted electrodes to auditory nerve fibers lying on the basilar membrane of the cochlea. As the basilar membrane contains a representation of sound frequencies, known as a tonotopic map, auditory prostheses deliver high-frequency information to the basal region of the cochlea, and low-frequency signals to the apical region, to mimic normal auditory processing.

In contrast to auditory prostheses, visual prostheses encounter much bigger difficulties which seem still hard to overcome. An encouraging preliminary success has been obtained by connecting a television camera to the visual cortex (Dobelle, 2000). In this approach the role played by the prosthesis is to acquire the "sensory signal" and, to encode the information appropriately to be transferred to the CNS. In fact, the digital video camera was mounted on glasses to capture an image and send it to a small computer on the patient's belt: the images are processed and sent to electrodes implanted in the patient's visual cortex. The electrodes stimulate the brain, producing a pattern of bright spots that form an image. With such a device the patient might be blind to some objects, some situations, but not totally blind anymore.

In parallel, a number of research groups are developing electrical implants that can be attached directly to the retina in an attempt to restore vision to patients suffering from retinal degeneration (Zrenner, 2002). There are two kinds of retinal implant under development: subretinal and epiretinal. With a subretinal implant, the rods and cones should be replaced by a silicon plate carrying thousands of light-sensitive microphotodiodes, each equipped with a stimulation electrode. The stimulation injects current into whichever neurons remain of the retinal network, the middle and inner retina thus taking over the information-processing part of vision. In this approach the prosthesis partially replaces the peripheral nervous system in acquiring the visual stimulus and directly transfers the information through the electrical stimulation to the next stage of the sensory peripheral visual system pathway. Encoding and conversion of the acquired information into the stimulation is very simple since the prosthesis acts in an early stage of the peripheral nervous system. In contrast, the epiretinal implant has no light-sensitive areas but receives electrical signals from a distant camera and processing unit outside of the body. Electrodes in the epiretinal implant

then directly stimulate the axons of the inner-layer ganglion cells that form the optic nerve. Unlike the subretinal implant, the epiretinal implant does not use the remaining network of the retina for information processing. Thus, the epiretinal sensor has to encode visual information as trains of electrical impulses that are then conveyed by the electrode array directly into the axons of ganglion cells, which unite to form the optic nerve. The visual information has to be translated into a spatiotemporal stimulation pattern of electrical impulses that can be understood by the brain's visual cortex. Despite promising results in animal experiments, there are still several major obstacles to overcome before retinal prostheses can be used clinically. Before retinal implants can be tested in patients, surgical techniques for implanting, removing, and fixing these electronic prostheses in the eye must be developed.

In the context of neuroimplants for brain-machine interfaces, a new field of neuroengineering, referred as "cognitive engineering", is emerging. In this ambit, Kennedy and Bakay (1998) have developed a neurotrophic electrode brain implant that is allowing speech-impaired patients to communicate through a computer. They recorded action potentials in the brain of the patients over several months by means of an electrode that induces growth of myelinated fibers into its recording tip. The patients were able to control the neural signals in an on/off fashion. The patients were taught to control the strength and pattern of the electric impulses being produced in the brain. The patients learned to move the cursor to letters of the alphabet and spell words. This result is an important step towards providing such patients with direct control of their environment by interfacing with a computer. Additionally, it indicates that restoration of paralyzed muscles may be possible by using the signals to control muscle stimulators. The developments in this field would open up a tremendous opportunity for patients who have lost the ability to move and talk because of stroke or spinal cord injury. For spinal cord injured patients who have uncontrolled muscles, these neural signals could provide some control of electrical stimulators that activate the paralyzed muscles, thus bypassing the area of spinal cord injury ("spinal bypass").

In the context of movement disorder diseases, the development of deep brain stimulation in the treatment of Parkinson's disease as an effective and safe therapy has led clinicians to explore the treatment of disorders for which there has been no effective treatment (Aziz & Yianni, 2003).

2.4 Aims and strategies of the Ph.D. project

The major aim of the research presented in this thesis was to study general and basic mechanisms of information processing in neuronal networks. Therefore,

- as a possible general model of neuronal networks, dissociated neuronal cultures of rat hippocampal neurons were used;
- the cultures were grown on multielectrode arrays and the electrodes were used to deliver electrical stimuli to the networks (input) and to record the electrical activity evoked in the neurons (output).

In order to understand the neural coding and the role of single neurons and neuronal ensembles in information processing, I studied:

- the variability of firing in single neurons and in neuronal ensembles;
- the response of neurons to stimuli with different features (intensity, spatial profile and spatial location);
- neural coding mechanisms based on the firing rate and on the first spike latencies of a population of neurons;
- the role of excitatory and inhibitory transmission by applying appropriate synaptic blockers.

Information theory and classification analysis were used to evaluate and compare the ability of different neural coding schemes to convey information. In particular, information theory was used to quantify precisely the concept of information.

In order to explore the possibility of using neurons as computing elements in tasks commonly solved by conventional serial devices:

- neuronal cultures were used for image processing and pattern recognition, tasks which would optimally require parallel computation and learning;
- digital images and spatial patterns were mapped into the extracellular stimulation of the neuronal culture in a one to one correspondence between pixels and electrodes;
- pattern recognition and features extraction were studied after induction of learning.

Understanding the neural coding mechanisms and how information processing takes place in the neuronal networks would give a huge contribution to the development and creation of neuroprostheses and new computing devices.

-Paper 1-

Towards the neurocomputer: image processing and pattern recognition with neuronal cultures

IEEE transactions on Biomedical Engineering, vol. 52, No. 3, March 2005-10-19

Maria Elisabetta Ruaro, Paolo Bonifazi and Vincent Torre

Toward the Neurocomputer: Image Processing and Pattern Recognition With Neuronal Cultures

Maria Elisabetta Ruaro, Paolo Bonifazi, and Vincent Torre*

***Abstract*—Information processing in the nervous system is based on parallel computation, adaptation and learning. These features cannot be easily implemented on conventional silicon devices. In order to obtain a better insight of how neurons process information, we have explored the possibility of using biological neurons as parallel and adaptable computing elements for image processing and pattern recognition. Commercially available multielectrode arrays (MEAs) were used to record and stimulate the electrical activity from neuronal cultures. By mapping digital images, i.e., arrays of pixels, into the stimulation of neuronal cultures, a low and bandpass filtering of images could be quickly and easily obtained. Responses to specific spatial patterns of stimulation were potentiated by an appropriate training (tetanization). Learning allowed pattern recognition and extraction of spatial features in processed images. Therefore, neurocomputers, (i.e., hybrid devices containing man-made elements and natural neurons) seem feasible and may become a new generation of computing devices, to be developed by a synergy of Neuroscience and Material Science.**

***Index Terms*—Long-term potentiation, multielectrode array, neuronal culture, pattern recognition.**

I. Introduction

UNDERSTANDING differences and similarities between conventional computers and biological nervous systems is a fascinating problem, at the core of Neuroscience and Computer Science. This comparison can provide a deeper understanding of human intelligence and may pave the way to the design of new computing devices. Standard silicon devices solve serial problems very efficiently, but, despite their remarkable speed, are less suitable for solving the parallel problems of artificial intelligence, computer vision and robotics [1], [2]. Because of the difficulty of forming large numbers of interconnections, man-made devices are not ideal for massive parallel processing, a task for which biological neurons are very suitable. Biological neurons form connections and synapses between themselves very naturally. Despite being slow and often unreliable computing elements [3]–[5], neurons operate extremely well in parallel and can adapt and learn.

In order to capture basic computational properties of biological neuronal networks, artificial neural networks (ANNs) were developed [1], [2]; [6]–[8]. ANNs can be trained to recognize features and patterns. However, ANNs are usually implemented on conventional serial machines thereby losing their biological inspiration. Their implementation on genuinely parallel devices, ideally networks of natural neurons that are able to learn, is certainly desirable.

The major aim of the present manuscript is to explore the possibility of using biological neurons as computing elements in a task commonly solved by conventional silicon devices: image processing and pattern recognition.

Advances in the biocompatibility of materials and electronics have allowed neurons to be cultured directly on metal or silicon substrates, through which it is possible to stimulate and record neuronal electrical activity [9]–[16]. The work here described shows that by using commercially available multielectrode arrays (MEAs), it is possible to process simple patterns using two fundamental properties of natural neuronal networks: parallelism and learning. By mapping digital images into the extracellular stimulation of the neuronal culture (in a one to one correspondence between pixels and electrodes) a low-pass filtering of the images is obtained. This processing occurs in just few milliseconds, independently from the dimension of the image processed. In addition, neuronal cultures can be trained to potentiate the response to a simple spatial pattern, due to changes in synaptic efficacy or long-term potentiation (LTP) [17], [18]. Therefore, the neuronal culture can be trained to recognize simple spatial patterns. Moreover filtering and learning can be combined to extract features from processed images.

These results show that biological neurons can be effectively used as computing elements for massively parallel problems and support the feasibility of neurocomputers, i.e., hybrid devices composed of biological neurons and artificial elements.

II. Methods

A. Neuronal Culture Media

Dissection Medium: Hanks' modified $-Ca^{2+}/Mg^{2+}$ free-solution supplemented with 4.2 mM $NaHCO_3$, 12 mM Hepes, 33 mM D-glucose, 200 μM kynurenic acid, 25 μM DL-2-amino-5phosphonovaleric acid (APV), 5 $\mu g/ml$ gentamycin, 0.3% BSA.

Digestion Medium: 137 mM NaCl, 5 mM KCl, 7 mM Na_2HPO_4, 25 mM Hepes, 4.2 mM $NaHCO_3$, 200 μM kynurenic acid, 25 μM APV).

Culture Medium: Minimal Essential Medium with Earle's salts (GIBCO-Brl) supplemented with 5% fetal calf serum, 0.5% D-glucose, 14 mM Hepes, 0.1 mg/ml apo-transferrin, 30 $\mu g/ml$ insulin, 0.1 $\mu g/ml$ d-biotin, 1 mM Vit. B12 and 2 $\mu g/ml$ gentamycin.

B. Neuronal Dissection and Dissociation

The hippocampus from three-day-old Wistar rats was dissected in ice-cold dissection medium. Slices, were cut with a

Manuscript received October 17, 2003; revised August 5, 2004. This work was supported in part by the EU under Grant INPRO and in part by a FIRB grant from the Italian Ministers. *Asterisk indicates corresponding author.*

M. E. Ruaro and P. Bonifazi are with the INFM section and International School for Advanced Studies, I-34014 Trieste, Italy

*V. Torre is with the International School for Advanced Studies (SISSA), Via Beirut 2-4, 34014 Trieste, Italy (e-mail torre@sissa.it).

Digital Object Identifier 10.1109/TBME.2004.842975

razor blade, transferred in a 15-ml centrifuge tube and washed twice with the dissection medium. Slices were then treated with 5 mg/ml Trypsin and 0.75 mg/ml DNAseI in digestion medium for 5 min at RT to perform enzymatic dissociation. Trypsin was then neutralized by 1 mg/ml trypsin inhibitor in dissection medium for 15 min on ice. After three washes with the dissection medium, mechanical dissociation was performed by 10 passages through a P1000 blue tip. The cell suspension was then centrifuged at 100 g for 5 min, and pellet was re-suspended in culture medium.

C. MEA Coating

MEA dishes were coated by overnight incubation at 37 °C with 1 ml of 50 μg/ml polyornithine (in water). Dishes were then air-dried and a film of BD-Matrigel (Beckton–Dickinson) was added on the electrode matrix region 20 min before seeding.

D. Cell Culture

100 μl of cell suspension was laid on the electrode array of precoated MEA at the concentration of 8×10^5 cells/cm^2. Cells were let to settle at room temperature for 20 min, and then 1 ml of culture medium was added to the MEA and incubated in a 5% CO_2 atmosphere at 37°C. After 48 hours 5 μM cytosine-β -D-arabinofuranoside (Ara-C) was added to the culture medium, in order to block glial cell proliferation, and re-incubated with gentle rocking.

E. Maintenance of Neuronal Cultures

Neuronal cultures were kept in an incubator providing a controlled level of CO_2 (5%), temperature (37°C) and moisture (95%). Half the medium was changed twice a week. Recordings were performed, in culture medium, from 3 weeks after seeding for up to 3 months. To decrease water evaporation and to maintain sterile conditions outside the incubator [19], during electrical recordings dishes were sealed with a cap manufactured by ALA Science and distributed by MCS (MultiChannelSystem). After termination of the experiment, usually after 3 to 10 hours, the cap was removed, the medium was changed and the dish was moved back to the incubator. The same dish could be used for other experiments in the following days and often repetitively over a month. In some cases the same dish was used for more than four different experiments.

F. Electrical Recordings and Electrode Stimulation

MultiChannelSystems commercially supplied the MEA system used for electrical recording. We used a 10×6 microelectrode array, with 500 μm spacing between adjacent electrodes. Each titanium-nitride microelectrode has a 30 μm diameter circular shape; its frequency-dependent impedance is of the order of 100 kΩ at 1 kHz. Through gold contacts it is connected to a 60 channel, 10 Hz –3 kHz bandwidth preamplifier/filter-amplifier (MEA 1060-AMP) which redirects the signals toward a further electronic processing (i.e., amplification and AD conversion), operated by a board lodged within a high performance PC. Signal acquisitions are managed under software control. A thermostat (HC-X) maintains the temperature at 37 °C underneath the MEA. The MEA provided by MCS is able to digitize in real time at 20 kHz all voltage recordings obtained from the 60 metal electrodes. One electrode was used as ground [see Fig. 1(c)]. Sample data were transferred in real time to the hard disk for later processing. Each metal electrode could be used for recording or for stimulation, but the present MCS system does not allow a computer-controlled switch from one mode to the other. Therefore, during a trial, each electrode can be used either for stimulation or recording. Voltage stimulation consisted of bipolar pulses lasting 100 μs at each polarity, of amplitude varying from 0.2 V to 1 V, injected through the STG1004 Stimulus Generator. An artifact lasting 5 – 20 ms caused by the electrical stimulation was induced on the recording electrodes but was removed from the electrical recordings during data analysis.

Tetanus: The tetanus, i.e., a high frequency stimulation, consisted of 40 trains of bipolar pulses of $+/-0.9$ V lasting for 200 μs delivered every 2 s. Every train consisted of 100 pulses at 250 Hz. Test stimuli before and after tetanus were delivered every 2 s. The tetanus had a spatial profile usually composed by two perpendicular bars of electrodes meeting in a corner, or by a vertical or horizontal bar of electrodes.

G. Data Analysis

Acquired data were analyzed using the software MatLab (The Mathworks, Inc., Natick, MA).

Artifact Removal: The artifact at each electrode and for each pattern of stimulation was estimated and subtracted from the voltage recordings. The artifact was estimated in the following way: for each pattern of stimulation and at each electrode the voltage response was averaged over all trials (typically 50), computed and fitted by 2 polynomials of ninth degree. Using polynomials of a lower order provide similar results in most of experiments, but not in all, therefore, ninth degree polynomials were routinely used. The 2 polynomials fitted respectively the data in the time windows of 0.5–25 ms and 7.5–100 ms after stimulation. The first polynomial was used to evaluate the artifact in the time window of 0.5 to 7.5 ms, while the second in the time window of 7.5 and 82.5 ms. The artifact, so evaluated, was subtracted from the original voltage signal. The time window between 0 and 1 ms after stimulation was not considered in the data analysis.

Computation of Firing Rate ($FR_{ij}(t)$) and Related Quantities ($AFR_{ij}(t)$, $\underline{FR}(t)$, $\underline{AFR}(t)$, $IntAFR_{ij}$, $Int\underline{AFR}$, $Int\underline{FR}$): Let $V_{ij}(t)$ be the voltage recorded at electrode (i,j) and σ_{ij} be the standard deviation of the noise computed considering a period of at least 1 s where no spikes were visually observed. The σ_{ij} of the noise ranged for individual electrodes from 3 to 6 μV. Action potentials are considered to be events exceeding 5 σ_{ij}. The firing rate per electrode $FR_{ij}(t)$ is computed with a binwidth of 10 ms centered on t. The $FR_{ij}(t)$ counts spikes from different neurons, making a good electrical contact with electrode (i, j). The average firing rate $AFR_{ij}(t)$ was computed by averaging $FR_{ij}(t)$ over the entire set or a subset of identical stimulations [Figs. 1(e), (f) and 5(a), (b)]. Let active electrodes be the electrodes showing a clear electrical contact with the neuronal culture, i.e., where spikes can be recorded. Generally, in order to have a simple measure of the overall evoked firing rate, the firing rate spatially averaged $\underline{FR}(t)$ was obtained by averaging $FR_{ij}(t)$ over the entire set of active recording electrodes. Only for the computation, shown in Figs. 2(a) and 3(a), the spatial average was limited to a row of electrodes. The average overall

TABLE I

Abbreviations / Names of variables	Definitions	Figure
$FR_{ij}(t)$ Firing rate	Firing rate per electrode in either 5 or 10 ms bins with centers specified by t	
$AFR_{ij}(t)$ Average firing rate	Firing rate per electrode averaged over the entire set or a subset of identical stimulations	1E, 1F, 5A, 5B
$\underline{FR}(t)$ Firing rate spatially averaged	Firing rate spatially averaged over a set of recording electrodes	
$\underline{AFR}(t)$ Average overall evoked response	Average of $\underline{FR}(t)$ over the entire set or a subset of identical stimulations	3B, 4C, 5C, 5D
$IntAFR_{ij}$	Integral between t=1 ms and t=50 ms of $AFR_{ij}(t)$	4A
$Int\underline{AFR}$	Integral between t=1 ms and t=50 ms of $\underline{AFR}(t)$	7
$Int\underline{FR}$	Integral between t=1 ms and t=50 ms of $\underline{FR}(t)$	6

evoked response $\underline{\mathrm{AFR}}(\mathrm{t})$ is the average of $\underline{\mathrm{FR}}(\mathrm{t})$ over the entire set or a subset of identical stimulations [Figs. 3(b), 4(c), and 5(c), (d)]. The coefficient of variation $\mathrm{CV}(\mathrm{t})$ of $\mathrm{AFR_{ij}}(\mathrm{t})$ was computed as the ratio of the standard deviation of $\mathrm{FR_{ij}}(\mathrm{t})$ to the $\mathrm{AFR_{ij}}(\mathrm{t})$. Similarly, the coefficient of variation $\mathrm{CV}(\mathrm{t})$ of $\underline{\mathrm{AFR}}(\mathrm{t})$ was computed as the ratio of the standard deviation of $\underline{\mathrm{FR}}(\mathrm{t})$ to the $\underline{\mathrm{AFR}}(\mathrm{t})$. In order to describe the properties of the neuronal culture to learn and discriminate patterns, the integrals respectively of $\mathrm{AFR_{ij}}(\mathrm{t})$, $\underline{\mathrm{FR}}(\mathrm{t})$, $\underline{\mathrm{AFR}}(\mathrm{t})$ in a time window between 1 and 50 ms have been calculated and defined as, $\mathrm{IntAFR_{ij}}$, $\mathrm{Int}\underline{\mathrm{FR}}$, $\mathrm{Int}\underline{\mathrm{AFR}}$. $\mathrm{IntAFR_{ij}}$ and $\mathrm{Int}\underline{\mathrm{AFR}}$ were used to compare the average response evoked by an identical stimulation before and after the tetanization, at a single electrode and when all the MEA electrodes were considered [see Figs. 4(a), 7, respectively]. $\mathrm{Int}\underline{\mathrm{FR}}$ was used to compare at the level of a single-trial the response evoked by different patterns of stimulation, detected by all the MEA electrodes (see Fig. 6). The different quantities used to characterize the firing of the neuronal culture are reported in Table I.

H. Pattern of Stimulation and Image Processing

The input to the device is the set of extracellular voltage stimulations, delivered at time $\mathrm{t} = 0$, applied to the neuronal culture through the MEA electrodes. If (i,j) is an electrode of the MEA, the input is the matrix $\mathrm{S_{ij}}$ of voltage stimulations applied to the electrode (i,j). A binary image or pattern I_{ij} of $\mathrm{M} \times \mathrm{N}$ pixels [Fig. 1(a)] is coded into the input of a MEA with $\mathrm{M} \times \mathrm{N}$ electrodes [Fig. 1(b)], so that the gray level of pixel (i,j) of I_{ij} is converted into the appropriate voltage stimulation $\mathrm{S_{ij}}$ of electrode (i,j). The matrix of voltage signals $\mathrm{V_{ij}}(\mathrm{t})$ recorded with the MEA [Fig. 1(c)], composed of action potentials or spikes produced by the neurons in the culture [Fig. 1(b)] is analyzed. The output of the device is the matrix $\mathrm{FR_{ij}}(\mathrm{t})$. MEAs with at least 54 electrodes providing electrical recordings of clear spikes were used for image processing. For each pattern of electrodes used for stimulation, let $\mathrm{S}_{1/2}$ be the voltage stimulation evoking half of the maximal $\underline{\mathrm{AFR}}(\mathrm{t})$ in the time window between 1 and 11 ms after the onset of the voltage pulse. If I_{ij} is the corresponding binary image or the pattern to be processed and its gray levels are either 0 or 1, then S_{ij} will be $3/2 * \mathrm{S}_{1/2}$ if I_{ij} is 1, 0 otherwise.

Filling Silent Electrodes and Smoothing: The procedure here described has been applied only for image processing [Figs. 2(b), (c), 3(d), and 8]. MEAs with at least 54 electrodes providing electrical recordings of clear spikes were used. When one electrode (i,j) is silent, i.e., no spikes can be recorded, the corresponding hole in the processed image is filled in by assigning to $\mathrm{FR_{ij}}(\mathrm{t})$ the value obtained by averaging the firing rate from neighboring electrodes – i.e., electrodes at a distance of 500 $\mu\mathrm{m}$. $\mathrm{FR_{ij}}(\mathrm{t})$ of stimulated electrodes was determined by extrapolation from the neighboring active electrodes using (1). All processed images had at most 3 silent electrodes, including the one used as ground. The value of $\mathrm{FR_{ij}}(\mathrm{t})$ was smoothed over the neighboring electrodes $(\mathrm{i}-1,\mathrm{j})$ $(\mathrm{i}+1,\mathrm{j})$, $(\mathrm{i},\mathrm{j}-1)$ and $(\mathrm{i},\mathrm{j}+1)$.

Processing of 8 Bit Images: The 8-bit image O_{ij} was described by

$$\sum_{p=1}^{8} I_{\mathrm{ij}}^{(p)} 2^{(p-1)}$$

where $I_{\mathrm{ij}}^{(p)}$ is a 1-bit image. The 8 $I_{\mathrm{ij}}^{(p)}$ 1-bit images are processed as described below and their output was summed as described in (4) and (5).

Scaling of $\mathrm{FR_{ij}}(\mathrm{t})$, $\mathrm{AFR_{ij}}(\mathrm{t})$ *and Output Color-Coding:* In order to display processed images using a standard color-coding, the values of $\mathrm{FR_{ij}}(\mathrm{t})$, $\mathrm{AFR_{ij}}(\mathrm{t})$ or their combination (for bandpass filtering) were rescaled. The scaling procedures described in this section refer to the factors α and $\alpha^{(p)}$ of (2), (4) and (5) (see Results). For low-pass filtered images, the values of $\mathrm{FR_{ij}}(\mathrm{t})$ [Fig. 3(d)] or $\mathrm{AFR_{ij}}(\mathrm{t})$ [Fig. 2(b), upper row] were scaled between 0 and 1 by dividing for the corresponding maximal value among all electrodes in the time-window 1–30 ms. Digitally low-pass filtered images [Fig. 2(b) lower row] were scaled between 0 and 1 dividing by their maximal value. Bandpass filtered image [Fig. 2(c) top panel] was obtained as the difference of $\mathrm{AFR_{ij}}(\mathrm{t})$ calculated in time bins 1–6 ms and 4–9 ms and the resulting matrix was scaled between -1 and $+1$, dividing by its maximum absolute value. For digitally bandpass filtered images [Fig. 2(c) lower panel], obtained as the difference of digitally low-pass filtered images, the resulting output was scaled between -1 and $+1$, dividing for its maximum absolute value. The color map (of 256 colors) was always scaled between -1 and 1. For 8-bit processed images [Fig. 8(a)], the values of $\mathrm{AFR_{ij}}(\mathrm{t})$ were scaled as described above, and were added according to (4). When it was necessary to compare 8-bit image processing before and after tetanization [see Fig. 8(b)], the values of $\mathrm{AFR_{ij}}(\mathrm{t})$ obtained

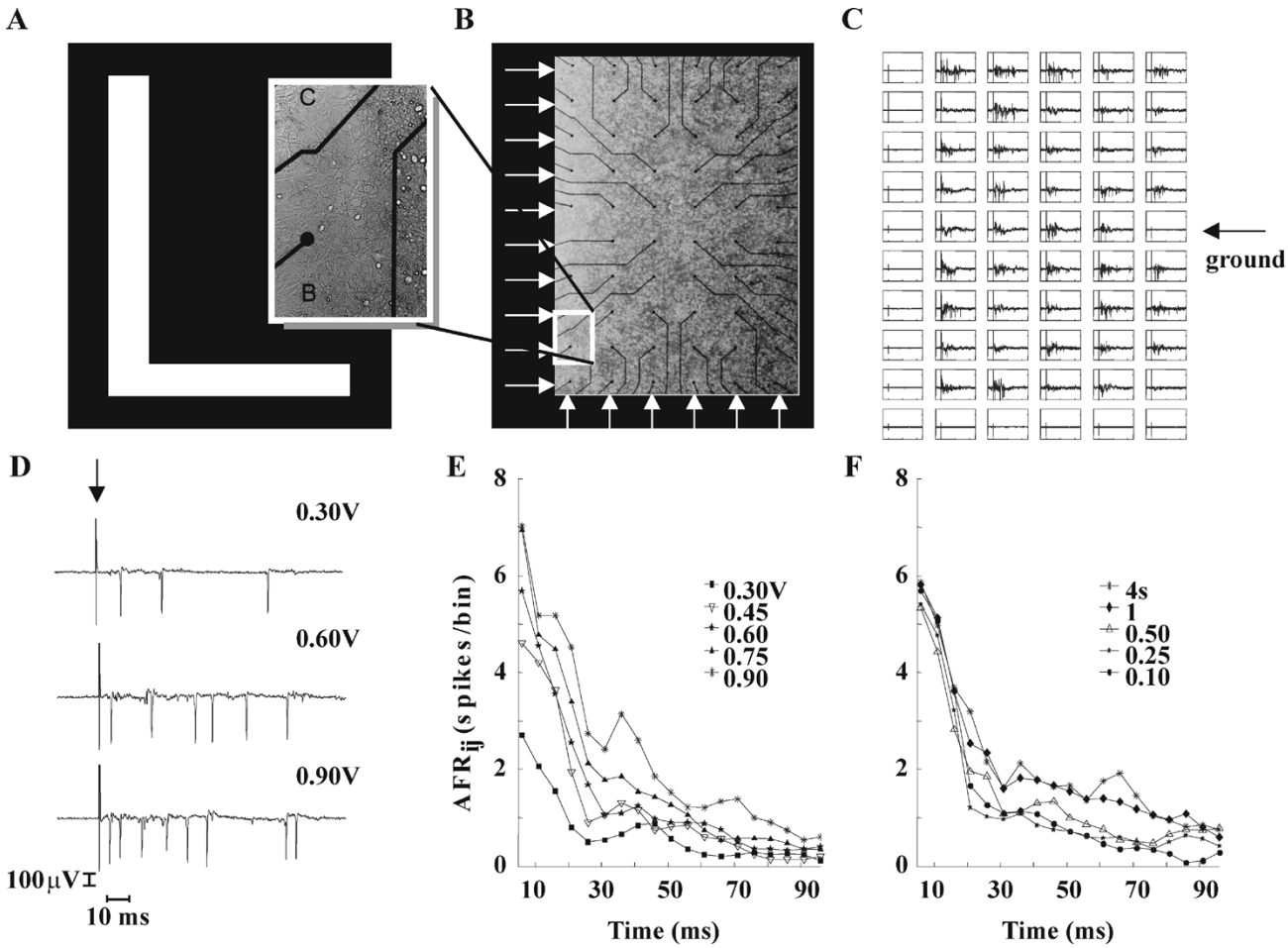

Fig. 1. Mapping an image into the stimulation of a neuronal culture. (A) 10×6 binary image of a ⌊ used as the stimulation pattern of a neuronal culture grown over a 10×6 MEA manufactured by MCS. (B) Photo of dissociated hippocampal neurons grown on the MEA. Magnification of the neuronal culture on the area marked by the letters B and C (white rectangle) shown in the inset. (C) Electrical recordings of electrical activity evoked by the electrodes stimulation with bipolar voltage pulses of 0.9 V. The silent electrode indicated by the arrow was used as the ground. (D) Three voltage recordings evoked by voltage pulses of 0.3, 0.6, and 0.9 V when the 6 electrodes of the upper row were stimulated. (E) $\mathrm{AFR_{ij}(t)}$ (see Section II) recorded by a representative electrode in response to five different voltage stimulations, as indicated in the panel. (F) $\mathrm{AFR_{ij}(t)}$ recorded by a representative electrode at different repetition rates as indicated in the panel Data in (E) and (F) are averaged from 50 different trials of the same stimulation. Time 0 ms corresponds to the voltage stimulation.

after tetanization were scaled dividing by the maximal value of $\mathrm{AFR_{ij}(t)}$ measured before tetanization. In this case the scaled values of $\mathrm{AFR_{ij}(t)}$ before tetanization varied between 0 and 1, but, after tetanization, they could be larger than 1. The scaled values of $\mathrm{AFR_{ij}(t)}$ were added according to (5). The color map (of 256 colors) was scaled between 0 and 256. Therefore, with this coding, the processing of images at 1 or 8-bit has the same map, i.e., the output has 256 different colors.

III. Results

A. The Device

The great majority of MEAs presently available and charge-coupled device (CCD) arrays share the same geometry of a square grid. Therefore, CCD pixels and MEA electrodes can be put in a simple one-to-one correspondence preserving their neighborhood [see Fig. 1]. This observation inspired the design of a new device for processing images and patterns, using a MEA and a neuronal culture grown on its surface. The image is mapped to the voltage stimulation of the neuronal culture and the evoked electrical activity is taken as the output of the device. The computing elements of the device are the neurons of the culture.

The input to the device is the set of extracellular voltage stimulations, delivered at time $\mathrm{t} = 0$, applied to the neuronal culture through the MEA electrodes, coding for the image $\mathrm{I_{ij}}$ to be processed. The output of the device is the matrix $\mathrm{FR_{ij}(t)}$, counting the number of times in which the extracellular voltage recorded at electrode (i,j) exceeds a given threshold in the time window between $\mathrm{t}-\Delta\mathrm{t}$ and $\mathrm{t}+\Delta\mathrm{t}$. Several average quantities – in space, time and over different trials – were computed from $\mathrm{FR_{ij}(t)}$ (see Section II for further details).

B. Dynamic Range and Cycle Time

In order to explore the dynamic range and cycle time of the proposed device, a row of electrodes, was repeatedly used for stimulation. Brief (200 μs) bipolar voltages with amplitude varying from 0.3 V to 0.9 V were used. When the voltage stimulation was increased, the frequency of evoked spikes increased and often spikes with a novel shape, produced by a different neuron, appeared [Fig. 1(d)]. The average firing

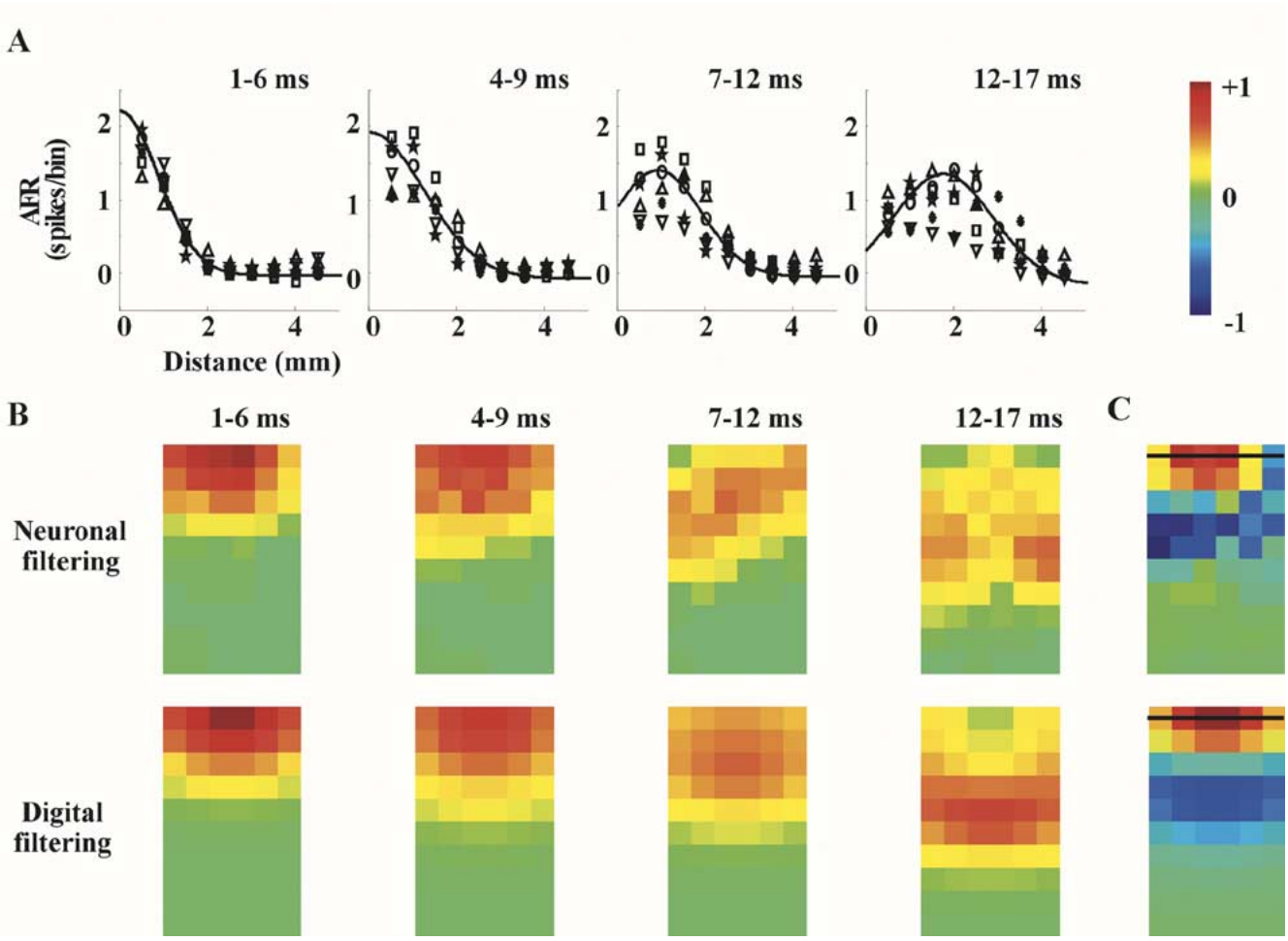

Fig. 2. Spread of excitation through the neuronal culture. (A) $\mathrm{AFR_{ij}(t)}$ averaged by row ($\underline{\mathrm{AFR}}(\mathrm{t})$) and calculated in the time windows of 1–6, 4–9, 7–12 and 12–17 ms after the stimulation of the uppermost row of electrodes with a voltage pulse of 0.6 V. Different symbols indicate experimental data from 6 different neuronal cultures. Thick curves are theoretical fits calculated from (1). Data obtained in the time windows 1–6 and 4–9 ms were fitted by setting $\widetilde{\rho}$ equal to 0 and σ respectively, to 890 and 1240 $\mu\mathrm{m}$. Data in the time windows 7–12 and 12–17 ms were obtained with $\widetilde{\rho}$ equal to 920 and 1750 and σ equal to 980 and 1130 $\mu\mathrm{m}$ respectively. (B) Comparison between neuronal and digital filtering. (Upper row) images obtained from the processing performed by the neuronal culture in the corresponding time windows. (Lower row) digital Gaussian filtering of the original binary image with the uppermost row of pixels equal to 1 and 0 elsewhere. (C) (Upper panel) bandpass filtering of the neuronal culture obtained by subtracting the AFRs in the time windows 1–6 and 4–9 ms; (lower panel) digital filtering obtained by convolving the original binary image with the difference of two Gaussians fitting the experimental data in the first and second panel of Fig. 2(a). The thin bars indicate the stimulated electrodes. Color-coding is reproduced at the right side of panel A.

$\mathrm{AFR_{ij}(t)}$ increased with the voltage stimulation [Fig. 1(e)], but its dynamic range was rather narrow: usually no spikes were evoked by voltage pulses below 0.2 V and a saturating maximal response was evoked with voltage stimulation of about 1 V. In the vast majority of the experiments, it was possible to distinguish reliably 4 levels of evoked activity.

In order to determine the cycle time of the device, the same stimulation was repeated at intervals from 0.1 s to 10 s. With a repetition interval higher than 1 or 2 s the $\mathrm{AFR_{ij}(t)}$ had two components: one which was evoked with a delay of very few ms and lasting for about 15 ms, followed by a second lasting around 0.1 s. The amplitude of the first component was not significantly affected by decreasing the repetition time from 4 to 0.1 s [see Fig. 1(f)]. The amplitude of the second component was clearly depressed at short repetition times and it was stable for repetition times greater than 4 s (data not shown).

C. Filtering Properties of the Neuronal Culture

The neuronal culture grown on the MEA constitutes a two-dimensional (2-D) network. Given a homogenous culture, its filtering properties can be simply analyzed by using a long bar as a spatial stimulus, thus reducing a 2-D problem to a much simpler one-dimensional. In these experiments the six electrodes of the upper row were used for stimulation and the average firing rate evoked in each electrode was measured (see Section II) and averaged by row ($\underline{\mathrm{AFR}}(\mathrm{t})$). At early times, i.e., in the time window between 1 and 6 ms [Fig. 2(a)] the $\underline{\mathrm{AFR}}(\mathrm{t})$ decayed as a Gaussian function with a standard deviation σ of about 900 $\mu\mathrm{m}$ corresponding to 1.8 pixels (solid line). In the time window between 4 and 9 ms the electrical activity decayed similarly as a Gaussian function but with a larger σ of about 1200 $\mu\mathrm{m}$ corresponding to 2.5 pixels (solid line). A very similar decay and spread of electrical excitation was consistently observed in all the 24 analyzed neuronal cultures. Data collected from 6 different dishes are shown in Fig. 2 as different symbols.

After about 10 ms from the stimulus, the peak of the $\underline{\mathrm{AFR}}(\mathrm{t})$ moved away from the stimulated electrodes and the spread of the electrical activity could be described by a Gaussian function centered at a distance $\widetilde{\rho}$ from the stimulated electrodes [Fig. 2(a), time interval of 7–12 ms]. After 15 ms the evoked electrical ac-

tivity decayed even further, maintaining a Gaussian-like profile [Fig. 2(a), time interval of 12–17 ms]. While the same qualitative behavior was observed in all neuronal cultures, after at least 25 days of cultivation, the speed at which the electrical activity moved from the stimulating electrodes varied between 70 to 250 $\mu\mathrm{m/ms}$. The electrical activity in young cultures, i.e., with less than 20 days, did not propagate well throughout the culture.

A comparison between the spatio-temporal filtering performed by the neuronal culture and a digital gaussian filtering is shown in Fig. 2(b). The processing of the bar-stimulus by the neuronal culture represented by the color-coding of the evoked $\mathrm{AFR_{ij}(t)}$ is shown in the upper row of Fig. 2(b) in the four time windows. The corresponding digital convolution of the binary image correspondent to the bar-stimulus (see Section II) is shown in the lower panels of Fig. 2(b). Between 1 and 9 ms the neuronal filtering is a good approximation of a Gaussian digital filtering which used the σ extracted from the fit of Fig. 2(a). Between 7 and 12 ms (and 12–17 ms), the Gaussian filtering with the values of $\widetilde{\rho} = 1250\ \mu\mathrm{m}$ and $\sigma = 850\ \mu\mathrm{m}$ (and $\widetilde{\rho} = 1750\ \mu\mathrm{m}$ and $\sigma = 1130\ \mu\mathrm{m}$) shows the same features of the neuronal filtering. Therefore, at later times, $\mathrm{AFR_{ij}(t)}$ is a noisy displaced low-pass filtering of the original image.

When an horizontal bar in a different location or a vertical bar of electrodes was used to stimulate the neuronal culture, the electrical activity propagated from the stimulation site with almost the same properties of the horizontal bar in the upper part shown in Fig. 2(a) and (b). Experiments where a row (or a column) of electrodes or individual electrodes were stimulated indicate that the spatial-temporal processing of the neuronal culture is – to a first approximation – spatially invariant and can be described by a radial impulse response with a Gaussian function or kernel, centered on $\widetilde{\rho}$ and with a time varying variance $\sigma^2(\mathrm{t})$

$$h(\rho, t) = \exp\left(-\frac{(\rho - \widetilde{\rho}(t))^2}{2\sigma^2(t)}\right) \tag{1}$$

and ρ is the polar coordinate of the electrode.

Therefore, given a 1-bit image I_{ij} the output of the proposed device $\mathrm{FR_{ij}(t)}$ varies in time according to

$$\mathrm{FR_{ij}}(t) = \alpha \cdot I_{\mathrm{ij}} ** h(\rho, t). \tag{2}$$

** indicates a 2-D convolution and α is a scaling factor (see Section II). As shown in Fig. 2(b), in the time window 1–6 ms, the impulse response of the neuronal culture is a Gaussian function with a σ of about 900 $\mu\mathrm{m}$, but 2 or 3 ms later with a larger value of σ of about 1200 $\mu\mathrm{m}$. The neuronal filters obtained in the time windows 1–6 ms and 4–9 ms are low pass, and their difference is bandpass (see Section II). Bandpass filtering of the binary image corresponding to the bar-stimulus obtained with the neuronal culture, is shown in the upper panel panels of Fig. 2(c). This neuronal filtering is rather similar to that obtained by a digital band-pass filtering, shown in the lower panel of Fig. 2(c) (see Section II).

D. Reproducibility of Neuronal Firing and Filtering

Unlike silicon devices, biological neurons are affected by a significant noise and their reliability is variable. In our neuronal cultures, during repetitions of the same stimulations, the number of evoked spikes measured by a single electrode was variable, but often the first evoked spike was rather reliable with a jitter varying from just a few hundreds $\mu\mathrm{s}$ to some ms.

The reproducibility of neuronal firing measured by a single electrode was evaluated computing the coefficient of variation $\mathrm{CV(t)}$ of $\mathrm{AFR_{ij}(t)}$ (see Section II). When the value of CV is less than 0.4, the firing is considered reproducible. Fig. 3(a) shows the $\mathrm{CV(t)}$ of the evoked response recorded by the electrodes in the 2nd (left panel, open symbols) and in the 7th (right panel, open symbols) rows of the array [Fig. 3(c)]. For the electrodes in the 2nd row, in the time window between 1 and 11 ms, the $\mathrm{CV(t)}$ was for most electrodes smaller than 0.5 and could approach 0.2. For the electrodes in the 7th row, in the time window between 11 and 16 ms, the $\mathrm{CV(t)}$ was always smaller than 0.75 and could approach 0.3. The value of the $\mathrm{CV(t)}$ was slightly higher at increasing distances of the recording electrode from the stimulation site. These results indicate that there is a " reliability window " soon after the stimulation in which the $\mathrm{CV(t)}$ of the evoked activity at most electrodes is less than 0.5 and often around 0.3.

The $\mathrm{CV(t)}$ of the evoked response was further decreased by considering all the spikes recorded from a row of electrodes, as shown in Fig. 3(a) (thick line). The $\mathrm{CV(t)}$ was between 0.1 and 0.2 for both the electrode rows and the $\mathrm{CV(t)}$ remains less than 0.5 for at least 20 ms. When all the spikes recorded from all electrodes on the MEA were pooled together, the $\mathrm{CV(t)}$ of the evoked response was transiently lower than 0.1 (in the time window between 11 and 21 ms) and remained less than 0.3 for at least 45 ms [see Fig. 3(b)]. Therefore, considering larger pools of neurons, the reliability of the response is improved and extended to larger time windows.

Fig. 3(d) illustrates images obtained from three single trials when the uppermost row of electrodes was stimulated with the same voltage pulse of 0.6 V. While at early times, during the so called "reliability window," the spread of the evoked activity in different trials was rather similar, at later times, the spread differed from trial to trial consistently with the high $\mathrm{CV(t)}$ of the electrical recordings [see Fig. 3(a)]. Neuronal cultures obtained from different rats and cultivated in different dishes had a variable number of active electrodes, i.e., providing good electrical recordings, ranging from 30 to 58. All neuronal cultures, with a sufficient number of electrically active electrodes to allow a quantitative characterization of the filtering of the neuronal network, i.e., larger than 40, had the same behavior illustrated in Fig. 2(a). A very similar decay and spread of electrical excitation was consistently observed in all the analyzed neuronal cultures. At early times the spread of electrical excitation was characterized by a Gaussian function with a standard deviation increasing from 800 to 1200 $\mu\mathrm{m}$ in about 3 ms. At later times the behavior of different neuronal cultures [Fig. 2(a)] was more variable than the response of an individual culture [see Fig. 3(a)]. These data show that immediately after the voltage stimulation there is a "good" time window during which the processing of the neuronal culture is reproducible leading to a reliable computation. This reproducibility is observed among trials from the same neuronal culture [see Fig. 3] and in different cultures [see Fig. 2(a)]. Since neuronal cultures could be maintained up to six months, it was possible to repeat several times the same experiment in the same culture and to verify that the spread of electrical excitation in the same culture had identical properties

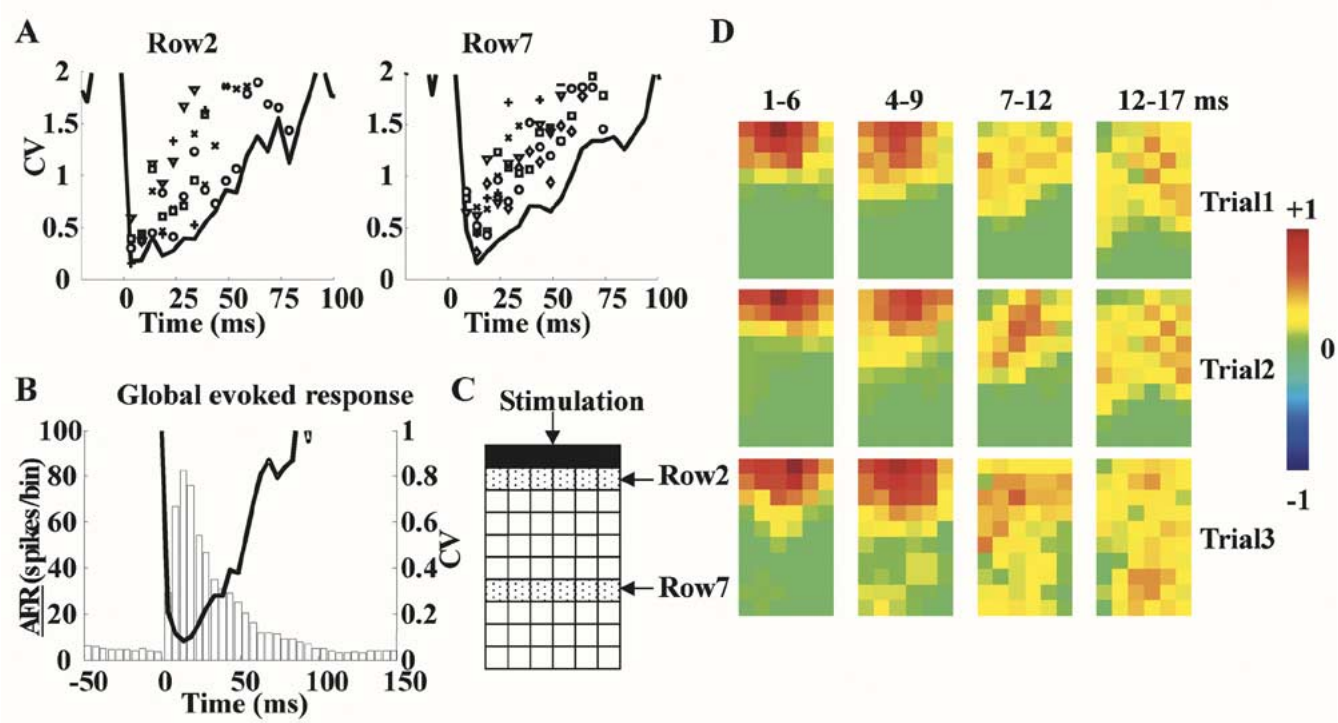

Fig. 3. Reproducibility of the neuronal firing and reproducibility of the spread of the excitation. Data obtained stimulating the uppermost row of electrodes (shown as black squares in panel C). (A) $\mathrm{CV(t)}$ of the evoked response considering the spikes recorded from each single electrode (open symbols) and from the row of electrodes (thick line), in the second (left panel) and the seventh (right panel) rows of the array. (B) $\underline{\mathrm{AFR}}(\mathrm{t})$ and $\mathrm{CV(t)}$ of the spikes recorded from the entire array of active recording electrodes (excluding the 1st row used for stimulation). (C) Map of the MEA electrodes analyzed in (A) and (B). (D) Spread of the excitation in different trials of stimulation. Each row reproduces images obtained from a single sweep or trial, in the four time windows after stimulation indicated at the top of each column. The $\mathrm{FR_{ij}(t)}$ in each image is represented according to the color map reproduced at the right side of the figure.

when analyzed in different days (in a time window of approximately two weeks).

E. Learning

Having characterized the filtering properties of the neuronal cultures, we investigated whether it was possible to induce learning in the neuronal culture [20]–[23] in a consistent and controlled way. If so, is it possible to train the neuronal culture to recognize a specific spatial pattern?

Learning in neurons is associated with changes in synaptic efficacy, leading to a persistent increase in amplitude of the response to the "learnt" stimulus. This is usually referred to long-term potentiation (LTP) and can be induced by delivering a tetanus (usually trains of stimuli at 100 Hz or more) to the neuronal culture. We refer to a $\lfloor$-stimulus ($\lceil$-stimulus) when the stimulation was applied to two perpendicular bars of electrodes forming an $\lfloor(\lceil)$ and to a $\lfloor$-tetanus when the tetanus had the same spatial profile of the $\lfloor$-stimulus.

To test the ability of hippocampal cultures to learn, the electrical response to a $\lfloor$-stimulus before and after the application of a $\lfloor$-tetanus was compared. The $\lfloor$-stimulus was delivered to the neuronal culture every 2 s. The evoked electrical activity was monitored by computing $\mathrm{IntAFR_{ij}}$ (see Section II). After the $\lfloor$-tetanus, the $\mathrm{IntAFR_{ij}}$ [Fig. 4(a)] and the electrical activity in individual traces [Fig. 4(b)] evoked by the $\lfloor$-stimulus were significantly increased for at least 1 hour.

The firing rate averaged over different trials and over all MEA electrodes, $\underline{\mathrm{AFR}}(t)$, is a global indicator of the changes induced by LTP. The $\underline{\mathrm{AFR}}(t)$ evoked by the $\lfloor$-stimulus clearly increased after $\lfloor$-tetanus in the time window between 10 and 90 ms after the stimulation. Fig. 4(c) shows the averaged data from 4 neuronal cultures before (left panel) and after (right panel) $\lfloor$-tetanus.

As LTP can be induced in the neuronal cultures, it is necessary to establish its spatial structure. Therefore, the electrical activity evoked by stimuli with different spatial profiles was compared. Neuronal cultures were stimulated every 2 s with $\lfloor$-stimulus and $\rceil$-stimulus. Prior to $\lfloor$-tetanus, the $\lfloor$-stimulus and the $\rceil$-stimulus evoked a similarly diffused response [see $\mathrm{AFR_{ij}(t)}$ in left and right panel of Fig. 5(a)]. This was also evident when the firing rate was averaged over different trials and over all recording electrodes ($\underline{\mathrm{AFR}}(\mathrm{t})$) [see left and right panels in Fig. 5(c)]. After the $\lfloor$- tetanus, only the response to the $\lfloor$-stimulus significantly increased [Fig. 5(b)] being more than twice the response evoked by the $\rceil$- stimulus [compare left and right panels in Fig. 5(d)].

In Figs. 4 and 5, learning and pattern discrimination was examined by averaging responses over different trials. A useful device, however, must be able to discriminate between patterns on the basis of a single trial, and its learning capabilities should be evident by inspection of a single trial. The single response was evaluated computing $\underline{\mathrm{IntFR}}$ (see Section II). Fig. 6(a) shows single-trial responses for a $\rceil$-stimulus (open symbols) and a $\lfloor$-stimulus (filled symbols). Prior the application of the $\lfloor$-tetanus, single-trial responses to the two stimuli could not be distinguished reliably. After $\lfloor$-tetanus the single-trial response to the $\lfloor$-stimulus was consistently larger than the single-trial response evoked by the $\rceil$-stimulus.

Fig. 6(b) reproduces the distribution of single-trial responses for the $\rceil$-stimulus (white bars) and the $\lfloor$- stimulus (black

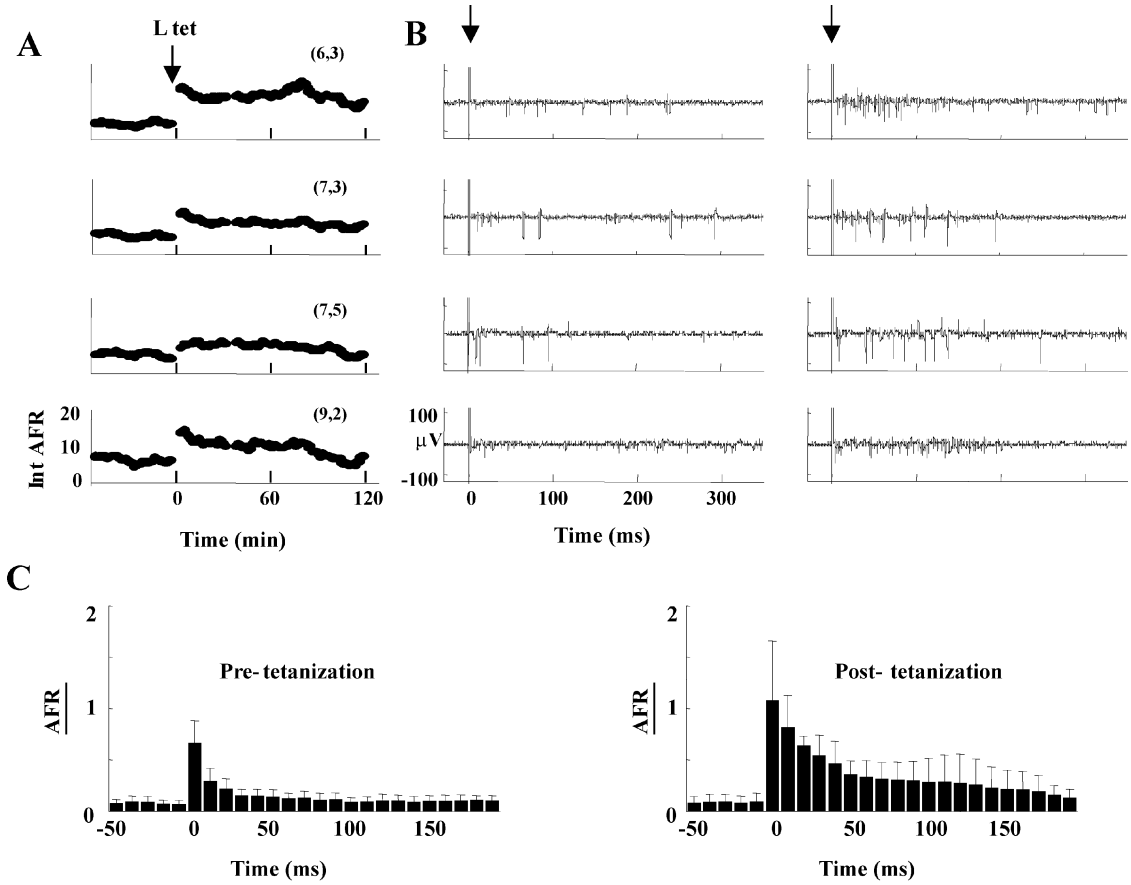

Fig. 4. Induction of LTP in a neuronal culture from hippocampal neurons. (A) Time-dependence of $\mathrm{Int}\,\mathrm{AFR}_{ij}$ prior to and after ⌊-tetanus for the electrodes (6,3), (7,3), (7,5), and (9,2), with tetanus indicated by an arrow. Each point was obtained by averaging 20 responses to the same stimulation repeated every 2 s. ⌊-tetanus was performed as described in Section II. (B) Single extracellular voltage response obtained before (left) and after tetanization (right) from the electrodes shown in A. Time zero, indicated by the arrow, corresponds to the delivery of the stimulation. The large transient at time zero is the residual artifact after its subtraction (see Section II). (C) $\underline{\mathrm{AFR}}(\mathrm{t})$ and standard deviation of an ⌊- stimulus calculated averaging 4 different experiments before and after the ⌊-tetanus. $\underline{\mathrm{AFR}}(\mathrm{t})$ was obtained averaging single sweeps measured in a time window of 30 min.

bars) before (left panel) and after (right panel) ⌊-tetanus. The experimental distributions were fitted with Gaussian functions of unitary area and the superimposed area of the two curves was calculated. Before ⌊-tetanus the average value of the single-trial responses for the ⌉– and the ⌊- stimulus was $4.7 + / - 0.8$ and $5.6 + / - 0.8$ respectively. In 58% of cases the presented stimulus could not be recognized on the basis of the single-trial response (superimposed area). After tetanus the average value of single-trial responses for the ⌉ and ⌊-stimuli was $4.1 + / - 0.5$ and $6.4 + / - 0.7$ respectively. Now, the superimposed area of the two Gaussian functions fitting the experimental distributions was reduced to 5.5%. As a consequence, after tetanus, it was possible to recognize the presented stimulus from its single-trial response with an accuracy of about 94.5%.

Results of similar experiments from 4 neuronal cultures are presented in Fig. 6(c). The distribution of single-trial responses ($\mathrm{Int}\underline{\mathrm{FR}}$) before (left panels) and after (right panels) ⌊-tetanus for the ⌊ and ⌉-stimulus are shown as black and white bars respectively. Before ⌊-tetanus, the distributions of the $\mathrm{Int}\underline{\mathrm{FR}}$ for the 2 patterns were almost completely overlapping. After ⌊-tetanus in all 4 neuronal cultures, single-trial responses were modified so that it was possible to discriminate the stimulating pattern from the great majority of single-trial responses. In fact, after tetanus, single-trial responses for the two stimuli were distinguishable for 80%, 98%, 78% and 95% in the 4 neuronal cultures. In general, when the tetanus was applied to two perpendicular bars of electrodes meeting in a corner, the response to the stimulation applied to the same bars of electrodes increased, while the response to the stimulation applied to distinct perpendicular bars of electrodes meeting in the opposite corner was never potentiated.

If the neuronal culture can be trained to discriminate between a ⌊-stimulus and a ⌉–stimulus it is important to analyze the selectivity of this recognition and verify whether it degrades "gracefully" with the corruption of the stimulus. Therefore, the evoked responses to stimuli with different spatial profiles prior to and after ⌊-tetanus were compared.

Prior to ⌊-tetanus, the response of the neuronal culture was not specific to the spatial profile of the stimulus [Fig. 7(a) open circles]. On the contrary, after ⌊-tetanus, the neuronal culture preferentially responded to stimuli resembling to an ⌊ [Fig. 7(a) filled circles]: in fact, after ⌊-tetanus, the $\mathrm{Int}\underline{\mathrm{AFR}}$ was significantly larger for stimuli with a spatial profile similar to ⌊ (for the five stimuli from the left of the x-axis, t-test $\mathrm{p} < 0.001$). The relative change of the $\mathrm{Int}\underline{\mathrm{AFR}}$ after ⌊-tetanus was clearly

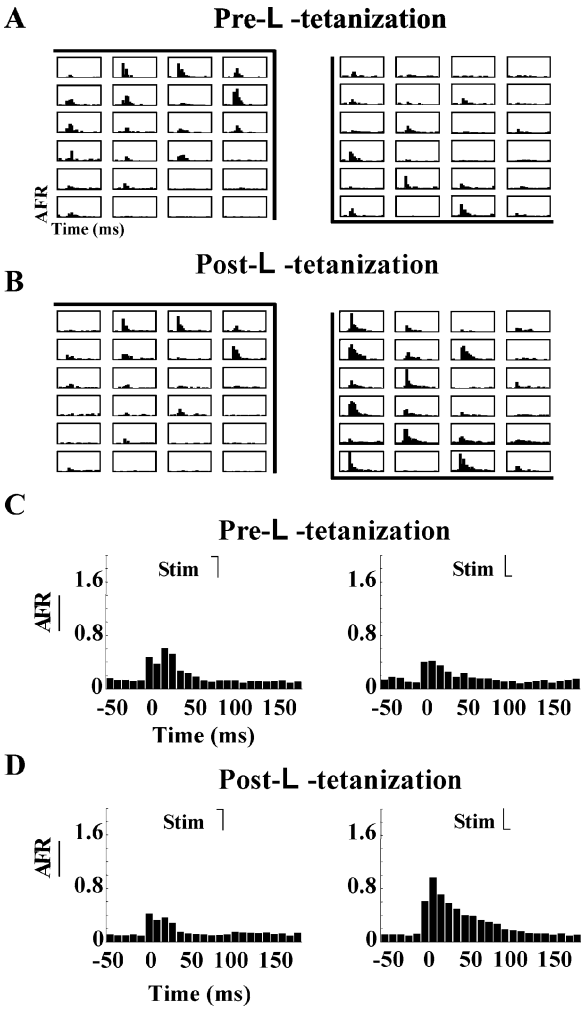

Fig. 5. Neuronal cultures can learn to distinguish between two different spatial profiles. (A) $\mathrm{AFR_{ij}(t)}$ evoked by the ⌉-stimulus (left) and the ⌊-stimulus (right) recorded from 24 electrodes (Y-axis limits: 0 to 10 spikes/bin; X-axis limits: -50 to 200 ms). During the experiment the ⌊-stimulus and a ⌉-stimulus were alternated every 2 s. $\mathrm{AFR_{ij}(t)}$ in (A) were obtained averaging the individual responses recorded in a time window of 30 min before tetanus. (B) As in (A) but in the time window of 30 min after the ⌊-tetanus. (C) $\underline{\mathrm{AFR}}(t)$ obtained by averaging the $\mathrm{AFR_{ij}(t)}$ over all the active recording electrodes. The 2 $\underline{\mathrm{AFR}}(t)$ shown refer to the responses to the ⌉-stimulus (left) and the ⌊-stimulus (right) before ⌊-tetanus. (D) $\underline{\mathrm{AFR}}(t)$ obtained by averaging the $\mathrm{AFR_{ij}(t)}$ over all the active recording electrodes. The 2 $\underline{\mathrm{AFR}}(t)$ shown refer to the responses to the ⌉-stimulus (left) and the ⌊-stimulus (right) after ⌊- tetanus.

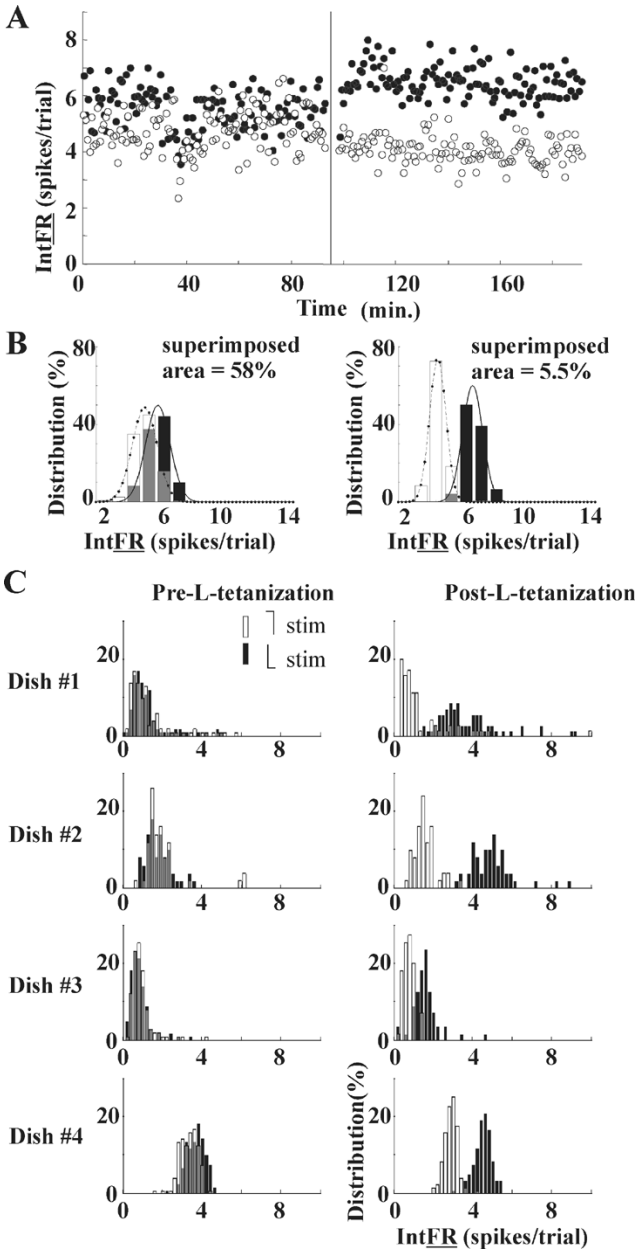

Fig. 6. Discrimination at single-trial level before and after ⌊-tetanus for a neuronal culture. ⌊-stimulus and ⌉-stimulus have been analyzed. (A) Time-evolution of the $\underline{\mathrm{IntFR}}$ evoked by a ⌉-stimulus (open symbols) and an ⌊- stimulus (black symbols) prior and after a ⌊- tetanus (indicated by a black vertical line). (B) Distribution of the $\underline{\mathrm{IntFR}}$ before (left panel) and after (right panel) L-tetanus for the ⌊-stimulus (black bars) and the ⌉-stimulus (white bars). (C) Distribution of the $\underline{\mathrm{IntFR}}$ before (left panel) and after (right panel) L-tetanus for the ⌊-stimulus (black bars) and the ⌉-stimulus (white bars) for 4 different neuronal cultures. In the left panels the distributions of $\underline{\mathrm{IntFR}}$ for the 2 stimuli are almost entirely overlapping. In the right panels, as consequence of LTP induction, the overlap of the distributions for the ⌊-stimulus and ⌉-stimulus is enormously decreased.

selective [Fig. 7(b)] and showed positive value for similar spatial profiles.

F. Image Processing of 8-Bit Images and Feature Extraction

The neuronal culture can be used also for processing digital images at 8 bits. Let O_{ij} be an image with 8 bit gray levels at location (i,j). Then O_{ij} can be represented by the decomposition

$$O_{\mathrm{ij}} = \sum_{p=1}^{8} I_{\mathrm{ij}}^{(p)} 2^{(p-1)} \tag{3}$$

where $I_{\mathrm{ij}}^{(p)}$ is a 1-bit image.

Given this decomposition, according to (2), the processing of an 8-bit image is obtained as

$$\sum_{p=1}^{8} \alpha^{(p)} 2^{(p-1)} I_{\mathrm{ij}}^{(p)} **h(\rho,t) \tag{4}$$

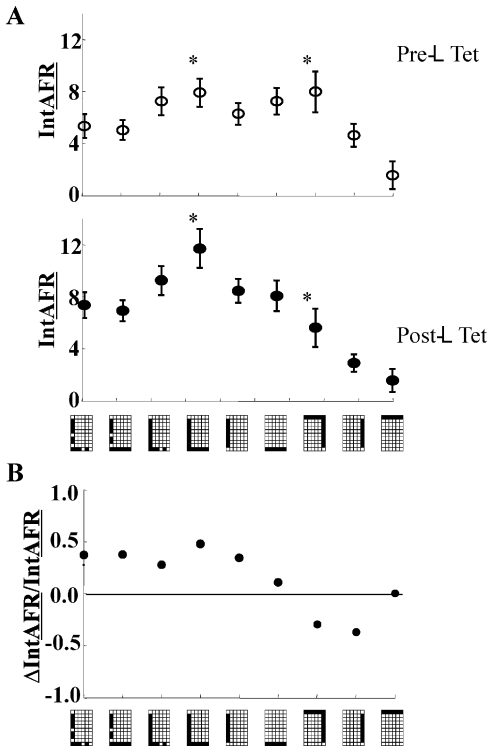

Fig. 7. Spatial selectivity of LTP. (A) $\mathrm{Int}AFR$ before (open symbols) and after (filled symbols) ⌊-tetanus for stimuli shown with the shape indicated in the abscissa. $\mathrm{Int}AFR$ before and after tetanus was obtained as an average during 30 min before and after tetanus respectively. The voltage intensity of the stimulation was 0.6 V. Stars indicate the response to the ⌊-stimulus and ⌉-stimulus. (B) Relative change of the $\mathrm{Int}AFR$ produced by the ⌊-tetanus. Data obtained from those shown in A before and after ⌊-tetanus.

where $\alpha^{(p)}$ is a scaling factor (see Section II). By processing independently the 8 1-bit images with the neuronal culture, a low or a bandpass filtering of an 8-bit image is obtained. A low-pass filtering of the original 8 bit images [Fig. 8(a) left panels], obtained by the neuronal culture in the time bin 1–6 ms and by a digital filtering with a Gaussian function, are shown in the central and right panels respectively of Fig. 8(a). The high similarity of images in the central and right panel shows that the proposed hybrid device can process efficiently 8 bit images. After a neuronal culture has learned, its temporal-spatial filtering is different. First of all, it is not anymore spatially invariant and, therefore, cannot be described by a temporal and spatial convolution as in (4). In fact, the firing rate $\mathrm{FR}_{\mathrm{ij}}(\mathrm{t})$ evoked by a given image I_{ij} cannot be predicted from (1) and (2) but must be measured. The processing of an 8-bit image is, therefore, obtained as

$$\sum_{p=1}^{8} \alpha^{(p)} 2^{(p-1)} FR_{\mathrm{ij}}^{(p)}(t) \tag{5}$$

where $FR_{\mathrm{ij}}^{(p)}(t)$ is the measured response to $I_{\mathrm{ij}}^{(p)}$ after tetanization and $\alpha^{(p)}$ is a scaling factor (see Section II). Having lost spatial invariance, the device is now able to extract a specific pattern from a complex image. When the neuronal culture has learned to recognize an ⌊ [see Fig. 8(b)], the processing of original images [Fig. 8(b) left column] is modified [see central column of Fig. 8(b)] and becomes tuned and selective to ⌊-stimulus [right column of Fig. 8(b)]. It is evident that after learning, the neuronal culture is able to extract the ⌊ from the rest of the image, in both processed images. The upper image shows clearly that, before learning, the neuronal filtering is symmetric and becomes asymmetric after learning, allowing, in this way, the extraction of the learned feature.

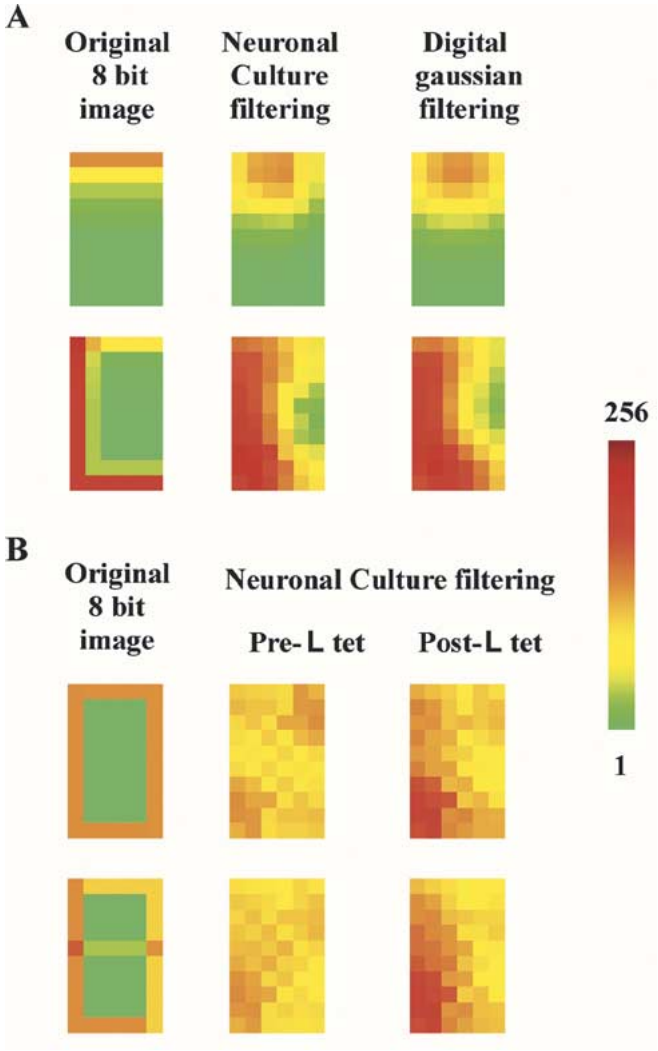

Fig. 8. Image processing of 8-bit images. (A) Low-pass filtering of two different 8-bit images. (Left panels) The original 8 bit images. (Central panels) Low-pass filtering of the images obtained with the neuronal culture. (Right panels) Low-pass filtering of the images, obtained by digital convolution of the original 8-bit image, with the Gaussian profile shown in 2A in the time window between 1 and 6 ms. Color-coding is reproduced at the right side of the figure. (B) Features extraction obtained by low-pass filtering of two different 8-bit images before and after learning. (Left columns) The original 8 bit images. (Central columns) Low-pass filtering of the images obtained with the neuronal culture before the tetanization. (Right columns) Low-pass filtering of the images obtained with the neuronal culture after ⌊-tetanus. Color-coding is reproduced at the right side of the figure. Original 8-bit images are obtained according to (3). For 1-bit processed images, the values of the $\mathrm{AFR}_{\mathrm{ij}}(\mathrm{t})$ were scaled between 0 and 1 by dividing for the corresponding maximal value among all electrodes in the time-window of 1–30 ms. 8-bit processed images are then obtained by (4). For features extraction, the values of $\mathrm{AFR}_{\mathrm{ij}}(\mathrm{t})$ obtained after the tetanization were scaled by dividing for the same maximal value calculated before the tetanization. 8-bit processed images are then obtained by (5) (see Section II).

G. Consistency of Potentiation and Learning

Neural plasticity is certainly a major advantage for Neurocomputers if LTP or LTD can be evoked in a neuronal culture

consistently and in a repeated way. As shown by Jimbo *et al.* [23] when a tetanizing train of pulses is applied through a single electrode of a MEA both LTP and LTD can be observed. The induction of LTP occurred when neurons before tetanus fired in a correlated way; while LTD occurred when the firing of neurons were poorly correlated. Therefore, when a single electrode was used the induction of LTP or LTD could not be controlled but depended from the intrinsic connectivity of the network. This situation is not satisfactory if neuronal cultures have to be used for information processing and learning. Therefore, we looked for experimental conditions in which LTP could be induced consistently. LTP described in previous sections was always evoked when the same tetanizing pulse was applied to many electrodes, more than 10, with a spatial profile of two perpendicular bars. With this pattern of stimulation, LTP was successfully induced in 10 (over 12 tested) neuronal cultures. LTP could be evoked in the same neuronal culture on different days over a period of 6 weeks. When the tetanus was applied through a smaller number of electrodes, i.e., less than 7, LTP was not consistently induced and both LTP and LTD was observed. When a bar-tetanus was delivered, LTP was never induced in 6 experiments. In 3 experiments performed with young (less than 20 days) neuronal cultures, stimulation applied to a bar of electrodes, either horizontal or vertical, produced an electrical excitation confined around the electrodes used for stimulation, and LTP could not be induced by an $\lfloor$- tetanus. In one dish the two tetanization protocols were combined: a bar-tetanus was first applied and, after 2 hours, an $\lfloor$- tetanus was applied. The response to the $\lfloor$- stimulus after the bar-tetanus was unchanged, while the $\lfloor$- tetanus clearly induced LTP. LTP could be evoked in the same neuronal culture, on different days over a period of 6 weeks. When 50 micromolar DL-2-amino-5-phosphonovaleric acid (APV), a well known blocker of NMDA channels, was added to the extracellular medium bathing the neuronal culture, the evoked electrical activity did not spread significantly from the electrodes used for stimulation, as in cortical neuronal cultures [24]. Under these conditions LTP could not be induced in the neuronal cultures.

IV. Discussion

The work described here demonstrates that, by growing neuronal cultures over multi electrode arrays (MEA), a new hybrid-computing device, composed of biological neurons and metal electrodes, can be foreseen. The biophysical mechanisms underlying the low-pass and band-pass filtering of digital images, here described, originate from membrane properties of cultivated neurons and their mode of interaction. Synaptic properties limit and shape the propagation of action potentials in the culture. The combination of these biophysical mechanisms determines the exact parameters of the filtering. The consistency of the experimental set up was discussed in the two sections on the reproducibility of neuronal filtering and consistency of potentiation and learning. The major difference with previous work on neuronal culture grown on MEA [23]–[25] is the controlled induction of LTP and its use for pattern recognition. The presented results, show, in our opinion, that neuronal cultures grown on MEA can constitute the basis for the development of Neurocomputers, possibly new computing devices.

A. Comparison With Previous Work

The present work is a continuation of previous analysis of the behavior of neuronal cultures grown on MEAs [23]–[25] and confirms several previous observations on how the evoked electrical activity spreads throughout the neuronal culture. Jimbo *et al.* [23] have shown that when a tetanizing train of pulses is applied through a single electrode of a MEA, both LTP and LTD can be observed and that the induction of LTP or LTP depended from the intrinsic connectivity of the network. The present work shows that, when many electrodes are used for tetanizing, LTP is preferentially induced and, therefore, the induction of LTP can be controlled. The controlled induction of LTP allows the use of neuronal cultures for pattern recognition (see Figs. 5 and 6) and opens the way for using neuronal cultures as new computing devices, i.e., Neurocomputers. Although the molecular mechanisms controlling the induction of LTP and/or LTD have not yet been fully revealed [26], it is well established that a moderate elevation of intracellular Ca^{2+} favors the induction of LTD, while a larger increase is more likely to induce LTP. As neuronal firing leads to an elevation of intracellular Ca^{2+}, it is not surprising that a massive electrical excitation preferably induces LTP instead of LTD. As stated in the Results section, LTP was induced in 10 over 12 tested neuronal cultures. However, in all neuronal cultures, after an $\lfloor$-tetanus, the discriminability between an $\lfloor$ and $\rceil$-stimulus increased. Therefore, in all tested cultures learning was observed, provided that the tetanus was applied through a sufficiently large number of electrodes. LTP was not observed when the frequency of tetanization was lower than 100 Hz.

B. Reproducibility and Reliability of Neuronal Firing

The reliability of the evoked response increases by pooling the electrical activity recorded from a larger number of neurons, as shown by the decrease of the $\mathrm{CV(t)}$ calculated for a single electrode, a row of electrodes or the 60 electrodes of the MEA. These conclusions, drawn from an investigation in a dissociated culture of hippocampal neurons, are remarkably similar to those obtained in an isolated leech ganglion (5) and in a semi-intact leech [27]. In the leech nervous system, motoneurons coactivated during the same behavioral reaction, fire spikes in an almost statistically independent way. As a consequence of statistical independence pooling, the electrical activity over all co-activated motoneurons makes highly variable spike trains underlying reproducible motor reactions.

These results suggest that, analogously to nervous systems, reliability and reproducibility of neurocomputers can be obtained by pooling the neuronal electrical activity over populations of neurons, as already shown by several previous investigations with intelligent prostheses [28]–[31]. The extent of pooling depends on the task to be solved: in fact, when it is necessary to discriminate between patterns, it is convenient to average the neuronal activity over a very large number of neurons (of the order of 100) in order to obtain a successful discrimination over a single trial, as shown in Fig. 6. When the MEA is used to filter images, averaging is restricted to neurons recorded from the same electrode, i.e., less than 6 or so different neurons. In this case the resulting computation is noisier. In a population of N neurons firing spikes in an almost unrelated way, the CV decreases as the square root of N [32]. Therefore, if each neuron

has a CV between 0.5 and 1 [27], a good reproducibility – with a CV of less than 0.1 – can be obtained by pooling the electrical activity of 100–1000 neurons, i.e., the same order of magnitude of neurons thought to be present in a column in the cortex [33]. This requirement may pose severe constraints on the construction of MEA and on the development of future Neurocomputers.

C. Limitations of the Tested Device

The tested device, based on the MEA supplied by MultiChannelSystem, has several limitations, which may be overcome by future technological improvements. First of all, in the present release it is not possible to stimulate and record simultaneously from the same electrode, contrary to the MEA developed by Jimbo and coworkers [25]. As a consequence, the electrical activity evoked in the stimulated electrode cannot be measured but has to be interpolated (see Section II) from the neighboring recording electrodes. In addition, switching between recording and stimulation cannot be obtained via software and has to be performed manually, reducing the possible experimentation and the analysis of parallel processing with the neuronal culture. Recently new circuits for distributing stimuli to all electrodes electronically (from Multichannel Systems, MEA1060-BC) and for stimulating and recording on the same electrode [34] have been developed. These circuits will allow to overcome the limitations discussed above. The implementation of on-line analysis [21], [35] allows the exploration of alternative parallel processing and learning with the neuronal culture.

Another disadvantage of the present device, possibly shared by a large variety of Neurocomputers, is the presence of silent electrodes or of electrodes making good electrical contacts with a limited number of neurons. The ideal device is composed of electrodes all making good electrical contact with a large number of healthy neurons. Since it is necessary to measure individual spikes and not field potentials, the number of neurons in good electrical contact with each electrode cannot be too high. Therefore, it is necessary to develop standard protocols in order to have MEA with almost all electrodes making good electrical contact with approximately the same number of neurons.

The training procedure, by which a neurocomputer learns to recognize a spatial feature, is simply an appropriate tetanus, i.e., a relatively simple procedure, representing, therefore, an obvious advantage of the Neurocomputer. On the other side the Neurocomputer – at least in its present form – seems to be primarily a coprocessor, which cannot be easily programmed for a different tasks, as usual digital processor can. After the decline of LTP, the neurocomputer can be trained to learn a new pattern and, therefore, can be reprogrammed and becomes reusable. Several issues, however, must be addressed such as the duration of induced LTP, the possibility of encoding new inputs and to erase stored information – possibly by inducing LTD. Once these issues will be properly addressed, the exploitation of LTP, as here demonstrated, and of LTD [18], [36], may provide a natural implementation of algorithms based on artificial neural networks (ANN).

D. Future of Neurocomputers

The use of biological neurons as computing devices opens a new avenue in which computer science can capitalize on the expertise and technology of cell biology and genetic engineering. Taking advantage of stem cell technology [37]–[39] we are trying to obtain a standard source of neurons in order to eliminate the variability intrinsic to individual rats, possibly leading to computing devices with a much higher reproducibility. Stem cell technology could provide also populations of neurons with specific properties, for example neurons that release selected neurotransmitters. In this way neuronal cultures with controlled ratios of inhibitory and excitatory neurons could be constructed. The possibility of guiding neuronal growth along specific spatial directions [40]–[43] will allow the fabrication of large variety of spatial filters, imitating the receptive field properties of neurons in early visual area [44]. Neurocomputers can become promising new computing devices if their reliability can be increased. In order to do so, besides using stem cell technology for obtaining a standardized source of neurons, it will be necessary to automate with appropriate robots all the subsequent procedures necessary for preparing and maintaining neuronal cultures. It will be very important to standardize the handling of MEAs, neuron deposition on the MEAs and their maintenance.

ACKNOWLEDGMENT

The authors would like to thank Dr. E. Cherubini and Dr. G. Musso for helpful comments and D. Dean for carefully reading the manuscript.

REFERENCES

[1] D. Marr, *Vision: A Computational Investigation into the Human Representation and Processing of Visual Information*. San Francisco, CA: Freeman, 1982.

[2] D. E. Rumelhart and J. L. McClelland, *Explorations in Parallel Distributed Processing*. Cambridge, MA: MIT Press, 1988.

[3] J. G. Nicholls, B. G. Wallace, A. R. Martin, and P. A. Fuchs, *From Neuron to Brain: A Cellular and Molecular Approach to the Function of the Nervous System*, 4th ed. Sunderland, MA: Sinauer, 2000.

[4] M. N. Shadlen and W. T. Newsome, "Noise, neural codes and cortical organization," *Curr. Opin. Neurobiol.*, vol. 4, pp. 569–579, 1994.

[5] D. Zoccolan, G. Pinato, and V. Torre, "Highly variable spike trains underlie reproducible sensory-motor responses in the medicinal leech," *J. Neurosci.*, vol. 22, pp. 10 790–10 800, 2002.

[6] J. Hertz, A. Krogh, and R. G. Palmer, "Introduction to the theory of neural computation," in *Studies in the Sciences of Complexity*. Santa Fe, NM: Santa Fe Institute, 1991, vol. 1.

[7] J. J. Hopfield, "Neural networks and physical systems with emergent collective computational ability," *Proc. Nat. Acad. Sci.*, vol. 79, pp. 2554–2558, 1982.

[8] M. Minsky and S. Papert, *Perceptrons: An Introduction to Computational Geometry*. Cambridge, MA: MIT Press, 1988.

[9] G. W. Gross, E. Rieske, G. W. Kreutzberg, and A. Meyer, "A new fixed-array multimicroelectrode system designed for long-term monitoring of extracellular single unit neuronal activity *in vitro*," *Neurosci. Lett.*, vol. 6, pp. 101–105, 1977.

[10] J. Pine, "Recording action potentials from cultured neurons with extracellular microcircuit electrodes," *J. Neurosci. Meth.*, vol. 2, pp. 19–31, 1980.

[11] J. L. Novak and B. C. Wheeler, "Recording from the aplysia abdominal ganglion with a planar microelectrode array," *IEEE Trans, Biomed. Eng.*, vol. BME-33, pp. 196–202, 1986.

[12] Y. Jimbo and A. Kawana, "Electrical stimulation and recording from cultured neurons using a planar electrode array," *Bioelectrochem. Bioenergetics*, vol. 29, pp. 193–204, 1992.

[13] S. Martinoia, M. Bove, G. Carlini, C. Ciccarelli, M. Grattarola, C. Storment, and G. Kovacs, "A general purpose system for long-term recording from a microelectrode array coupled to excitable cells," *J. Neurosci. Meth.*, vol. 48, pp. 115–121, 1993.

[14] S. Vassanelli and P. Fromherz, "Neurons from rat brain coupled to transistors," *Appl. Phys. A*, vol. 65, pp. 85–88, 1997.

[15] G. Zeck and P. Fromherz, "Noninvasive neuroelectronic interfacing with synaptically connected snail neurons immobilized on a semiconductor chip," *Proc. Nat. Acad. Sci.*, vol. 98, pp. 10 457–10 462, 2001.
[16] P. Bonifazi and P. Fromherz, "Silicon chip for electronic communication between nerve cells by noninvasive interfacing and analog-digital processing," *Advanced Mater.*, vol. 14, pp. 1190–1193, 2002.
[17] T. V. P. Bliss and G. L. Collingridge, "A synaptic model of memory: Long-term potentiation in the hippocampus," *Nature*, vol. 361, pp. 31–39, 1993.
[18] O. Paulsen and T. J. Sejnowski, "Natural patterns of activity and long-term synaptic plasticity," *Curr. Opin. Neurobiol.*, vol. 10, pp. 172–179, 2000.
[19] S. M. Potter and T. B. DeMarse, "A new approach to neural cell culture for long-term studies," *J. Neurosci. Meth..*, vol. 110, pp. 17–24, 2001.
[20] S. Marom and G. Shahaf, "Development, learning and memory in large random networks of cortical neurons: Lessons beyond anatomy," *Quart. Rev. Biophys.*, vol. 35, pp. 63–87, 2002.
[21] G. Shahaf and S. Marom, "Learning in networks of cortical neurons," *J. Neurosci.*, vol. 21, pp. 8782–8788, 2001.
[22] W. L. Rutten, "Selective electrical interfaces with the nervous system," *Annu. Rev. Biomed. Eng.*, vol. 4, pp. 407–452, 2002.
[23] Y. Jimbo, T. Tateno, and H. Robinson, "Simultaneous induction of pathway-specific potentiation and depression in networks of cortical neurons," *Biophys. J.*, vol. 76, pp. 670–678, 1999.
[24] Y. Jimbo, A. Kawana, P. Parodi, and V. Torre, "The dynamics of a neuronal culture of dissociated cortical neurons of neonatal rats," *Biol. Cybern.*, vol. 83, pp. 1–20, 2000.
[25] Y. Jimbo, N. Kasai, K. Torimitsu, T. Tateno, and H. P. C. Robinson, "A system for MEA-based multisite stimulation. Biomedical engineering," *IEEE Trans. Biomed. Eng.*, vol. 50, no. 2, pp. 241–248, Feb 2003.
[26] M. Sheng and M. J. Kim, "Postsynaptic signaling and plasticity mechanisms," *Science*, vol. 298, no. 5594, pp. 776–80, 2002.
[27] I. Arisi, D. Zoccolan, and V. Torre, "Distributed motor pattern underlying whole-body shortening in the medicinal leech," *J. Neurophysiol.*, vol. 86, pp. 2475–2488, 2001.
[28] J. Wessberg, C. R. Stambaugh, J. D. Kralik, P. D. Beck, M. Laubach, J. K. Chapin, J. Kim, S. J. Biggs, M. A. Srinivasan, and M. A. Nicolelis, "Real-time prediction of hand trajectory by ensembles of cortical neurons in primates," *Nature*, vol. 408, no. 6810, pp. 361–365, 2000.
[29] M. A. Nicolelis, "Brain-machine interfaces to restore motor function and probe neural circuits," *Nat. Rev. Neurosci.*, vol. 4, no. 5, pp. 417–422, 2003.
[30] A. E. Grumet, J. L. Wyatt Jr., and J. F. Rizzo, III, "Multi-electrode stimulation and recording in the isolated retina," *J. Neurosci. Meth.*, vol. 101, no. 1, pp. 31–42, 2000.
[31] R. A. Normann, E. M. Maynard, P. J. Rousche, and D. J. Warren, "A neural interface for a cortical vision prosthesis," *Vis. Res.*, vol. 39, no. 15, pp. 2577–87, 1999.
[32] A. Papoulis, *Probability, Random Variables and Stochastic Processes*. New York: McGraw-Hill, 1984.
[33] V. B. Mountcastle, "The columnar organization of the neocortex," *Brain*, vol. 120, pp. 701–722, 1997.
[34] D. A. Wagenaar and S. M. Potter, "A versatile all-channel stimulator for electrode arrays, with real-time control," *J. Neural Eng.*, vol. 1, pp. 39–45, 2004.
[35] T. B. DeMarse, D. A. Wagenaar, A. W. Blau, and S. M. Potter, "The neurally controlled animat: Biological brains acting with simulated bodies," *Autonomous Robot.*, vol. 11, pp. 305–310, 2001.
[36] D. J. Linden and J. A. Conner, "Long-term synaptic depression," *Ann. Rev. Neurosci.*, vol. 18, pp. 319–357, 1995.
[37] T. Barberi, P. Klivenyi, N. Y. Calingasan, H. Lee, H. Kawamata, K. Loonam, A. L. Perrier, J. Bruses, M. E. Rubio, N. Topf, V. Tabar, N. L. Harrison, M. F. Beal, M. A. Moore, and L. Studer, "Neural subtype specification of fertilization and nuclear transfer embryonic stem cells and application in parkinsonian mice," *Nat. Biotechnol.*, vol. 21, pp. 1200–1207, 2003.
[38] H. Kawasaki, H. Suemori, K. Mizuseki, K. Watanabe, F. Urano, H. Ichinose, M. Haruta, M. Takahashi, K. Yoshikawa, S. Nishikawa, N. Nakatsuji, and Y. Sasai, "Generation of dopaminergic neurons and pigmented epithelia from primate ES cells by stromal cell-derived inducing activity," *Proc. Nat. Acad. Sci.*, vol. 99, pp. 1580–1585, 2002.
[39] J. J. Westmoreland, C. R. Hancock, and B. G. Condie, "Neuronal development of embryonic stem cells: A model of GABAergic neuron differentiation," *Biochem. Biophys. Res. Commun.*, vol. 284, pp. 674–680, 2001.
[40] J. C. Chang, G. J. Brewer, and B. C. Wheeler, "Modulation of neural network activity by patterning," *Biosensors Bioelectron.*, vol. 16, pp. 527–533, 2001.
[41] F. Nakamura, R. G. Kalb, and S. M. Strittmatter, "Molecular basis of semaphorin-mediated axon guidance," *J. Neurobiol.*, vol. 44, pp. 219–229, 2000.
[42] J. A. Raper, "Semaphorins and their receptors in vertebrates and invertebrates," *Curr. Opin. Neurobiol.*, vol. 10, pp. 88–94, 2000.
[43] M. Tessier-Lavigne and C. S. Goodman, "The molecular biology of axon guidance," *Science*, vol. 274, pp. 1123–1133, 1996.
[44] D. H. Hubel and T. N. Wiesel, "Early exploration of the visual cortex," *Neuron*, vol. 20, pp. 401–412, 1998.

Maria Elisabetta Ruaro received the Laurea degree in biological science from the University of Trieste, Trieste, Italy, in 1984.

In 1987, she worked at the EMBL in Heidelberg in the group of Lennard Philipson, where she learned different cell biology and molecular biology techniques. From 1991 to 1997, she was responsible for the microinjection facility at the ICGEB-UNIDO at the Area Science Park while maintaining scientific collaboration with scientific groups in Italy, U.K., and USA. From 1998 to 2000, she was a Scientific Collaborator at the LNCIB, where she studied two growth arrest specific genes Gas1 and Gas6, and became an expert in cell culture of different cell type and cell biology techniques. Since 2001, she has been a Research Fellow in the group of V. Torre at the International School for Advanced Studies where she participated to the neurocomputer project in particular to the cell culture and electrophysiological aspects. During this period she visited the laboratory of Dr. Studer at the Sloan Kettering Institute in New York where she learned the methodology to differentiate neurons from embryonic stem cells. Since 1996 she has been teaching cell biology, as an external teacher, at the University of Udine (IT) and Trieste (IT).

Paolo Bonifazi was born in Sassoferrato, Italy, in 1975. He received the Laurea degree in physics from the University of Perugia, Perugia, Italy, in May 2001. He is currently working toward the Ph.D. degree in neurobiology at the International School for Advanced Studies (ISAS/SISSA), Trieste, Italy. From January 2000 to July 2001, he was a trainee and a postgraduate student at the department of "Membrane and Neurophysics" of the Max-Planck-Institute for Biochemistry in Munich, under the supervision of Prof. P. Fromherz.

His research interests include electrophysiology, neuroengineering, computational neuroscience.

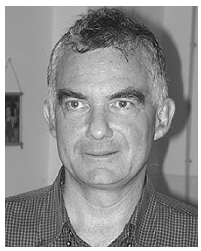

Vincent Torre received the degree in theoretical physics from Genoa University, Genoa, Italy, in 1973.

In the early 1980s, along with T. Poggio and C. Koch, he pioneered in the area of computational neuroscience. For several years he was a Post Doc and Visiting Scientist in Sir Alan Hodgkin Lab, Cambridge, U.K., where he learned a variety of electrophysiological methods and became expert in modeling biological process. In the late 1980s and early 1990s he worked on computer vision and in particular, edge detection and motion perception. Since 1997 he has been a Full Professor at International School of Advanced Studies, Trieste, Italy and is the Head of the Department of Neurobiology. He has a well-established expertise in electrophysiology, computer vision, computational neuroscience and modeling biological process. He is the author of more than 100 full papers.

-Paper 2-

Statistical properties of information processing in neuronal networks

European Journal of Neuroscience, in press

Paolo Bonifazi[1], Maria Elisabetta Ruaro[1] and Vincent Torre

[1] Paolo Bonifazi and Maria Elisabetta Ruaro equally contributed to this work

Abstract

Information processing and coding were analyzed in dissociated hippocampal cultures, grown on multielectrode arrays. Multi-site stimulation was used to activate different neurons and pathways of the network. The neural activity was binned into firing rates and the variability of the firing of individual neurons and of the whole population was analyzed. In individual neurons, the timing of the first action potential (AP) was rather precise from trial to trial whereas the timing of later APs was much more variable. Pooling APs in an ensemble of neurons reduced the variability of the response and it allowed to distinguish reliably in a single trial stimuli varying in intensity. A similar decrease of variability was observed pooling the first evoked APs in an ensemble of neurons. The size of the neuronal pool (about 50-100 neurons) and the time bin (about 20 ms) necessary to provide reproducible responses are remarkably similar to those obtained in *in vivo* preparations and in small nervous systems. Blockage of excitatory synaptic pathways mediated by NMDA receptors improved the mutual information between the evoked response and stimulus properties. When inhibitory GABAergic pathways were blocked by bicuculline the opposite effect was obtained. These results show how ensemble averages and an appropriate balance between inhibition and excitation allow neuronal networks to process information in a fast and reliable way.

Introduction

Understanding the neural code requires the identification of electrical events occurring consistently and reliably from trial to trial. These electrical events could correspond to the exact timing of action potentials (APs) in individual neurons or to the firing rate averaged over a population of neurons. These two neural codes are usually referred to as the temporal and the rate code, respectively (Georgopoulos *et al.*, 1986; Hopfield, 1995; DeCharms & Merzenich, 1996; de Ruyter van Steveninck *et al.*, 1997; Nicolelis *et al.*, 1998; Parker & Newsome, 1998; Panzeri *et al.*, 2001; Zoccolan *et al.* 2002; Johansson & Birznieks, 2004). Whether the computational unit in the nervous system is a single neuron or a neuronal assembly is still an open debate (Cohen & Nicolelis, 2004; Johansson & Birznieks, 2004; Osborne *et al.,* 2004).

The analysis of neuronal networks has been carried out by intracellular recordings from a small number of neurons (Silberberg *et al.*, 2004) or by using multielectrode arrays (MEA) either implanted in the cortex (Nicolelis *et al.*, 1997), or in the hippocampus (Harris *et al.*, 2003) Optical methods have also been used to analyze the dynamics of cortical neurons and to characterize the global states of cortical networks (Jancke *et al.*, 2004) and to visualize plasticity in the hippocampal CA1 area (Aihara *et al.*, 2004). Recording the electrical activity from neuronal networks in vivo provides valuable information on how the brain works, but has a number of limitations. Firstly, given the high convergence of inputs to the cortex it is difficult to control exactly, in every trial performed with the same stimulation, the effective input reaching the neuronal network. Secondly, it is not easy to change in a controlled way the properties of the stimulus applied to the cortical network and its chemical environment. These limitations are overcome by studying neuronal cultures grown over MEAs (Eytan *et al.*, 2003; Gross, 1979; Jimbo *et al.*, 1999; Pine, 1980; Potter, 2001). These cultures with random connections, provide a more general view of neuronal networks and assemblies, not depending on the circuitry of a neuronal network *in vivo,* and allow a more detailed and careful experimental investigation.

In order to investigate statistical properties of information processing in neuronal networks, rat hippocampal neurons were cultured on a MEA. After few weeks in culture the network established synaptic contacts, showed spontaneous activity (Van Pelt *et al.*, 2004; Maeda *et al.*, 1995) and was largely composed of excitatory glutamatergic neurons with few percent of inhibitory GABAergic neurons. Extracellular electrical stimuli were delivered to the network, through the MEA. The neural activity was binned into firing rates over time windows of different length and its statistical properties were analyzed. The variability of firing of individual neurons and of the whole population was first studied. In individual neurons, the timing of the first AP was rather precise whereas the timing of the following APs was much more variable. Pooling evoked APs in an ensemble of neurons reduced the variability of the response across different trials. As a consequence, it was possible to distinguish at the level of a single trial stimuli varying in intensity. A similar decrease of variability was observed counting the first evoked APs in an ensemble of neurons. Blockage of excitatory synaptic pathways mediated by NMDA receptors improved the mutual information between the evoked response and the stimulus. The opposite effect was observed when inhibitory GABAergic pathways were blocked by bicuculline. The estimations of the size of the neuronal pool and time bin necessary to process information in a reliable way are remarkably similar to those obtained in *in vivo* preparations (Shadlen & Newsome, 1998; Nicolelis *et al.*, 1998) and in small nervous systems (Lewis & Kristan, 1998; Zoccolan *et al.*, 2002). These results show how an appropriate ensemble average and a balanced presence of inhibition and excitation allow neuronal networks to process information in a fast and reliable way.

Materials and Methods

Neuronal culture preparation. Hippocampal neurons from Wistar rats (P0-P2) were prepared as described previously (Ruaro et al., 2005). Cells were plated on polyorhitine/matrigel pre-coated MEA (Ruaro et al, 2005) at a concentration of 8 x 10^5 cells/cm^2 and maintained in Minimal Essential Medium with Earle's salts (GIBCO-Brl) supplemented with 5% fetal calf serum, 0.5% D-glucose, 14 mM Hepes, 0.1 mg/ml apo-transferrin, 30 μg/ml insulin, 0.1 μg/ml D-biotin, 1 mM Vit. B12, and 2μg/ml gentamycin. After 48 hours 5 μM cytosine-β-D-arabinofuranoside (Ara-C) was added to the culture medium, in order to block glial cell proliferation. Half of the medium was changed twice a week. Neuronal cultures were kept in an incubator providing a controlled level of CO_2 (5%), temperature (37^{o}C) and moisture (95%).

Immunohistochemistry. Cells were fixed in 4% paraformaldehyde-0.15% picric acid and were stained with the following primary antibodies: mouse monoclonal antibodies against Nestin (Chemicon) GFAP (Sigma-Aldrich), Tubulin (TUJ1) (Covance), Glutamate (Sigma-Aldrich). Rabbit polyclonal antibodies against CaMKII and GABA (Sigma-Aldrich) serotonin (Sigma-Aldrich) and TH (DiaSorin). Appropriate FITC-labeled and TRITC-labeled secondary antibodies and Hoechst33345 nuclei counterstain were used for visualization. Images were acquired under a Zeiss Axioshop2 fluorescent microscope using an Optronics camera.

Density of Neuronal cultures. Cell density on the MEA after 4 weeks in culture was evaluated with incubation of the culture with 2μg/ml of Hoechst 33342 in PBS which stain all nuclei (Latt & Stetten, 1976), for 10 minutes at RT. After washing with PBS the cells were covered with a round coverslip and observed under a fluorescent microscope. Images of microscope fields covering 500mm^2 (the region comprised among a square of 4 electrodes on the MEA, as shown in fig. 1 B) were taken and the number of cell nuclei counted. The mean was obtained counting 4 fields of 5 different preparations. To evaluate the relative composition of neurons and glial cells in the

preparation, parallel cultures were obtained at the same density on coverslip and double immunofluorescence assays were performed with the primary antibody TUJ1 which binds to a neuron-specific class III beta-tubulin (Geisert & Frankfurter, 1989) (Fig. 1C) and with anti Glial fibrillary associated protein (GFAP; Fig. 1D) (Debus *et al.*, 1983). Total nuclei were counterstained with Hoechst 33342 dye. The percentage of neurons and glia in the culture was therefore evaluated by counting the number of TUJ1 or GFAP labeled cells over the total number of nuclei. The graph of fig 1F shows the results of these counts after 1,2,3 and 4 weeks culture. At each time point about 20% of the cells is positive for GFAP. The percentage of neurons increases from the first to the second week in culture and remains stable in the following weeks. The remaining cells in the first week samples are positive to nestin, a marker for neural precursors (Renfranz *et al.*, 1991). In similar cultures, the neuronal composition was evaluated by double immuno-fluorescence assays. Neurons were recognized by the antibody TUJ1. GABAergic, glutamatergic, or serotonergic neurons were revealed by specific antibodies binding to their neurotransmitters; dopaminergic neurons were revealed with specific antibodies against the enzyme tyrosine hydroxylase (TH), which is required for the production of catecholamine neurotransmitter. (Molinoff & Axelrod, 1971). The percentage of neurotransmitter specific neurons relative to the total number of neurons was therefore counted under the fluorescence microscope. To estimate the number of synaptic contacts between cells an immunofluorescence assay against the synaptic vesicle marker protein SV2 and the neuron-specific class III beta-tubulin (TUJ1) was performed. 5 fields were photographed under the normal fluorescent microscope and the confocal microscope, then the number of dots per field were counted and divided by the number of cells in the field to give an approximate number of synapses per neuron.

(Fig. 1 near here)

Electrical recordings and electrode stimulation. The multi electrode array (MEA) system used for electrophysiology was commercially supplied by Multi Channel Systems (MCS). MEA dishes had 10x6 TiN electrodes with an interelectrode spacing of 500 μm and each metal electrode had a

diameter of 30 μm. The MEA is connected to a 60 channel, 10 Hz – 3 kHz bandwidth pre-amplifier/filter-amplifier (MEA 1060-AMP) which redirects the signals towards a further electronic processing (i.e. amplification and AD conversion), operated by a board lodged inside a high performance PC. Signal acquisitions are managed under software control and each channel was sampled at a frequency of 20kHz. One electrode was used as ground (see Figure 2A). Sample data were transferred in real time to the hard disk for later processing. In order to keep the desired environmental conditions during the electrical recordings, the dish was moved to a different incubator providing only a controlled level of CO_2 (5%) and temperature (37^{o}C) and it was sealed by a cap distributed by MultiChannelSystem in order to eliminate evaporation and contamination. The neuronal culture was then allowed to settle for about 1 hour in order to reach a stationary state. After conclusion of the experiment, usually after 3 to 10 hours, the medium was changed and the dish was moved back to the original incubator. Recordings were performed, in culture medium, from 3 weeks after seeding for up to 6 months. The same culture could be used repeatedly for other experiments for up to one month. Each metal electrode could be used either for recording or for stimulation. Voltage stimulation was used and consisted of bipolar pulses lasting 100 μs at each polarity injected through the STG1004 Stimulus Generator. The voltage pulse generated by the STG1004 was applied in parallel to the set of electrodes manually selected for stimulation (simultaneous multi-site stimulation). A thermostat (HC-X) maintained the temperature at 37°C underneath the MEA.

The amplitude of the voltage pulse varied between 200 and 900 mV. The minimum amplitude required to evoke an electrical response varied between 200 and 300 mV depending on the responsiveness of the culture and on the geometry of the stimulus. Analogously the lower amplitude giving the maximum response varied between 750 and 900 mV. In order to avoid invasive effects due to the stimulus itself, intensities higher that 900mV were not applied. Once the lowest and highest intensity for a specific culture were selected, two intermediate values were chosen to complete the experiment. In most of the experiments the intensities applied were 300,

450, 600 and 900mV. For each different spatial stimulus, once the amplitude of the voltage pulse was selected, the neuronal culture was usually stimulated for 100 trials with a fixed inter-pulse interval, selected between 2s and 4s. In general, every 30 minutes, test stimulation was repeated in order to test the stability of the response.

Pharmacology. The following chemicals were used as synaptic blockers: 2-amino-5-phosphonovalerate (APV, Sigma-Aldrich), bicuculline (Sigma-Aldrich) and 6-cyano-7-nitroquinoxaline-2,3-dione disodium salt (CNQX, Sigma-Aldrich). Synaptic blocker/s was/were added to the extracellular medium in their required amount. After completion of the planned measurements, blockers were washed out by four medium replacements, and the original extracellular medium was restored.

Data analysis. Acquired data were analyzed using MATLAB (The Mathworks, Inc.). An artifact lasting 5 – 20 ms, caused by the electrical stimulation, was induced on the recording and was removed during data analysis (Wagenaar & Potter, 2002; Ruaro *et al.*, 2005). As the artifact removal was not reliable during the first 2 ms following the stimulation, we excluded this time bin from the analysis. Antidromically evoked APs were identified in two different ways: first, all APs observed in the presence of a cocktail of synaptic blockers (50 μM APV, 10 μM bicuculline and 100 μM CNQX) were classified as antidromic APs; second, – in agreement with Wagenaar et al 2004 - all APs with a reliability close to 100% and with a temporal jitter of less than 0.25 ms were classified as antidromic (Wagenaar *et al.*, 2004). In our analysis of the variability of neuronal firing we excluded those APs classified as antidromic. For each individual electrode, we computed the standard deviation (σ) of the noise, which ranged from 3 to 6 μV, and only APs crossing the threshold of -5σ were counted as APs used for data analysis. AP sorting was obtained using principal component analysis and open source toolboxes for the analysis of multi-electrode data (Egert *et al.*, 2002) with MATLAB. For the analysis on the first evoked APs, for each electrode,

only the timing of the first evoked AP was considered. Taken a pool of neurons, we define first the AP response as the number of neurons within the pool firing at least an AP in the time bin *t* after the stimulation ($FAPR_t$, fig. 7 B). In order to calculate the average firing rate (AFR) of the neurons, peri-stimulus time histograms (PSTHs) were calculated for the sorted neurons (fig. 3A) using a 10 ms time bin, where time 0 ms corresponds to the delivery of the stimulation. When APs recorded from sorted neurons were pooled, the PSTH over the population of neurons (PPSTH) was similarly calculated, counting in each time bin the APs of all neurons (fig. 3B). In the same way, when APs recorded from the whole array of electrodes were pooled, the population PSTH (APSTH) was calculated (fig. 3C, 8A and 9A). We define single neuron response (SR_t) the number of APs fired in a single trial by a single neuron in the time bin *t* after the stimulation. Summing the SR_t of a pool of neurons, a population response (PR_t) is defined. Analogously, when all the APs recorded by an electrode or by a population of electrodes are counted in the time bin *t* in a single trial, respectively an electrode response (ER_t) and an electrode population response (EPR_t) are obtained. The coefficient of variation (CV) of any analyzed variable, is the standard deviation over the mean of the variable. If $CV_{\#i}$ is the CV of the single neuron #i response (SR_t), $\langle CV \rangle$ is the average $CV_{\#i}$ over a population of M selected neurons.

Calculation of correlation and statistical independence of neuron firing. The degree of correlation and of statistical independence of neuronal firing was measured on short (i.e. few ms) and longer time scales (i.e. few tens of ms). On short time scales, i.e. with binwidth of 2 ms as in fig. 4 C, for each pair of neurons #i and #j the product of the probability of firing $p_i \cdot p_j$ was compared to the joint probability of firing p_{ij}, as described by Pinato *et al.* (2000). The same procedure was used to measure the statistical independence of the neuronal firing recorded for each pair of electrodes #i and #j (fig. 4F). On longer time scales, i.e. with a time bin of 50 ms, the cross correlation between pairs of single neuron responses (SR_t) were calculated (CSN_t) as shown in Fig. 4B. The same

procedure was applied to calculate the cross correlation between single electrode responses (ER_t) for a pair of electrodes (CSE_t), as shown in Fig.4E.

Calculation of the mutual information. In order to decode the stimulus intensity, we analyzed and compared neural codes based on the firing rate of single neurons (SR_t), on the firing rate of an ensemble of neurons (ER_t, EPR_t) and on the first evoked APs in an ensemble of neurons ($FAPR_t$). We used information theory (Shannon & Weaver, 1949) and in particular mutual information to estimate the amount of information which can be decoded by the different neural codes in different time bins (i.e. varying *t*) and for different extent of pooling (i.e. different number of electrodes considered). In particular, the mutual information was calculated as follows:

$$I_t \equiv I_t(R,S) = \sum_{s \in S} p(s) \sum_{r \in R} p_t(r \mid s) \cdot \log_2 (p_t(r \mid s) / p_t(r)) \qquad (1)$$

where

$$p_t(r) = \sum_{s \in S} p(s) \cdot p_t(r \mid s) \qquad (2)$$

I_t quantifies in bits the amount of information that a single response, *r*, (i.e. SR_t, ER_t, EPR_t, or $FAPR_t$ depending on the different neural code) provides about the intensity of the stimulus *s*. $p_t(r)$ is the total probability of observing the response *r* considering the time bin 1 to *t* ms after the stimulus, averaged over all stimuli. In our case, all stimuli occurred with equal probability, $p(s)$. In order to minimize the effects of finite sample size on our estimates of information, the real response *r* have been binned into different intervals, following the methods of Panzeri and Treves (1996).

Results

Characterization of the neuronal culture

Hippocampal neurons from neonatal rats were grown over a 10 x 6 MEA (fig. 1A). After 4 weeks in culture, the density of neurons was evaluated by counting the cell nuclei on the surface delimited by 4 adjacent electrodes on the MEA (Fig. 1B). The obtained density was 1756± 255 cells/mm^2 (n=4). By immunofluorescence assays, it was possible to clearly identify neurons (fig. 1C) and astrocytes (fig. 1D). The neuronal culture composition was analyzed over a period of 4 weeks. As shown in fig 1, during the first four weeks, the fraction of glial cells was always about 20%. The percentage of neurons increased between the first and the second week in culture and remained stable afterwards. The remaining cells during the first week were positive to nestin, a marker for neural precursors (Renfranz *et al.*, 1991) (fig. 1H). Neurons had long dendrites extending in all directions and often it was possible to recognize an axonal structure. Due to the difference in cell body size, although much less abundant in number, glial cells occupied most of the space of the culture and neurons appeared to be growing over and beneath glial cells. Approximately 8% of neurons were GABAergic (fig. 1E) and 90% were glutamatergic. No serotonin or dopaminergic neurons were detected and we were unable to determine the nature of the few remaining neurons. With double immunofluorescence assay against the synaptic vesicle marker protein SV2 and the neuronal masker TUJ1, (fig. 1F and G) we estimated the number of synapses between 450 and 500 per cell, in agreement with the data published for cortical neurons in culture (Tateno *et al.*, 2002).

Electrophysiology, single neuron detection and antidromically evoked APs

MEAs allow the recording of the extracellular voltage signals, produced by APs of all neurons establishing a good electrical contact with MEA electrodes (fig. 2A). Often extracellular APs

larger than 100 μV were measured. The neuronal culture was stimulated by a brief bipolar voltage pulse applied to a set of electrodes. The electrical stimulation produced an artifact lasting 5 – 20 ms (removed off-line, see Methods) in all electrodes (indicated by an arrow in fig. 2 A and B), followed by clear evoked APs. Extracellular signals larger than five times the standard deviation of the voltage noise (5σ) were considered as reliable APs. The number of neurons recorded by different MEAs ranged from few dozen to hundreds of units. APs clearly produced by the same neuron (indicated in red and blue in fig. 2 C lower panel) were identified using AP sorting algorithms (see Methods) and the reproducibility of their firing during repetitive stimulations was studied. The population of neurons which could be identified on different MEAs ranged between 10 and 50 units. As neurons of our cultures had long axons (see Fig. 1), some detected APs were produced by a direct antidromic stimulation of the neuron and were not evoked through synaptic pathways (Wagenaar et al. 2004). In order to identify these antidromic evoked APs, we compared recordings in the absence and in the presence of a cocktail of synaptic blockers (50 μM APV, 10 μM bicuculline and 100 μM CNQX). In addition to what reported by Wagenaar et al. (2004), we observed highly reliable APs with a low temporal jitter (less than 0.25ms) which were abolished by the cocktail, indicating that they were traveling through synaptic pathways (fig. 2D). We also observed APs with a low temporal jitter (less than 0.25ms) detected only in presence of synaptic blockers (fig. 2E). These APs are likely to be antidromically evoked but in control conditions are blocked by inhibitory synapses.

(Fig. 2 near here)

Reproducibility, pooling and statistical independence of neuronal firing

When the same voltage pulse was repetitively applied to the same electrodes, the number of evoked APs in a single neuron varied, but often the first evoked AP was reliable with a jitter varying from just a few hundreds μs to some ms. The evoked average firing rate (AFR) and the associated coefficient of variation (CV, see Methods) computed on a time window of 10 ms, for 10

individual neurons, at progressively longer distances from the stimulated electrodes are shown in fig. 3A.

(Fig. 3 near here)

The 10 neurons were recorded at distances varying between 500 μm to 4000 μm from the row of electrodes used for stimulation (black bar in the grid). Neurons #1 and #10 were not activated and their firing was almost abolished by the electrical stimulation. The CV of their firing increased following the electrical stimulation. On the contrary, the firing of neurons #2-9 increased significantly, whereas their CV decreased. Neuron #4 responded to the stimulation by firing an AP in the time window between 1 and 11 ms, in each of the 50 trials, with a jitter of less than 0.25 ms and the corresponding CV was 0. Other identified neurons, were less reliable, their firing was more distributed over time and, at the peak of the evoked response, their CV was between 0.2 and 0.8. When antidromically evoked APs were excluded (see methods) and the firing of the 10 identified neurons was pooled, the CV was about 0.25 and remained less than 0.4 for at least 20 ms at the peak of the evoked response (fig. 3B). Similar results were obtained from 5 additional neuronal cultures. When we pooled together all APs recorded from all electrodes on the MEA, the CV was transiently lower than 0.1 and remained lower than 0.3 for at least 40 ms (fig. 3C). When antidromically evoked APs were included in the pool, the CV did not change significantly, since antidromic APs are extremely reliable (fig. 3B and C).

(Fig. 4 near here)

When pooling single neuron responses (SR_{50ms}) with a similar CV (fig. 4A), the CV of the pooled activity decreased as $\langle CV \rangle / \sqrt{N}$ (thick black line), where $\langle CV \rangle$ is the average CV ad N is the number of pooled neurons. Fig. 4A shows how the CV varies when neurons with the lowest (black symbols) and the highest CV (gray symbols) were progressively pooled one by one. Single neurons had an average CV of 0.5 and, when 12 neurons were pooled, the CV approached 0.15. Therefore at least two dozens of neurons are needed to obtain a CV of about 0.1, i.e. a very reliable response. Pooling the electrical activity from different neurons reduces the corresponding CV only

if their evoked firing is not correlated (Shadlen & Newsome, 1994, 1998; Gawne & Richmond, 1993). The correlation between single neuron responses (SR_{50ms}) of pooled neurons, was on average 0.11+-0.02 (mean and standard deviation of the mean for 5 preparations) (fig. 4B) considering all possible pairs of neurons. Also on shorter time scales, i.e. at a binwidth of 2 ms, neuronal firing was very poorly correlated as shown in fig. 4C: for each pair of neurons #i and #j the product of the probability of firing $p_i \cdot p_j$ was very similar to the joint probability of firing p_{ij}, of neurons #i and #j firing simultaneously. As a consequence, on short time scales the binned firing of pairs of neurons is close to statistical independence and therefore is almost uncorrelated.

Similar results were obtained when all APs recorded in a single electrode were counted in the first 50ms following the stimulation (ER_{50ms}) and pooled (fig. 4D). In this case, when APs from approximately 10 electrodes were pooled, the CV approached 0.1. As each electrode of the MEA detects APs from different neurons (usually between 2 and 5), a pool of 20 to 50 neurons provides a reliable response.

The correlation between pairs of ER_{50ms} was 0.17+-0.05 (fig. 4E). Similarly, at a binwidth of 2 ms, APs recorded by pairs of electrodes were almost statistically independent and therefore not correlated (fig. 4F). These results, although obtained on a small fraction of neurons forming the network under investigation, suggest that coactivated neurons on a time scale of some milliseconds are poorly correlated and therefore averaging their electrical activity reduces the variability of the evoked response.

(Fig. 5 near here)

Statistical properties of neuron firing, when a single bar of electrodes was stimulated, for a population of 99 neurons identified in the 5 neuronal cultures analyzed (different colors correspond to different cultures) are reproduced in fig. 5. The jitter of the first evoked AP on its average latency were significantly correlated with coefficient of correlation $\rho = 0.76$ (fig. 5A). Since the latency of an evoked AP is primarily determined by the number of synapses between the

stimulating site and the neuron, the significant correlation between jitter and latency shows that the reliability of the firing of a single neuron decreases with the number of synapses that the signal has to cross. The minimum CV (min_{CV}) of the AFR and the time of its occurrence ($time_{minCV}$) were correlated to the latency of the first evoked AP respectively with $\rho = 0.87$ and $\rho = 0.89$ (fig. 5B and D), indicating that the firing of the first evoked AP is the most reliable part of the neural response. The average latency increases with the physical distance (*d*) between the recording electrode and the bar of stimulating electrodes (fig. 5C). The slope of the line provides the maximum speed of APs propagation in the cultures, which is approximately 350mm/s, in agreement with our previous report (Ruaro *et al.*, 2005).

Processing information: coding stimulus intensity by pooling neuron firing

The neural code is expected to distinguish - and therefore to encode - important features of the stimulus, such as its intensity. Therefore, the coding of stimulus intensity was investigated and compared at the level of a single neuron and when APs were pooled from a population of neurons. More precisely it is assumed that N stimulus intensities can be distinguished in a reliable way - and therefore properly coded – if, by analyzing features of the response, it is possible to determine in almost all trials the exact stimulus intensity. In this case, the response distributions for the N stimuli do not overlap appreciably and it is possible to code $\log_2 N$ bits of information.

The first evoked AP is usually highly reliable and these APs may carry most of the relevant information for recognition (Thorpe *et al.*, 2001; Abeles, 1991; Van Rullen & Thorpe, 2001; Delorme, 2003; Delorme & Thorpe, 2001) and later processing. The first evoked APs are possibly the fastest signals achievable within the nervous system and are ideal for a fast neural code.

Voltage pulses of different intensities were applied to an electrode row. By increasing the voltage pulse, APs recorded on each electrode became more frequent and often APs with a new shape, produced by a different neuron, appeared (Ruaro *et al.*, 2005). Usually, no APs were evoked by voltage pulses below 200mV and a saturating maximal response was evoked with a voltage of

about 1V. Four voltage pulses, varying between 200 mV and 900 mV, were considered (see methods) and coding was measured by computing the mutual information I_t (see methods) between the evoked response in each trial and the stimulus intensity.

(Fig. 6 near here)

The maximal mutual information I_t carried by binned firing rates of single neurons (see methods), was on average 0.34 bits. The analysis was performed on 91 neurons from 5 different preparations (fig. 6A). In the great majority of these neurons, I_t was much less than 1 bit and only in 10 neurons I_t approached to 1 bit. Therefore, by counting the number of evoked APs in single neurons, it is not possible to reliably distinguish two stimulus intensities. Very similar results were obtained, computing I_t carried by the first evoked AP ($FAPR_t$, see methods) (fig. 6B). In this case I_t was, on average, 0.32 bits and in 7 neurons out of 91 the value of I_t approached 1 bit.

(Fig. 7 near here)

As binned firing rates of single neurons cannot reliably distinguish the stimulus intensity, we investigated population coding in which APs from different neurons were pooled. Each electrode of the MEA usually detects APs from different neurons (between 2 and 5, data not shown) and therefore we pooled all APs recorded by a single electrode (ER_t) and by an ensemble of electrodes of the array (EPR_t). I_t was maximal (1.48±0.22 bits, mean and standard deviation over 5 cultures) when APs recorded by a population of at least 20 electrodes were pooled in a time bin of about 30 ms. Similar results were obtained when the first evoked APs in all electrodes were counted, in this case I_t was 1.35±0.18 bits in a similar time bin.

Fig. 7 shows, in one preparation, the dependence of I_t on the number of electrodes pooled and on the time bin *t*, when the first evoked APs were counted (fig. 7A upper panel) and when all APs were pooled (fig. 7A lower panel). In this case, the network distinguishes clearly 4 stimulus intensities, both when the first evoked APs were counted (fig. 7B upper panel) and when all APs were pooled (fig. 7B lower panel).

The effect of APV and bicuculline

Hippocampal neuronal cultures are composed of GABAergic and of glutamatergic neurons (fig. 1). Therefore, we analyzed the effect of blockers of these synaptic pathways such as APV and bicuculline on the mutual information. APV is a well known blocker of excitatory synaptic transmission mediated by NMDA receptors and bicuculline blocks inhibitory pathways mediated by GABAergic synapses.

(Fig. 8 near here)

Increasing the extracellular concentration of APV from 1 μM to 50 μM, the second component of the evoked response progressively decreased and in the presence of 50 μM APV was completely blocked (Fig. 8A). In the presence of 50 μM APV, the initial component of the AFR was almost unaltered, but the second component was significantly depressed leading to an increase of the corresponding CV. For single neurons, the late evoked response was also depressed but the timing and the occurrence of the first evoked AP was unaltered and had approximately the same latency and jitter (data not shown). The correlation between the electrode responses in the first 50 ms post stimulus (ER_{50ms}) did not significantly change.

The value of I_t when the first evoked APs were counted (fig. 8B) and when all APs were pooled (fig. 8C), significantly increased in the presence of APV of 15% (n=5, *t*-test, $p<0.01$).

(Fig. 9 near here)

The opposite effect was observed when bicuculline was added to the extracellular medium. Increasing the concentration from 200 nM to 10 μM, the spontaneous electrical activity increased and became progressively synchronized.

While the late component of the evoked response increased, the correspondent CV decreased (Fig. 9A). In the presence of 10 μM bicuculline, the correlation between the electrode responses (ER_{50ms}) of two electrodes increased drastically (0.61 ± 0.19). The mutual information based on first

evoked APs (Fig. 9B) and on rate coding (Fig. 9C) significantly decreased in the presence of 10 μM bicuculline respectively of 25% and 23% (n=5, *t*-test, $p<0.01$).

These results show that blockage of excitatory synaptic pathways mediated by NMDA receptors increases the mutual information and improves neuronal coding. We observed instead the opposite effect when inhibitory pathways mediated by GABA receptors are blocked.

Discussion

In order to investigate the statistical properties of information processing in neuronal networks, the reproducibility of the electrical activity evoked by multi-site stimulation in a neuronal culture from rat hippocampal neurons was investigated in single neurons and in neuronal assemblies. The neural activity was binned into firing rates over time windows of different length and its statistical properties were analyzed. Our analysis reaches three major conclusions. Firstly, although individual neurons are noisy and unreliable elements carrying a low amount of information, by averaging APs from a neuronal assembly of about 25-100 neurons, it is possible to decode at a single trial level a stimulus in about 20 ms. Secondly, a reliable information processing is obtained by averaging evoked APs or by counting the first evoked APs, provided that enough neurons are pooled. Thirdly, information processing depends critically on the balance between excitation and inhibition.

Variability of firing of individual neurons and of neuronal populations

When a neuron was postsynaptically excited by the stimulation, the evoked firing was composed by a first reliable AP followed by less reliable APs (fig. 3). The degree of correlation on short binwidths (i.e. less than 50 msec) between coactivated individual neurons and between all APs recorded by individual electrodes was usually small, often less than 0.1 (see Fig. 4). These results, although obtained on a small fraction of the neurons forming the neuronal network, suggest that coactivated neurons fire almost independently on a short time scale. This is not surprising as vesicle release at different synapses is an uncorrelated process at short time scales. As a consequence of this statistical independence, when the electrical activity was pooled over N coactivated neurons, the CV of the pooled electrical activity decreased as $1/\sqrt{N}$ (see fig. 4) (Papoulis, 1984; Pinato *et al.*, 2000). As neurons had an average CV of 0.5, a good reproducibility - with a CV of less than 0.1 - was obtained by pooling the electrical activity of 25 neurons or more.

These conclusions, drawn from an investigation carried out in a dissociated culture of rat hippocampal neurons, are remarkably similar to those obtained in intact neuronal tissues or small nervous systems. In the leech nervous system (Arisi *et al.*, 2001; Zoccolan *et al.*, 2002) motoneurons coactivated during the same behavioral reaction and fired APs in an almost statistically independent way. As a consequence of statistical independence, pooling the electrical activity over all coactivated motoneurons makes AP trains underlying reproducible motor reactions. Shadlen and Newsome (1998) suggested that in the cortex quantities are represented as rate codes in ensembles of 50-100 neurons, i.e. a column-like ensembles, providing a reliable estimation of rate in just one interspike interval (10-50 ms). Using multi-site recordings, Nicolelis *et al.* (1998) showed that in the primate somatosensory cortex, the electrical activity from a small neural ensemble – of about 30-40 neurons - coded correctly the location of a single tactile stimulus on a single trial.

Processing information by ensemble averaging

The large variability of firing of individual neurons is reflected in the low amount of information carried by binned firing rates of the single neurons (fig. 6). Since the first evoked AP is the most reliable, in the large majority of neurons the information carried by the first evoked AP is almost identical to the information carried by the firing rate (fig. 6). In order to decode a larger amount of information, it is necessary to average the response of a neuron population (fig. 7). By pooling the electrical activity of 50-100 neurons evoked in the first 20-50 ms, it was possible to extract more than 1.5 bits (fig. 7). Pooling over an ensemble of neurons the first evoked APs or the number of evoked APs (fig. 7) allowed the extraction of approximately the same amount of information (fig. 7). Therefore, pooling first evoked APs or firing rates is almost equivalent. First evoked APs also represent the fastest signal in the nervous system. *In vivo* experiments on the somatosensory cortex (Panzeri *et al.*, 2001) have shown the prominent role of the first AP, which contained about 83% of the total information. Recently, Johansson and Birznieks (2004) have

shown that first APs in ensembles of about 30 neurons of human tactile afferents can code, within 40 ms after the stimulus onset, complex spatial fingertip events.

Recognition of complex scenes and images occurs within 180 ms (Thorpe *et al.*, 2001) likely obtained in several steps, each completed within a short time interval of 10 to 20 ms. In this case, the best procedures are either averaging APs in a short time window or considering the first evoked APs in an ensemble of neurons. A faster and reliable processing such as that necessary in the auditory system requires an appropriate neuronal network composed of specific neurons and synapses (Koppl, 1997). For different tasks it may be necessary to have a different amount of temporal and spatial averaging. For instance in the leech nervous system, in order to guarantee reliability of important behavioral reactions, such as the escape from a noxious stimulus, a longer integration time is used – some hundreds of ms - but on 10-20 motoneurons (Zoccolan *et al.*, 2002).

The role of inhibition and excitation: variability, reliability and information processing

Inhibition and excitation seem to play a fundamental role in the mechanisms underlying variability and reliability of the evoked response and they influence the the network's potential to process information. Blocking the excitatory pathways mediated by NMDA-receptors had several major effects, in agreement with previous investigations (Jimbo *et al.*, 2000; Kamioka *et al.*, 1996). In the present investigation, it is shown (fig. 8) how the blockage of these synaptic pathways reduced and almost eliminated the second component of the evoked response and, most relevant for the present investigation, increased the mutual information between the evoked response and the stimulus, allowing a greater recovery of information. Blocking inhibitory pathways mediated by GABA-receptors had opposite effects as previously described (Jimbo *et al.*, 2000; Arnold *et al.*, 2005). The present investigation shows how, blocking these synaptic pathways, the mutual information between the evoked response and stimulus decreases and a very little information can be recovered. This remarkable deterioration of information processing was caused by an increased

variability of the early phase of the evoked response and by the occurrence of large spontaneous bursts of synchronized electrical activity. Under these conditions, the noise in the neuronal network became correlated and could not be eliminated or reduced by averaging or pooling. These results support the idea (Shadlen & Newsome, 1998; Mariño *et al.*, 2005; Turrigiano & Nelson, 2004; Wehr & Zador, 2003; Zhang *et al.*, 2003) that, in order to process information in a reliable way, neuronal networks require an appropriate balance of excitation and inhibition, so that a stimulus can generate a reliable neuronal response, distributed through the network.

Acknowledgements

This work was supported by the EU grants INPRO and NEURO, by a FIRB grant from the Italian Ministers and by the CIPE grant (GRAND FVG). We thank Dr. Davide Zoccolan, Prof. Alessandro Treves and Prof. Enrico Cherubini for the helpful comments and Ranken Shimakazi and Manuela Schipizza Lough for carefully reading the manuscript.

References

Abeles, M. (1991). *Corticonics*. Cambridge University Press.

Aihara, T., Y. Kobayashi, & M. Tsukada. (2004). Spatiotemporal visualization of long-term potentiation and depression in the hippocampal CA1 area. *Hippocampus* **15**:68-78 .

Arisi, I., D. Zoccolan, & V. Torre. (2001). Distributed motor pattern underlying whole-body shortening in the medicinal leech. *J. Neurophysiol.* **86**: 2475-2488.

Arnold, F.J., Hofmann, F., Bengtson, C.P., Wittmann, M., Vanhoutte, P., Bading, H. (2005). Microelectrode array recordings of cultured hippocampal networks reveal a simple model for transcription and protein synthesis-dependent plasticity. *J Physiol.* **563**: 3-19.

Cohen, D., & M.A. Nicolelis. (2004). Reduction of single neuron firing uncertainty by cortical ensembles during motor skill learning. *J. Neurosci*. **24**: 3574-3582.

Debus, E., K. Weber, & M. Osborn. (1983). Monoclonal antibodies specific for glial fibrillary acidic (GFA) protein and for each of the neurofilament triplet polypeptides. *Differentiation* **25**: 193-203.

DeCharms, R.C., & M.M. Merzenich. (1996). Primary cortical representation of sounds by the coordination of action-potential timing. *Nature* **381**:610-613.

Delorme, A., S.J. Thorpe. (2001). Face identification using one spike per neuron: resistance to image degradations. *Neural. Netw.* **14**:795-803.

Delorme, A. (2003). Early cortical orientation selectivity: how fast inhibition decodes the order of spike latencies. *J. Comput. Neurosci*. **15**: 357-365.

De Ruyter van Steveninck, R.R., G.D. Lewen, S.P. Strong, R. Koberle, & W. Bialek. (1997). Reproducibility and variability in neural spike trains. *Science* **275**:1805-1808.

Egert, U., Th. Knott, C. Schwarz, M. Nawrot, A. Brandt, S. Rotter, & M. Diesmann. (2002). MEA-Tools: an open source toolbox for the analysis of multi-electrode data with MATLAB. *J. Neurosci. Meth.* **17**: 33-42.

Eytan, D., N. Brenner, & S. Marom. (2003). Selective adaptation in networks of cortical neurons. *J. Neurosci*. **23**:9349-9356.

Gawne, T.J., & B.J. Richmond. (1993). How independent are the messages carried by adjacent inferior temporal cortical neurons? *J. Neurosci.* **13**:2758-2771.

Geisert, E.E. Jr, & A. Frankfurter. (1989). The neuronal response to injury as visualized by immunostaining of class III beta-tubulin in the rat. *Neurosci. Lett*. **102**:137-141.

Georgopoulos, A.P., A.B. Schwartz, & R.E. Kettner. (1986). Neuronal population coding of movement direction. *Science* **233**:1416-1419.

Gross, G.W. (1979). Simultaneous single unit recording in vitro with a photoetched laser deinsulated gold multimicroelectrode surface. *IEEE Trans. Biomed. Eng*. **26**:273-279.

Harris, K.D., J. Csicsvari, H. Hirase, G. Dragoland G. Buzsaki. (2003). Organization of cell assemblies in the hippocampus. *Nature* **424**: 552-556.

Hopfield, J.J. (1995). Pattern recognition computation using action potential timing for stimulus representation. *Nature* **376**:33-36.

Jancke, D., F. Chavane, S. Naaman, & A. Grinvald. (2004). Imaging cortical correlates of illusion in early visual cortex. *Nature* **428**:423-426.

Jimbo, Y., T. Tateno, & H. Robinson. (1999). Simultaneous induction of pathway-specific potentiation and depression in networks of cortical neurons. *Biophys. J.* **76**:670-678.

Jimbo, Y., Kawana, A., Parodi, P., Torre, V. (2000). The dynamics of a neuronal culture of dissociated cortical neurons of neonatal rats. *Biol Cybern.* **83**: 1-20.

Johansson, R.S., & I. Birznieks. (2004). First spikes in ensembles of human tactile afferents code. *Nat. Neurosci.* **6**: 750 – 757.

Kamioka, H., E. Maeda, Y. Jimbo, H.P.C. Robinson, & A. Kawana. (1996). Spontaneous periodic synchronized bursting during formation of mature patterns of connections in cortical neurons. *Neurosci. Lett.* **206**: 109-112.

Koppl, C. (1997). Phase locking to high frequencies in the auditory nerve and cochlear nucleus magnocellularis of the barn owl, Tyto alba. *J. Neurosci.* **17**:3312-3321.

Latt, S.A., & G. Stetten. (1976). Spectral studies on 33258 Hoechst and related bisbenzimidazole dyes useful for fluorescent detection of deoxyribonucleic acid synthesis. *J. Histochem. Cytochem.* **24**:24-33.

Lewis, J.E., & W.B. Jr Kristan. (1998). A neuronal network for computing population vectors in the leech. *Nature* **391**:76-79.

Maeda, E., H.P.C. Robinson, & A. Kawana. (1995). The Mechanisms of Generation and Propagation of Synchronized Bursting in Developing Networks of Cortical Neurons. *J. Neurosci.* **75**: 6834-6845.

Mariño, J., Schummers, J., Lyon, D.C., Schwabe, L., Beck, O., Wiesing, P., Obermayer, K., Sur, M. (2005). Invariant computations in local cortical networks with balanced excitation and inhibition. *Nat Neurosci.* **8**:194-201.

Molinoff, P.B., & J. Axelrod. (1971). Biochemistry of catecholamines. *Annu. Rev. Biochem*. **40**: 465-500.

Nicolelis, M.A., A.A. Ghazanfar, B.M. Faggin, S. Votaw, & L.M. Oliveira. (1997). Reconstructing the engram: simultaneous, multisite, many single neuron recordings. *Neuron* **18**:529-537.

Nicolelis, M.A., A.A. Ghazanfar, C.R. Stambaugh, L.M. Oliveira, M. Laubach, J.K. Chapin, R.J. Nelson RJ, & J.H. Kaas. (1998). Simultaneous encoding of tactile information by three primate cortical areas. *Nat. Neurosci*. **1**:621-630.

Osborne, L.C., W. Bialek, & S.G. Lisberger. (2004). Time course of information about motion direction in visual area of macaque monkeys. *J. Neurosci.* **24**:3210-3222.

Panzeri, S., & A. Treves. (1996). Analytical estimates of limited sampling biases in different information measures. *Network Comput. Neural. Syst.* **7**:87–107.

Panzeri, S., R.S. Petersen, S.R. Schultz, M. Lebedev, & M.E. Diamond. (2001). The role of spike timing in the coding of stimulus location in rat somatosensory cortex. *Neuron* **29**:769-777.

Papoulis, A. (1984). *Probability, random variables and stochastic processes*. McGraw-Hill, New York.

Parker, A.J., & W.T.Newsome. (1998). Sense and the single neuron: probing the physiology of perception. *Annu. Rev. Neurosci*. **21**:227-277.

Pinato, G., S. Battiston, & V. Torre. (2000). Statistical independence and neural computation in the leech ganglion. *Biol. Cybern.* **83**:119-130.

Pine, J. (1980). Recording APs from cultured neurons with extracellular microcircuit electrodes. *J. Neurosci. Methods* **2**:19-31.

Potter, S.M. (2001). Distributed processing in cultured neuronal networks. *Prog. Brain Res*. **130**:49-62.

Renfranz, P.J., M.G. Cunningham, & R.D. McKay. (1991). Region-specific differentiation of the hippocampal stem cell line HiB5 upon implantation into the developing mammalian brain. *Cell* **66**:713-729.

Ruaro, M. E, P. Bonifazi, & V. Torre. (2005). Towards the neurocomputer: image processing and pattern recognition with neuronal cultures. *IEEE Trans. Biomed. Eng.* **52**:371-383.

Shannon, C.E., & W. Weaver. (1949). A mathematical theory of communication. In: *The mathematical theory of communication*. Urbana, IL: University of Illinois.

Shadlen, M.N., & W.T. Newsome. (1994). Noise, neural codes and cortical organization. *Curr. Opin. Neurobiol*. **4**:569-579.

Shadlen, M.N., & W.T. Newsome. (1998). The variable discharge of cortical neurons: implications for connectivity, computation, and information coding. *J. Neurosci*. **18**:3870-3896, 1998.

Silberberg, G., M. Bethge, H. Markram, K. Pawelzik, & M. Tsodyks . (2004). Dynamics of population rate codes in ensembles of neocortical neurons. *J. Neurophysiol*. **91**:704-709.

Tateno, T., A. Kawana & Y. Jimbo. (2002). Analytical characterization of spontaneous firing in networks of developing rat cultured cortical neurons. *Phys. Rev. E* **65**: 051924.

Thorpe, S., A. Delorme, & R. Van Rullen. (2001). Spike-based strategies for rapid processing *Neural Network* **14**: 715-725.

Turrigiano, G.G., Nelson, S.B. (2004). Homeostatic plasticity in the developing nervous system. *Nat Rev Neurosci.* **5**:97-107.

Van Pelt, J., Wolters, P.S., Corner, M.A., Rutten, W.L., Ramakers, G.J. (2005). Long-term characterization of firing dynamics of spontaneous bursts in cultured neural networks. *IEEE Trans Biomed Eng.* **51**: 2051-62.

Van Rullen, R., & S:J: Thorpe. (2001). Rate coding versus temporal order coding: what the retinal ganglion cells tell the visual cortex. *Neural Comput*. **3**: 1255-1283.

Wagenaar, D.A., & S.M. Potter. (2002). Real-time multi-channel stimulus artifact suppression by local curve fitting. *J Neurosci. Methods* **120**: 113-120.

Wagenaar, D.A., Pine J., S.M. Potter (2004). Effective parameters for stimulation of dissociated cultures using multi-electrode arrays. *J Neurosci. Methods* **138**: 27-37.

Wehr, M., Zador, A.M. (2003). Balanced inhibition underlies tuning and sharpens spike timing in auditory cortex. *Nature* **426**:442-6.

Zhang, L.I., Tan, A.Y., Schreiner, C.E., Merzenich, M.M. (2003). Topography and synaptic shaping of direction selectivity in primary auditory cortex. *Nature* **424**:201–20.

Zoccolan, D., G. Pinato, & Torre, V. (2002) Highly variable AP trains underlie reproducible sensory-motor responses in the medicinal leech. *J. Neurosci*. **22**: 10790-10800.

Tables

Table 1: definition of variables

Abbreviations / names of variable	Definition	Unit
First AP response $FAPR_t$	number of neurons within the pool firing at least an AP in the time bin *t* after the stimulation).	# neurons
single neuron response SR_t	number of APs fired in a single trial by a single neuron in the time bin *t* after the stimulation	# APs
population response PR_t	sum of SR_t of a pool of neurons	# APs
electrode response ER_t	number of APs recorded by an electrode counted in the time bin *t* after the stimulation	# APs
electrode population response EPR_t	sum of ER_t of a pool of electrodes	# APs

Figure legends:

Figure 1. Characterization of the neuronal culture. A: image of dissociated hippocampal neurons on the MEA. B: cell nuclei of the dissociated culture stained with Hoechst33342. C: neurons expressing type III tubulin recognized by TUJ1 antibody (green); total nuclei (blue); D: glial cells expressing GFAP (green); total nuclei (blue). E: GABAergic neurons recognized by antiGABA specific antibody. F: synaptic vesicles stained by the protein specific for synaptic vesicle SV2 (green) and neurons expressing type III tubulin recognized by TUJ1 antibody (red) G: confocal image of the same preparation shown in F. In A and B the reference bar corresponds to 100μm; in C, D and E the reference bar corresponds to 50μm; in F the reference corresponds to 25μm. Images in C-G are from cells after 3 weeks in culture. H: cell composition of neuronal cultures after 1-4 weeks of culture.

Figure 2. Electrical recordings, AP sorting and APs antidromically evoked. A: electrical recordings obtained with a MEA composed by an array of 10x6 electrodes. The electrical artifact is indicated by the black arrow. A bipolar voltage pulse was applied to the fifth row of electrodes. The electrode framed in the gray box was used as ground. The stimulation evoked APs of different amplitude in most of the MEA electrodes. B: magnified electrical recordings obtained from the encircled electrode in panel A. Red and blue squares mark APs from two identified neurons. C: AP sorting. Upper panel shows all events exceeding a threshold of -50 μV. Lower panel shows APs sorted from two different neurons in red and blue. Same color in B and C indicates the same neuron. D: raster plots (left panel) and electrical recordings (right panel) from one electrode in normal conditions showing a highly reliable AP with a low temporal jitter (less than 0.25ms) which is suppressed in presence of synaptic blockers (10 μM bicuculline, 100 μM CNQX and 50 μM APV). E: raster plots (left panel) and electrical recordings (right panel) from one electrode in the presence of synaptic blockers (10 μM bicuculline, 100 μM CNQX and 50 μM APV), showing

a highly reliable AP with a low temporal jitter (less than 0.25ms) which is not evoked in normal conditions.

Figure 3. Reproducibility of neuronal firing. A: each panel reproduces the AFR (open bars) and the corresponding CV (black symbols) for 10 neurons identified in the electrodes indicated in the grid, where the black bar corresponds to the electrodes used for stimulation. B: AFR (open bars) and its CV (black symbols) when all APs of the 10 neurons identified in A were pooled. C: AFR (open bars) and its CV (black symbols) when all the APs recorded by the MEA were pooled. In B and C the shaded bar corresponds to antidromic APs, i.e. APs which were observed also in the presence of APV, CNQX and bicuculline.

Figure 4. Coefficient of variation of the population response and correlation of neuron firing. A: CV of the population response in the first 50 ms post-stimulus (PR_{50ms}) as a function of the number of neurons pooled (N). Neurons with a similar CV (i.e. less than 1) were pooled. In the gray (black) plot, neurons with an increasing (decreasing) CV were added one by one. The data are averaged over 5 different preparations. The thick black line represents $\langle CV \rangle / \sqrt{N}$, where $\langle CV \rangle$ is the average CV of the neurons. B: distribution of the coefficient of correlation of single neuron response in the first 50 ms post-stimulus (CSN_{50ms}). For each different preparation, all the possible pairs of neurons were considered. The data were averaged over 5 different preparations. C: average joint probability of firing of all possible pair-wise combinations of neurons. Considering all the possible pairs of neurons #i and #j, the average joint probability of firing p_{ij} (filled circles) is compared with the average product of individual probabilities $p_i * p_j$ (open circles). The data shown are from a single preparation and identical results were obtained in the other 4 preparations considered. D: CV of the electrode population response in the first 50 ms post-stimulus (EPR_{50ms}) as a function of the number of pooled electrodes. In the gray (black) plot, electrodes with an increasing (decreasing) CV were added one by one . The data were averaged over 5 different preparations. E: distribution of the coefficient of correlation of single electrode response in the first 50 ms post-stimulus (CSE_{50ms}). For each different preparation, all the possible pairs of electrodes

were considered. The data were averaged over 5 different preparations. F: average joint probability of firing of all possible pair-wise combinations of electrodes. Considering all the possible pairs of electrodes #i and #j, the average joint probability of firing p_{ij} (filled circles) is compared with the average product of individual probabilities $p_i * p_j$ (open circles). The data shown are from a single preparation and identical results were obtained in the other 4 preparations considered.

Figure 5. Statistical properties of single neuron firing, when a single bar of electrodes was stimulated. APs antidromically evoked are considered only in the statistic shown on panel C. A: relation between jitter and latency of first evoked AP. B: relation between the minimum CV (min_{CV}) of the AFR and latency of first evoked AP. C: relation between latency of first evoked AP and distance between stimulating and recording electrodes. The slope of the line estimates the maximum speed of propagation of action potentials in the cultures, which is approximately 350mm/s. D: relation between the time of the minimum CV ($time_{minCV}$) and latency of first evoked AP. The bin width considered is 10 ms. Only neurons, which had a CV of the evoked AFR lower than 4, were analyzed. A population of 99 neurons identified in five neuronal cultures was considered (different colors correspond to different cultures). In panel A, B and D the coefficient of correlation ρ is reported on the top. The red line is the linear regression.

Figure 6. Statistic of the maximal mutual information I_t carried by single neurons computed considering the highest and the lowest intensities of stimulation. 5 different preparations were considered. For each of the 91 neurons analyzed, the time bin *t* was varied in order to maximize the mutual information. A: distribution of the mutual information provided by the first evoked AP ($FAPR_t$). B: distribution of the mutual information provided by the single neuron response (SNR_t).

Figure 7. Coding stimulus intensity by pooling neuron firing. The statistics shown in the upper and lower panels were done respectively by pooling the first evoked APs ($FAPR_t$) and by pooling all the APs evoked (EPR_t) in the time bin *t* after the stimulus. A: mutual information I_t calculated for 4 different stimulus intensities as function of bin width (*t*) and of the number of pooled electrodes. B: distribution of the population response to the 4 different intensities of stimulation. The APs evoked

in the first 15 ms post-stimulus in all the electrode arrays were pooled. The data shown refer to one preparation.

Figure 8. The effect of APV on information processing. The statistics shown on the left panels and on the right panels were calculated in normal conditions and in the presence of 50 μM APV. The statistics shown in the upper and lower panels were done respectively by pooling the first evoked APs ($FAPR_t$) and by pooling all the APs evoked (EPR_t) in the time bin *t* after the stimulus. A: AFR (solid bars) and CV (black dots) of all APs recorded by the MEA. B and C: mutual information I_t calculated for 4 different stimulus intensities as functions of bin width *t* and of the number of pooled electrodes.

Figure 9. The effect of bicuculline on information processing. The statistics shown on the left panels and on the right panels were calculated in normal conditions and in the presence of 10 μM bicuculline. The statistics shown in the upper and lower panels were done respectively by pooling the first evoked APs ($FAPR_t$) and by pooling all the APs evoked (EPR_t) in the time bin *t* after the stimulus. A: AFR (solid bars) and CV (black dots) of all APs recorded by the MEA. B and C: statistics of the mutual information I_t calculated for 4 different stimulus intensities as functions of bin width (*t*) and of the number of pooled electrodes.

Figure 1

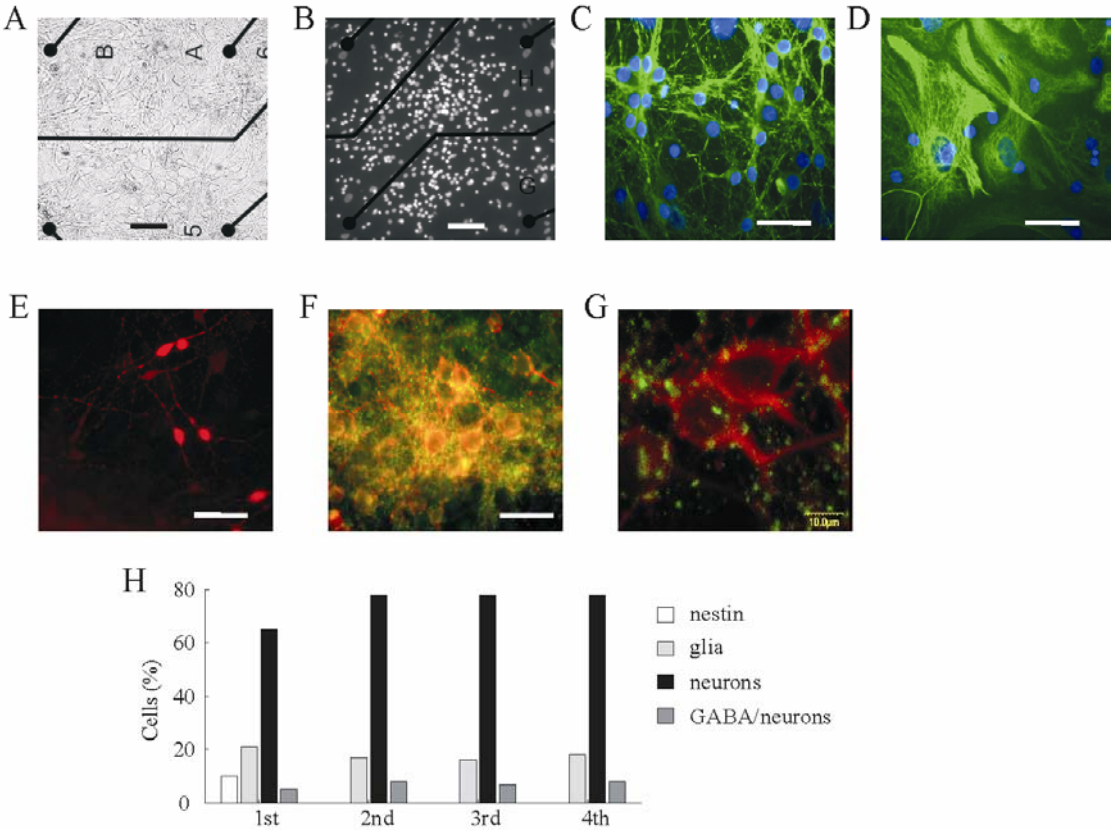
A
B
C
D
E
F
G
H
Cells (%)
80
60
40
20
0
1st
2nd
3rd
4th
nestin
glia
neurons
GABA/neurons

Figure 2

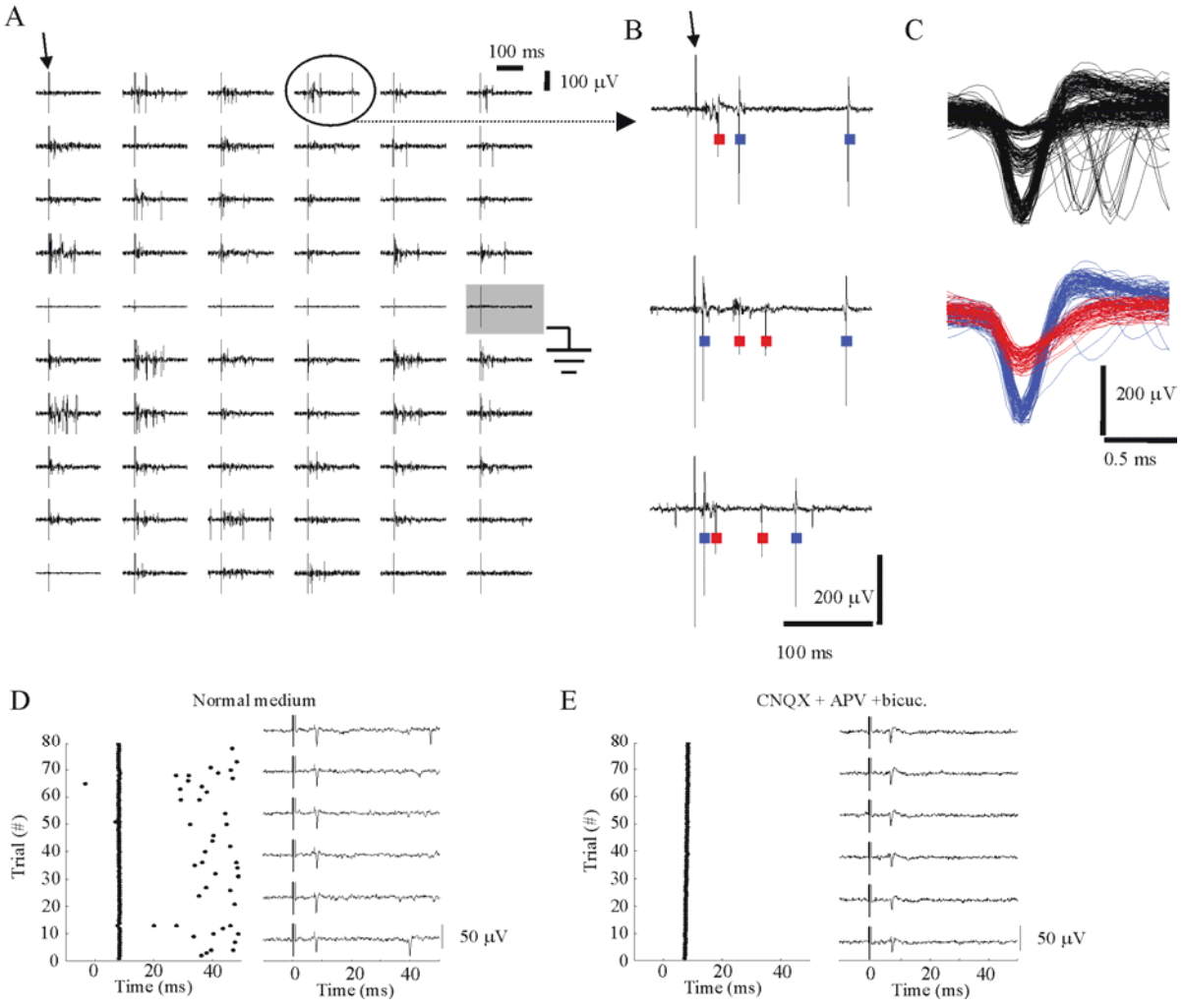
A
100 ms
100 µV
B
200 µV
100 ms
C
200 µV
0.5 ms
D
Normal medium
Trial (#)
Time (ms)
50 µV
E
CNQX + APV +bicuc.
Trial (#)
Time (ms)
50 µV

Figure 3

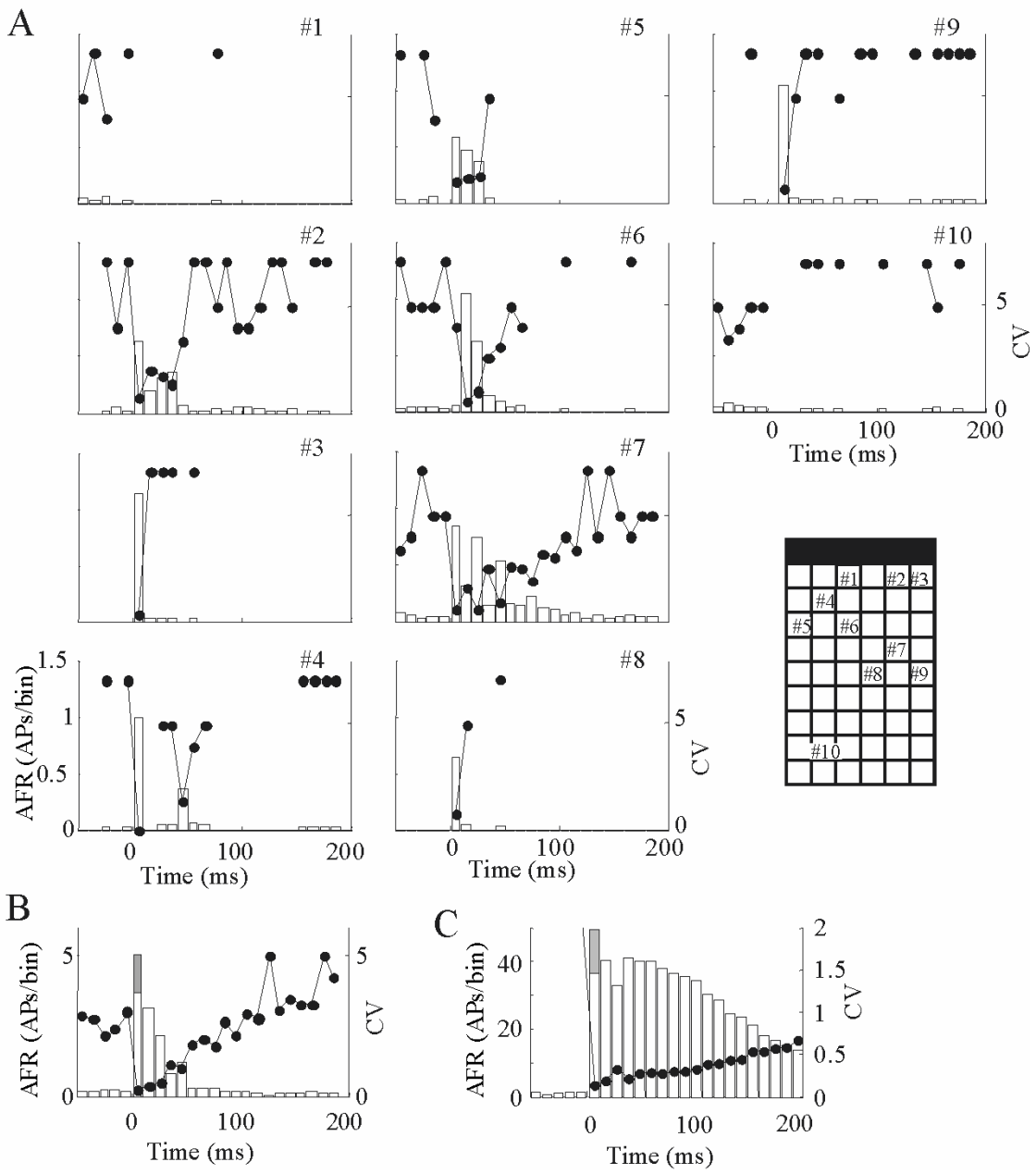
A
#1
#5
#9
#2
#6
#10
#3
#7
#4
#8
AFR (APs/bin)
CV
Time (ms)
0
100
200
1.5
1
0.5
5
#1
#2
#3
#4
#5
#6
#7
#8
#9
#10
B
C
40
20
2
1.5

Figure 4

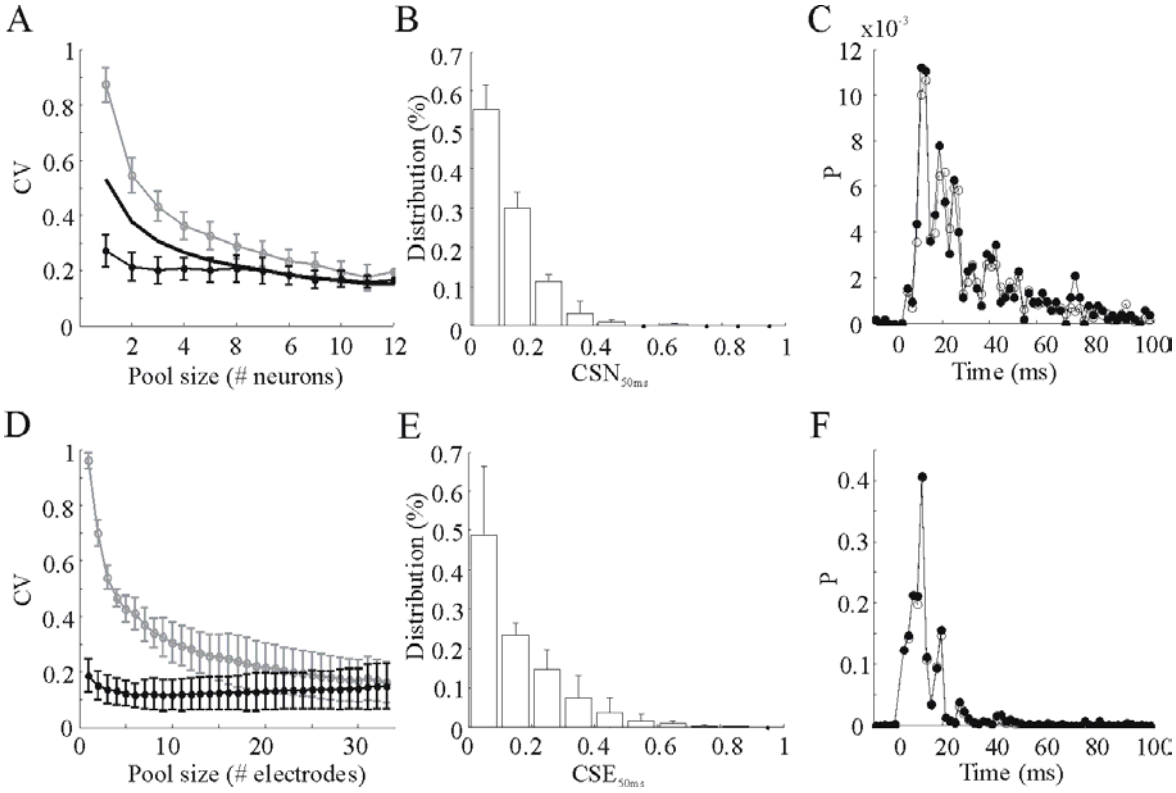
A
CV
Pool size (# neurons)
B
Distribution (%)
CSN50ms
C
x10-3
P
Time (ms)
D
CV
Pool size (# electrodes)
E
Distribution (%)
CSE50ms
F
P
Time (ms)

Figure 5

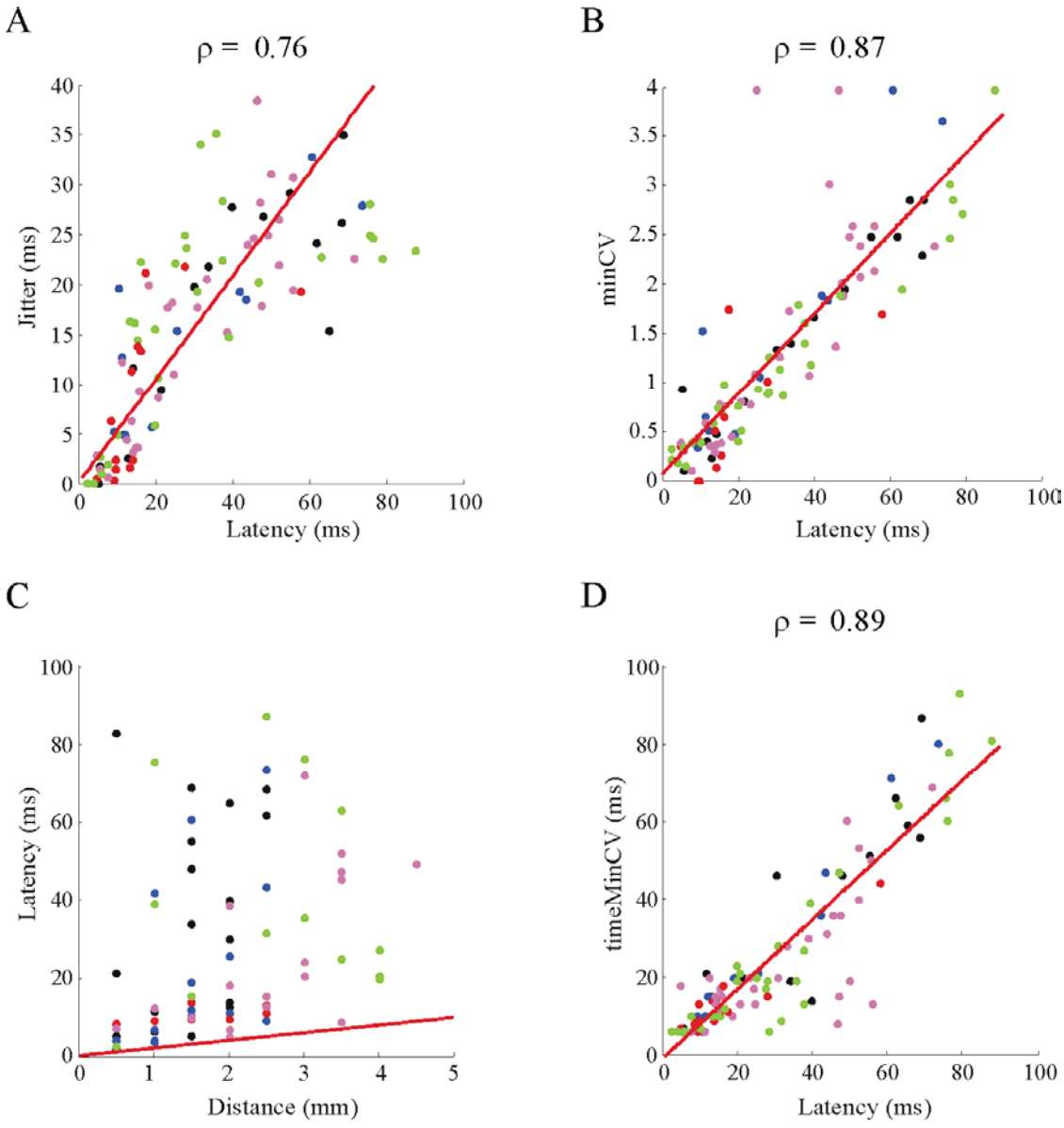
A
ρ = 0.76
Jitter (ms)
Latency (ms)
B
ρ = 0.87
minCV
Latency (ms)
C
Latency (ms)
Distance (mm)
D
ρ = 0.89
timeMinCV (ms)
Latency (ms)

Figure 6

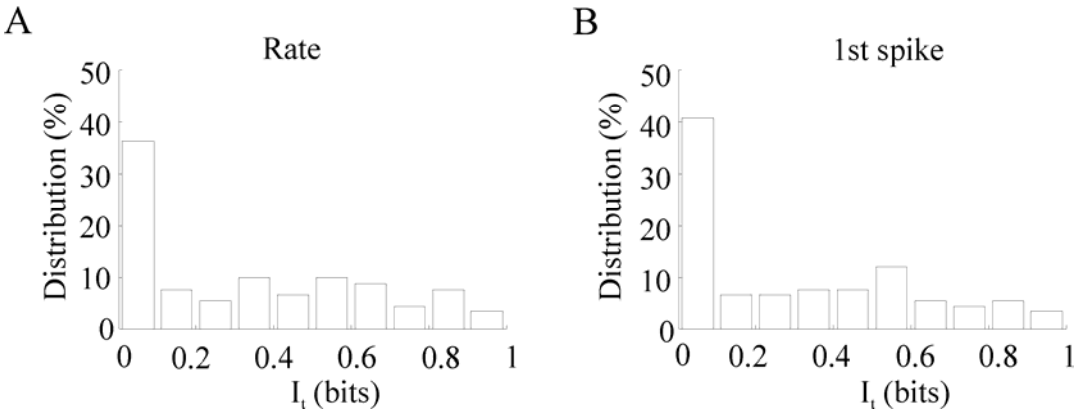
A
Rate
Distribution (%)
50
40
30
20
10
0
0
0.2
0.4
0.6
0.8
1
I_t (bits)
B
1st spike
Distribution (%)
50
40
30
20
10
0
0
0.2
0.4
0.6
0.8
1
I_t (bits)

Figure 7

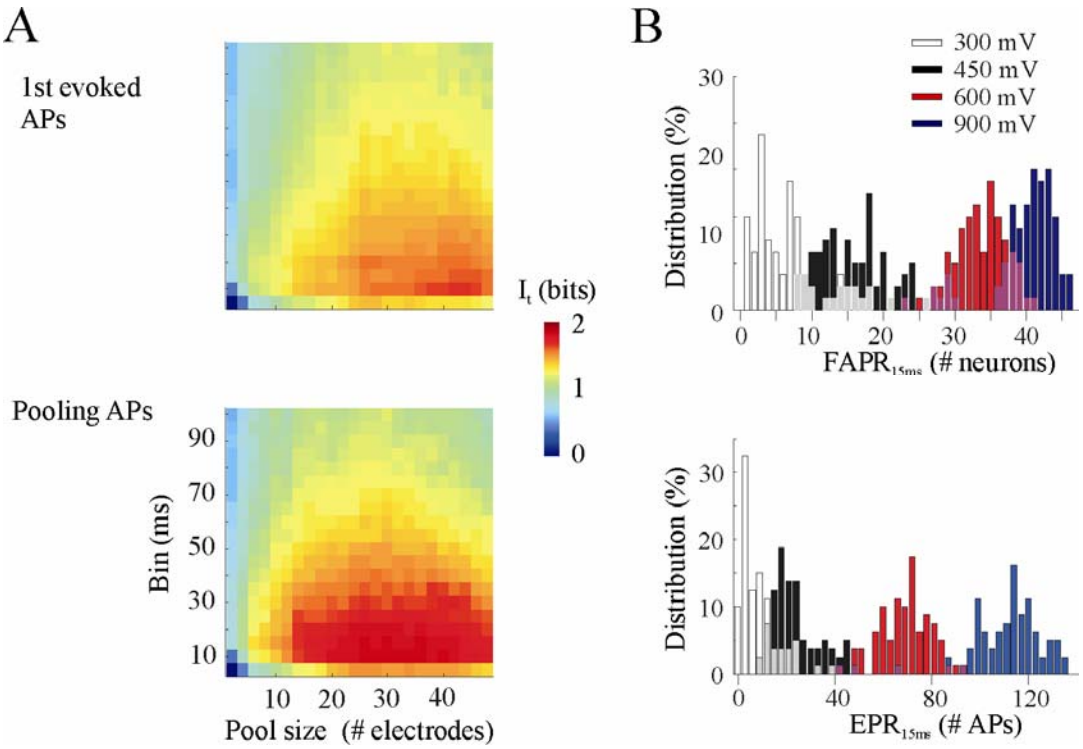
A
1st evoked APs
Pooling APs
Bin (ms)
90
70
50
30
10
10 20 30 40
Pool size (# electrodes)
I_t (bits)
2
1
0
B
300 mV
450 mV
600 mV
900 mV
Distribution (%)
30
20
10
0
0 10 20 30 40
$FAPR_{15ms}$ (# neurons)
Distribution (%)
30
20
10
0
0 40 80 120
EPR_{15ms} (# APs)

Figure 8

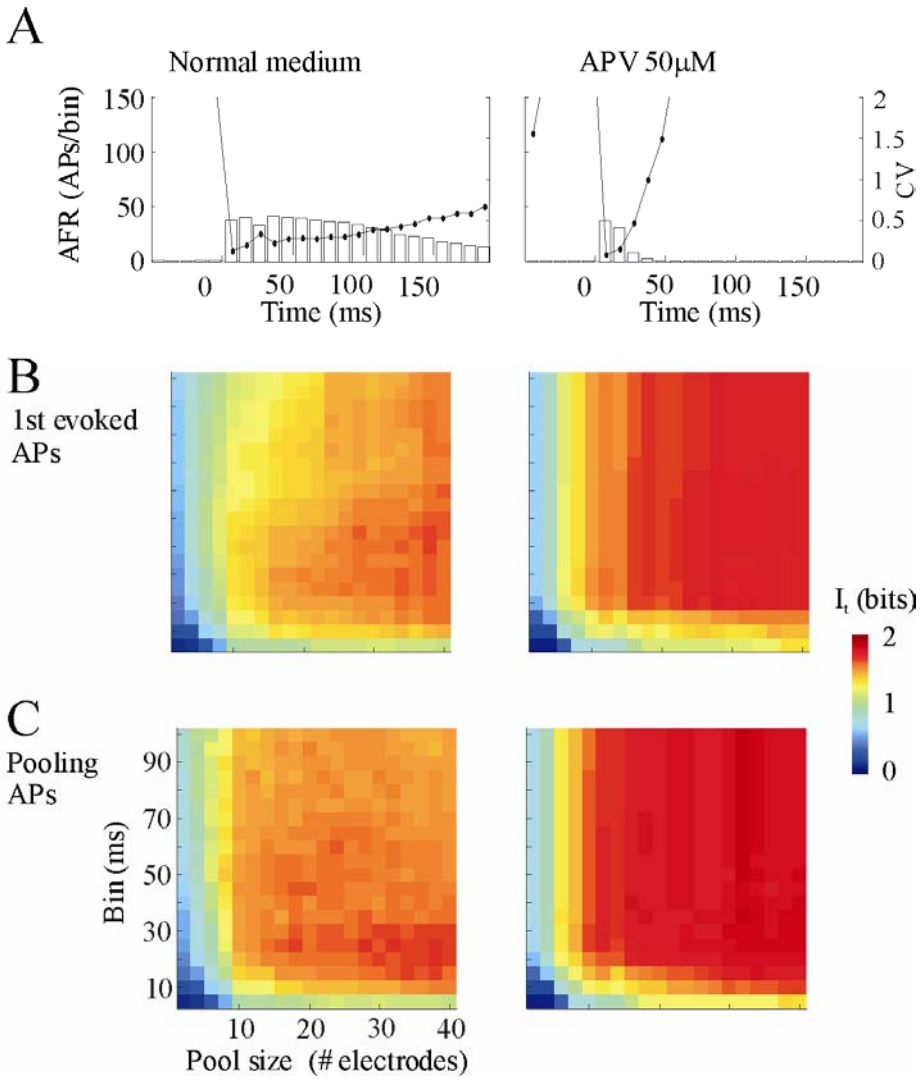
A
Normal medium
APV 50μM
AFR (APs/bin)
150
100
50
0
0
50
100
150
Time (ms)
2
1.5
1
0.5
0
CV
B
1st evoked
APs
C
Pooling
APs
Bin (ms)
90
70
50
30
10
10
20
30
40
Pool size (# electrodes)
I_t (bits)
2
1
0

Figure 9

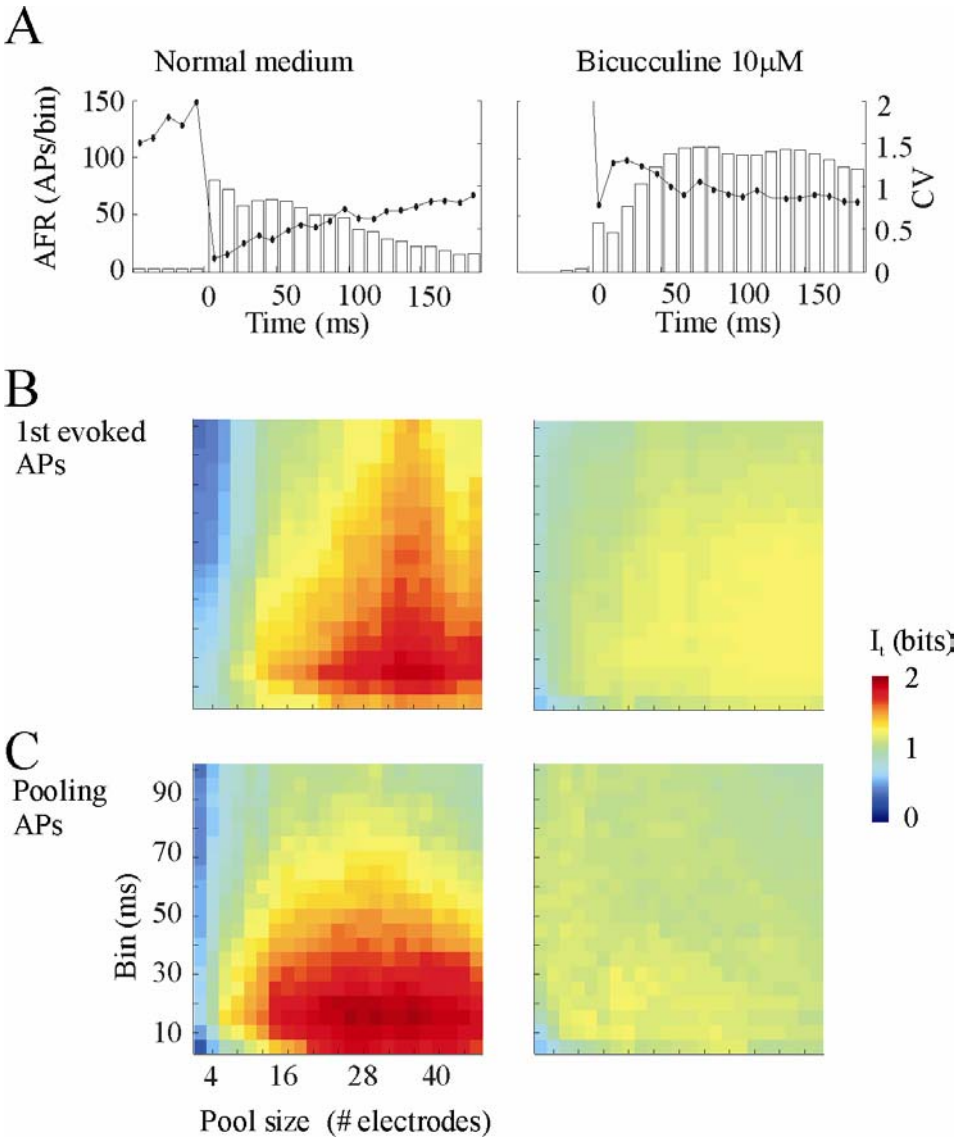
A
Normal medium
Bicucculine 10μM
AFR (APs/bin)
150
100
50
0
0
50
100
150
Time (ms)
2
1.5
1
0.5
0
CV
B
1st evoked
APs
C
Pooling
APs
Bin (ms)
90
70
50
30
10
4
16
28
40
Pool size (# electrodes)
I (bits)
2
1
0

-Paper 3-

Population coding in networks of rat hippocampal neurons

Artcicle in preparation

Paolo Bonifazi, Maria Elisabetta Ruaro, Frederick Broccard and Vincent Torre

Abstract

Neural coding was analyzed in dissociated hippocampal cultures, grown on multielectrode arrays. The efficiency of different coding schemes was considered and quantitatively compared by using criteria from information theory and pattern recognition. When neurons are tuned for the same stimulus pooling or averaging evoked action potentials (APs) provides a nearly optimal coding. On the contrary, when neurons are specific for different stimuli a distributed coding is advantageous. A distributed temporal coding based on the latency of the first evoked APs provided very similar performances as a rate coding integrating action potentials APs over a short time window. The efficiency of all these coding schemes was greatly affected when excitatory synaptic pathways mediated by NMDA receptors and/or inhibitory GABAergic pathways were blocked. Blockage of NMDA receptors improved the efficiency of all coding schemes while blockage of GABAergic synapses significantly deteriorated their efficiency. These results suggest that: i - a nearly optimal coding is represented by pooling the electrical activity of neurons with the same tuning and considering as distributed these averaged activity; ii – a distributed temporal coding based on the first evoked APs is reliable and is the fastest in the nervous system.

Introduction

In the great majority of invertebrate species and in almost all vertebrates, sensory signals are coded in trains of evoked action potentials (APs). In the central nervous systems (CNSs) of all vertebrates messages and signals are exchanged and processed as APs trains. Therefore, information processing in the CNS is based on the analysis of APs trains and on their transformation in other APs trains, ultimately reaching muscles, evoking a motor response. A fundamental problem of Systems Neuroscience is the understanding of the neural code, that is to identify how the stimulus and its characteristics are coded in trains of APs. A common way to tackle this problem is to look for features of the evoked trains of APs which are reproducible from trial to trial and are at the basis of the reliability and robustness of information processing in biological nervous systems (de Ruyter van Steveninck et al., 1997; Zoccolan et al. 2002; Panzeri et al., 2001; Johansson & Birznieks, 2004; Georgopoulos et al., 1986; Nicolelis et al., 1998; Bialek et al., 1991). These features are usually identified by decoding the evoked train of APs so to recover exactly – or almost - the stimulus and its characteristics in every single trial. Thus, by finding optimal ways to decode evoked trains of APs, good clues to understand neural coding and information processing are obtained (Johansson & Birznieks, 2004; Georgopoulos et al., 1986; Nicolelis et al., 1998; Foffani & Moxon, 2004; DeCharms & Merzenich, 1996; McAlpine et al., 2001; Nirenberg & Latham, 2003; Young & Yamane, 1992).

Two coding schemes seem at the basis of the operation of the nervous system: one scheme is based on the exact timing of APs in individual neurons and the other scheme on the firing rate of a population of neurons. These two neural codes are usually referred to as the temporal and the rate code, respectively (Georgopoulos et al., 1986; Hopfield, 1995; DeCharms & Merzenich, 1996; de Ruyter van Steveninck et al., 1997; Nicolelis et al., 1998; Parker & Newsome, 1998; Panzeri et al., 2001; Zoccolan et al. 2002; Johansson & Birznieks, 2004; Nirenberg & Latham, 2003). Experimental evidences from different preparations showed that the firing of individual neurons is noisy and unreliable but by averaging the firing of some dozens of neurons, it is possible to reduce

the variability so to reliably process stimuli (Shadlen & Newsome, 1998; Zoccolan et al. 2002; Bonifazi et al., in press). Instead of averaging, the firing rate of each neuron can be considered separately, i.e. a population rate vector is constructed and coding is based on the statistics of these vectors (Lewis & Kristan, 1998; Georgopoulos et al., 1986). On the other side, temporal codes are based on the precision of AP timing in a population of neurons and information can be encoded either in the synchrony of firing (Gray et al., 1989; Singer & Gray, 1995), or in the relative timing of APs (DeCharms & Merzenich, 1996; O'Keefe & Recce, 1993; Hopfield, 1995) or in the latency of first evoked APs (Thorpe et al., 2001; Johansson & Birznieks, 2004). Correlation can play an opposite role for different coding mechanisms, whereas in most neural codes correlation is deleterious, in the case of temporal coding based on synchronization, it can improve the encoding of information (Nirenberg & Latham, 2003; Schneidman et al., 2003).

In order to analyze population coding in a quantitative way and to compare the rate and temporal codes based on the latency of the first APs, hippocampal neurons from neonatal rats were cultured on a multielectrode array (Ruaro et al., 2005; Arnold et al., 2005). After few weeks in culture the network established synaptic contacts and exhibited the spontaneous firing typical of physiological neuronal networks (Van Pelt et al., 2004; Maeda et al., 1995; Bonifazi et al., in press). Extracellular electrical stimuli, with a different spatial profile and intensity, were delivered to the network, through the MEA. By changing the ionic medium it was possible to modulate the relative weight of excitatory and inhibitory synaptic pathways.

The efficiency of different coding schemes was considered and quantitatively compared by using criteria from information theory and pattern recognition. For neurons with similar tuning properties, a simple pooling of evoked APs provided a good coding/decoding scheme with an efficiency not significantly lower than of a more complex distributed coding. When stimuli differed in their amplitude and their spatial location, a distributed coding was necessary to achieve a good efficiency. A distributed temporal coding based on the latency of the first evoked APs provided very similar performances as a rate coding integrating APs over a short time window.

Blockage of excitatory synaptic pathways mediated by NMDA receptors decreased the correlation in the electrical activity of the network and improved the efficacy of the coding/decoding mechanisms. The opposite effects were observed when inhibitory GABAergic pathways were blocked by bicuculline.

Materials and Methods

Neuronal culture preparation. Hippocampal neurons from Wistar rats (P0-P2) were prepared as previously described (Ruaro et al., 2005). Cells were plated on polyorhitine/matrigel pre-coated MEA (Ruaro et al, 2005) at a concentration of 8 x 10^5 cells/cm^2 and maintained in Minimal Essential Medium with Earle's salts (GIBCO-Brl) supplemented with 5% fetal calf serum, 0.5% D-glucose, 14 mM Hepes, 0.1 mg/ml apo-transferrin, 30 μg/ml insulin, 0.1 μg/ml D-biotin, 1 mM Vit. B12, and 2μg/ml gentamycin. After 48 hours 5 μM cytosine-β-D-arabinofuranoside (Ara-C) was added to the culture medium, in order to block glial cell proliferation. Half of the medium was changed twice a week. Neuronal cultures were kept in an incubator providing a controlled level of CO_2 (5%), temperature (37°C) and moisture (95%).

Electrical recordings and electrode stimulation. The multi electrode array (MEA) system used for electrophysiology was commercially supplied by Multi Channel Systems (MCS). MEA dishes had 10x6 TiN electrodes with an interelectrode spacing of 500 μm and each metal electrode had a diameter of 30 μm. The MEA is connected to a 60 channel, 10 Hz – 3 kHz bandwidth pre-amplifier/filter-amplifier (MEA 1060-AMP) which redirects the signals towards a further electronic processing (i.e. amplification and AD conversion), operated by a board lodged inside a high performance PC. Signal acquisitions were managed under software control and each channel was sampled at a frequency of 20kHz. One electrode was used as ground. Sample data were transferred in real time to the hard disk for later processing. In order to keep the desired environmental conditions during the electrical recordings, the dish was moved to a different incubator providing only a controlled level of CO_2 (5%) and of temperature (37°C). It was also sealed with a cap supplied by MultiChannelSystem in order to eliminate evaporation and contamination. The neuronal culture was then allowed to settle for about 1 hour in order to reach a stationary state. Once the experiment was terminated, usually after 3 to 10 hours, the medium was changed and the dish was moved back to the original incubator.

Each metal electrode could be used either for recording or for stimulation. Voltage stimulation was used and consisted of bipolar pulses lasting 100 μs at each polarity injected through the STG1004 Stimulus Generator. The voltage pulse generated by the STG1004 was applied in parallel to the set of electrodes manually selected for stimulation (simultaneous multi-site stimulation). The amplitude of the voltage pulse was selected between 200 and 900 mV. The minimum amplitude required to evoke an electrical response varied between 200 and 300 mV depending on the responsiveness of the culture and on the geometry of the stimulus. Analogously the lower amplitude giving the maximum response varied between 750 and 900 mV. In order to avoid invasive effects due to the stimulus itself, intensities higher that 900mV were never applied. Once the lowest and highest intensity for a specific culture were selected, two intermediate values were chosen to complete the experiment. In most of the experiments the intensities applied were 300, 450, 600 and 900mV. Six electrodes forming a bar were used for stimulation. Given six electrodes laying on a line of the array, four different spatial patterns of stimulation were used (see fig. 1 A): three patterns composed of two electrodes and one pattern composed of all six electrodes. By using four different intensities and four different spatial configurations, a total of sixteen different stimuli were used. For each stimulus, hundred repetitions of the same stimulus were delivered. A fixed inter-pulse interval of 2s was used. In general, every 30 minutes, a test stimulation was repeated in order to test the stability of the response.

Pharmacology. The following chemicals were used as synaptic blockers: 2-amino-5-phosphonovalerate (APV, Sigma-Aldrich), bicuculline (Sigma-Aldrich) and 6-cyano-7-nitroquinoxaline-2,3-dione disodium salt (CNQX, Sigma-Aldrich). Synaptic blocker/s was/were added to the extracellular medium in their required amount. After completion of the planned measurements, blockers were washed out by four medium replacements, and the original extracellular medium was restored.

Data analysis. Acquired data were analyzed using MATLAB (The Mathworks, Inc.). An artifact lasting 5 – 20 ms, generated by the electrical stimulation, was induced on the recording and

was removed during data analysis (Wagenaar & Potter, 2002; Ruaro et al., 2005). As the artifact removal was not reliable during the first 2 ms following the stimulation, the first 2 ms following stimulation were excluded from the analysis.

Antidromically evoked APs were identified in two different ways: first, all APs observed in the presence of a cocktail of synaptic blockers (50 μM APV, 10 μM bicuculline and 100 μM CNQX) were classified as antidromic APs; second, – in agreement with Wagenaar et al 2004 - all APs with a reliability close to 100% and with a temporal jitter of less than 0.25 ms were classified as antidromic (Wagenaar et al., 2004). APs classified as antidromic were excluded from the analysis. For each individual electrode, we computed the standard deviation (σ) of the noise, ranging from 3 to 6 μV, and only APs crossing the threshold of -5σ were considered . Since each electrode could record the activity of several neurons, varying between 1 and 5, we define here as a multiunit recording the electrical (or neural) activity recorded by a single electrode. AP sorting was obtained using principal component analysis and open source toolboxes for the analysis of multi-electrode data (Egert et al., 2002) with MATLAB.

Calculation of correlation. The degree of correlation of firing in the network was measured by averaging the cross correlation analyzing among electrical recordings obtained from pairs of electrodes. The correlation of the spontaneous activity was computed in the following way: the spontaneous activity was recorded for about 30 minutes and the number of APs recorded at each electrode in a bin width Δt was computed so to obtain a time series (SA_1, …, SA_n). For each pair of electrodes (i, j), the cross correlation between the time series (SA_{i1}, …, SA_{in}) (SA_{j1}, …, SA_{jn}) was calculated according to the equation (Papoulis, 1984)

$$\frac{\sum_{k=1}^{n}(SA_{ik}-\overline{SA_i})(SA_{jk}-\overline{SA_j})}{\sqrt{\left(\sum_{k=1}^{n}(SA_{ik}-\overline{SA_i})^2\right)\left(\sum_{k=1}^{n}(SA_{jk}-\overline{SA_j})^2\right)}} \qquad (1)$$

and the average cross correlation over all the possible pairs of electrodes was computed The correlation of the evoked activity was obtained in the following way: for each electrode the

APs evoked in the time bin Δt following the stimulation were counted at each single trial so to obtain a series of single trial responses depending on the time bin Δt. For each pair of electrodes, the cross correlation between the "trial" series was calculated according to equation (1) and the obtained cross correlation was averaged over all the possible pairs of electrode. The cross correlation for the spontaneous and evoked activity shown in fig. 2, was obtained by varying the size of the bin width Δt.

Neural coding mechanisms. Given a set of different stimuli S_i, we investigated how information about S_i could be encoded in the evoked APs trains. Three distributed mechanisms were considered: a rate code, a 1st evoked APs code and a binary code. For each trial, a population vector was computed in the bin width Δt following the stimulus. The vector dimension N was equal to the number of neurons included in the population (or to the number of active electrodes when multiunit recordings were considered). A single time window Δt following the stimulation, was considered, as we are interested in fast coding mechanisms. In the case of the first evoked APs code, for each neuron (electrode) *i* the inverse of the latency τ_i of the first evoked AP was measured (see fig. 1 B and C) and the vector $(1/\tau_1,\ldots,1/\tau_N)$ was considered. When the latency was larger than the time window Δt, the latency was considered as infinite, i.e. the neuron was supposed not to fire. For the rate code (see fig. 1 B and C), the number of APs (FR_i) evoked in the bin width Δt was counted for each neuron *i* (electrode) and the vector ($FR_1,\ldots,FR_N$) was constructed. For the binary coding, the activity detected in the bin width Δt was converted to "0" when no APs were evoked or to "1" when one or more APs were evoked and a vector of 0 or 1 was obtained. The analysis shown in the paper was obtained varying the bin width Δt. Given S different stimuli and T repetitions of the same stimulus, a total of S*T vector responses were collected for each different coding mechanisms. For the population rate code, for each single trial, the APs evoked in the neural pool ($FR_1, \ldots, FR_N$) were summed (ΣFR_i).

Evaluation of neural coding mechanisms: mutual information and efficiency of decoding. In order to extract the information about the stimulus from the firing of populations of neurons, we used two different procedures: information theory (Shannon & Weaver, 1949) and classification analysis (Ghazanfar et al., 2000; Foffani & Moxon, 2004). Information theory was used to compare the information carried by single neurons and by pairs of neurons. In order to calculate the mutual information, a reliable estimate of conditional probabilities is required and this was not possible when more than two neurons were considered, due to the limited set of trials.

The mutual information *I* (Shannon & Weaver, 1949) was calculated as follow

$$I \equiv I(R,S) = \sum_{s \in S} p(s) \sum_{r \in R} p(r|s) \cdot \log_2 (p(r|s)/p(r)) \qquad (2)$$

where

$$p(r) = \sum_{s \in S} p(s) \cdot p(r|s) \qquad (3)$$

and *p(r)* is the total probability of observing the response *r*. In our case, all stimuli occurred with equal probability, *p(s)*. The response *r* could be the firing rate FR_i of a single neuron *i*, or the distributed firing rate (population vector response) (FR_i, FR_j) of neuron *i* and neuron *j*, or the pooled firing rate ($FR_i + FR_j$) of neuron *i* and neuron *j*. The response was measured in the bin width Δt following the stimulus and the data shown in fig. 4 represent the maximal mutual information obtained by varying Δt. In order to minimize the effects of finite sample size on our estimates of information, the real response *r* was binned into different intervals, following the methods of Panzeri and Treves (1996).

In order to measure the information encoded in the response of a neural population, classification analysis was used and the efficiency of decoding was calculated (Ghazanfar et al., 2000; Foffani & Moxon, 2004). The algorithm used to classify the pattern of neural response, was the *K*-nearest neighbor method (Foffani & Moxon, 2004). During training, half of the trials of stimulation were selected and for each different stimulus the average neural response was calculated (the average is a vector for the distributed codes and a scalar for the population rate code).

Therefore, given a set of S different stimuli, a set of S templates was constructed. During testing, half of the trials were used for classification. Each trial was classified according to its minimal distance (in the Euclidean sense) from the templates. Trials used for the training part were randomly selected and the remaining trails were used for testing (complete cross-validation, Foffani & Moxon, 2004). In order to eliminate any effect due to the random sample of the training trials, the complete cross-validation procedure was repeated 50 times and average values were considered. The analysis reported in fig. 5C, 6 and 7 show how the efficiency of decoding and time of optimal decoding varies as a function of the size of the ensemble of neurons (electrodes). When subsets of N elements (neurons or electrodes) were considered out of N_{max} possible elements, only a maximum of 1000 combinations were randomly selected and averages were calculated. The error bars in the graphics represent standard deviation calculated for 5 different experiments. The analysis shown in fig. 5, 6 (left panels) and 7 (first and second panels from the left) showed the maximal efficiency of retrieval which was computed for the bin width giving maximal efficiency. The analysis of the bin width with optimal response versus the ensemble size (fig. 6 right panels and 7 right panels), considered the minimal bin width where the efficiency was at least 95% of its maximal value.

Measures of the tuning properties of the neurons. The choice of the most appropriate coding scheme depends on the stimuli which have to be coded and on the tuning properties of neurons under consideration. Tuning properties of a neurons to a set of S stimuli were characterized in the following way: let be $AFR_i(S_k)$ the average number of APs of neuron i in the bin width of 50 ms following the stimulus S_k For each pair of neurons i and j and for pairs of stimuli S_k and S_l the relative specificity (RS) of their firing was defined as the minimum between

$$\frac{AFR_i(S_k)\cdot AFR_j(S_l)}{AFR_i(S_l)\cdot AFR_j(S_k)}$$

and its reciprocal.

RS is close to 1 when the two neurons have a similar selectivity for the two stimuli and is close to 0 when the two neurons respond very differently (see fig. 4 B).

When three stimuli or more (S_1,…, S_n) are considered it, neurons could respond in a progressive-like way, i.e.

$$AFR_i(S_1) < AFR_i(S_2) < \ldots\ldots < AFR_i(S_n)$$

This is the case when the stimuli differ in their intensity (with the intensity of S_j larger than the intensity of S_k when $j>k$) and the average firing rate of neuron i increases monotonically with the stimulus intensity. This kind of behavior can be detected by plotting $AFR_i(S_j)$ versus $AFR_i(S_k)$. If points cluster in one semisector for all pairs of stimuli (S_j, S_k) then the neuron i responds to the stimuli in a progressive-like way.

Results

Hippocampal neurons from neonatal rats were grown over a 10 x 6 MEA (fig. 1A). After three or four weeks of culture a well developed neuronal network was observed exhibiting bursts of spontaneous activity. Cultures were primarily composed by glutamatergic neurons and with a small proportion of GABAergic neurons (Bonifazi et al., in press). The MEA on which neurons are grown allows the recording of extracellular voltage signals, produced by APs of all neurons establishing a good electrical contact with MEA electrodes. Extracellular APs larger than 100 μV were often measured. The neuronal culture was stimulated with brief bipolar voltage pulses applied to the electrodes. Stimuli could differ in intensity and in their spatial location, i.e. different pattern of stimulated electrodes (fig. 1 A, see methods). The electrical stimulation produced an artifact lasting 5 – 20 ms (removed off-line, see Methods) in all electrodes, followed by clear evoked APs. Extracellular signals larger than five times the standard deviation of the voltage noise (5σ) were considered. The total number of neurons recorded by a MEA ranged from few dozens to hundreds of units. Out of these it was possible to identify APs originating from individual neurons and its number ranged from 10 to 25 units in different experiments. As neurons of our cultures had long axons, some detected APs were produced by a direct antidromic stimulation of the neuron and were not evoked through synaptic pathways (Wagenaar et al. 2004). In order to identify these antidromic evoked APs, recordings in the absence and in the presence of a cocktail of synaptic blockers (50 μM APV, 10 μM bicuculline and 100 μM CNQX) were compared as described in Bonifazi et al. (in press).

(Fig. 1 near here)

The purpose of the present investigation is to explore and compare coding mechanisms based on the response of a population of neurons. Given N distinct neurons (or electrodes, when multiunit recordings are considered, see Methods), the firing rate of the neurons can be summed (population rate code) or can be considered as distributed (distributed rate coding) (fig.1 B and C, see methods). Distributed codes based on the latency of the first evoked APs are also analyzed

(distributed temporal codings, fig.1 B and C). These coding schemes are compared in term of their ability to recover the stimulus and its characteristics in every trial (Panzeri et al., 2001; Petersen et al., 2001; Ghazanfar et al., 2000; Foffani & Moxon, 2004). In this view decoding is adopted as the criterium to evaluate coding mechanisms.

Two classes of decoding procedures have been proposed so far. One procedure is based on information theory and makes use of the mutual information *I* between features of evoked trains of APs and the stimulus (Panzeri et al., 2001; Petersen et al., 2001), as used in the analysis shown in Fig.4. This procedure requires an estimate of several probabilities, and, due to our limited set of trials, they could not be computed reliably when more than two neurons were considered. In this case, procedures based on pattern recognition and/or classification were used (Ghazanfar et al., 2000; Foffani & Moxon, 2004) as in Figs 5-7. These procedures are based on a training in which the correct mapping between evoked APs trains and stimulus is learned. The *K*-nearest neighbor procedure, possibly the simplest methods of classification, was here used.

Correlation of the spontaneous and evoked electrical activity

The amount of correlation among neurons is a key element of neural coding (Nirenberg & Latham, 2003; Schneidman et al., 2003). Therefore, we have investigated in detail the degree of correlation in the electrical activity of the neuronal culture in bin width time of increasing duration and in the presence of specific blockers of synaptic transmission. The cross-correlation (*CC*) among the number of APs detected on pairs of electrodes was computed as described in the Methods. Fig.2A and B illustrates collected data from 5 cultures for the spontaneous and evoked electrical activity respectively.

(Fig. 2 near here)

In normal conditions, when no synaptic blockers were present in the medium, at bin widths of about 5 ms, the *CC* was around 0.1, both for the spontaneous and for the evoked activity. By increasing the bin width from 5 to 200 ms, whereas for the evoked activity the *CC* slightly

increased from 0.1 to 0.25, while the CC of the spontaneous activity reached 50% of its saturating value for a bin width of about 25 ms. For bin widths larger than 15 ms there was a significant difference between spontaneous and evoked activity (*t*-test, $p<0.05$). When excitatory synaptic pathways mediated by NMDA receptors were blocked by the addition of 50 μM APV, the *CC* was drastically reduced for all bin widths and was less than 0.05 and 0.15 for the evoked and spontaneous activity respectively. The *CC* of the evoked activity in normal conditions and in the presence of APV was significantly different only for bin width larger than 60 ms (*t*-test, $p<0.05$), i.e. when the late phase of the evoked response, mediated by the NMDA receptors, was considered (Jimbo et al., 2000). A very different effect was observed when GABAergic inhibitory pathways were blocked by 10 μM bicuculline. In this case, the *CC* for both the spontaneous and the evoked activity was always significantly larger with respect to normal conditions (*t*-test, $p<0.05$). Moreover, even at a bin width of 25 ms the electrical activity showed a high correlation, larger than 0.5.

Tuning properties of the neurons in response to stimuli varying in intensity and in spatial location

The nervous system is able to process visual stimuli varying for their intensity and location in the visual field and mechanical stimuli applied to different regions of the skin with a different pressure. In order to study similar mechanisms, in the present investigation two classes of stimuli were studied: stimuli differing for their intensity, i.e. the amplitude of the voltage pulse used, and stimuli differing for their spatial location, i.e. delivered through distinct patterns of electrodes (see Methods and fig. 1 B and C). Therefore the response of neurons to three spatial stimuli (X1, X2 and X3, see the grid of fig. 3 C) and to three voltage intensities (300, 450 and 900 mV) was analyzed. Neurons responded in three modes, summarized by the three neurons N1, N2 and N3 shown in fig. 3A and B: neurons could respond only to the highest stimulation intensity and to only spatial stimuli (neuron N3), neurons could respond to more than one intensity but only to one

spatial stimulus (neuron N1) and finally neurons responding to one intensity and to several spatial stimulus (neuron N2). We never observed neurons (5 preparations for a total of 88 neurons) responding to all intensities and to all spatial stimuli. The majority of neurons behaved like neuron N3 (about 55 neurons), this class includes the case of neurons that poorly responded to all the stimuli. Some neurons behaved like neuron N2 (about 28 neurons) and only few neurons behaved like neuron N1 (about 5 neurons).

(Fig.3 near here)

Neurons responded to stimuli with different intensities in a "progressive-like way " (see Methods), i.e. they increased the number of evoked APs when the stimulus intensity increased (see Methods). This property is illustrated in the upper panels of fig. 3C where the *AFR* evoked by a stronger stimulus is plotted against the *AFR* evoked by a weaker stimulus (the three panels correspond to the three possible pairs of stimuli). Points $(AFR_i(S_k), AFR_i(S_j))$ cluster in one semi sector, showing that neurons respond to the stimuli in a progressive-like way (see Methods). On the contrary, when stimuli of different spatial location were considered (fig. 3C lower panels), neurons did not fire in a progressive-like way. This different tuning originates from the fact that a neuron responding to a stimulus of weak intensity responds also to the same stimulus but with stronger intensity. This different selectivity determines optimal distinct coding mechanisms.

Coding the location and the intensity of the stimulus: population and distributed rate code

As shown in Fig.3 neurons have different tuning properties for the intensity and the spatial location of the stimulus. Therefore we have studied how these two features are encoded in the firing of a population of neurons. Information theory and classification analysis were used to measure the decoding or retrieval efficiency.

Given N neurons with a firing FR_i in the bin width Δt , the population rate code is based on the pooled response (i.e. ΣFR_i) and the distributed rate code is based on the vector ($FR_1, \ldots, FR_N$). As shown in Fig. 4A the information encoded by the firing rate *FR* of single neurons (5

preparations for a total of 88 neurons) is generally low. Indeed the mutual information between *FR* and the stimulus was on average 0.2 and 0.4 bits for stimuli with different intensities (upper panel) and with different spatial locations (lower panel) respectively.

(Fig. 4 near here)

The information encoded in the rate slightly increased when pairs of neurons were considered (fig. 4B and C). Fig. 4B illustrates for stimuli varying in intensity, the relation between information encoded in the pooled (I_{pool}) and in the distributed (I_{dist}) responses. The experimental points clustering around the straight line $I_{pool} = I_{dist}$ indicate a substantial equivalence between the two codes. However, the average information encoded in the response of a pair of neurons (0.3 bits) was slightly larger compared to the response of single neurons (0.2 bits) (88 neurons, *t*-test, $p<0.05$). In the case of stimuli differing for their spatial location, for several pairs of neurons I_{dist} was larger than I_{pool}. In this case, the average information encoded in the distributed response (0.5 bits) was larger compared to the response of single neurons (0.4bits) (*t*-test, $p<0.05$). A distributed rate code is more advantageous when neurons in the pair are tuned to different spatial stimuli. Fig. 4D shows that the relative variation of the mutual information $((I_{dist}-I_{pool})/I_{pool})$ is larger when the relative specificity of the pair of neurons (*RS*, see Methods) is close to 0, i.e. when neurons are tuned to different stimuli.

Fig. 5 shows for both type of stimuli and for the distributed (continuous line) and pooled coding scheme (dotted line) how the retrieval efficiency varied, when neurons were added one by one to the ensemble. Figure 5 A shows the dependence of retrieval when the best predictors (i.e. the neurons with the highest mutual information) are one by one included in the ensemble for stimuli varying in intensity (left panel) and in spatial location (right panel). For all neural codes, the efficiency obtained by the four "best neurons" was more than 90%, i.e. few optimal neurons provide almost an optimal coding. The distributed code showed a slightly better efficiency when more than eight neurons were considered (*t-test*, $p<0.05$)

(Fig. 5 near here)

Figure 5 B shows how retrieval is affected when the best predictors are removed one by one from the ensemble (from right to left in the x-axes). The smooth degradation of the ensemble performance confirms that the information is distributed in the population response. Between the two extreme cases shown in fig. 5A and B, fig. 5 C shows the case when neurons are randomly added one by one (an average was calculated over a set of possible random combinations, see Methods). For a single neuron, the efficiency of retrieval of the spatial location (right panel) compared to the intensity (left panel), was higher – reflecting the different average mutual information carried by single neurons for the two features of the stimulus (fig. 4 A) - and increased more rapidly when more neurons were added to the ensemble. The efficiency of intensity retrieval (left) increased more rapidly for the distributed rate code (continuous line) than for the population rate code (broken line), and both codes were equally efficient (about 0.95%) when all the APs of the multiunit recordings (see Methods) were considered.

Comparison of distributed codes: rate, first AP and binary codes

First evoked APs are the fastest signals in the nervous system. In addition, they are usually highly reliable and often carry most of the relevant information (Gawne Richmond 1993, Johansonn 2004, Panzeri et al., 2001 Thorpe et al., 2001; Abeles, 1991; Van Rullen & Thorpe, 2001; Delorme, 2003; Delorme & Thorpe, 2001; Bonifazi et al., in press; Zoccolan et al., 2002;) : first evoked APs are ideal candidates for an efficient and fast code. Therefore we compared the distributed rate code and temporal codes based on the latency of the first evoked APs. Given an ensemble of N neurons and a bin width Δt following the stimulus, three distinct vectors describing the population response were computed: a rate vector, a first AP vector and a binary vector (see Methods and fig. 1).

(Fig. 6 near here)

Fig. 6 shows a comparison of the three neural coding mechanisms for the intensity (upper panels) and for spatial patterns (lower panels) respectively. The dependence of the maximal

efficiency on the ensemble size was not significantly different (n=5, *t*-test, p>0.05) (left panels). For the largest ensemble considered (12 neurons, central panels), the efficiency reached its maximum in a bin width of about 20ms for the intensity retrieval (upper central panel) and of about 10ms for the spatial retrieval (lower central panel). While for the latter case, measuring the response in larger bin widths did not alter retrieval efficiency, in the other task, at larger bin widths, the performance of the rate and of the binary coding schemes slightly decreased and a significant difference was observed between the rate code and the first AP code at a time window of 100 ms (n=5, *t*-test, p<0.05). By increasing the ensemble size, the time needed to obtain the optimal response decayed in an approximately equivalent way for the three neural codes (right panels).

Distributed analysis of pooled signals and effect of APV and bicuculline

Hippocampal neuronal cultures are composed of GABAergic and of glutamatergic neurons (Bonifazi et al., in press), therefore the effect of the selective blockage of excitatory synaptic pathways mediated by NMDA receptors (50 μM APV) and of inhibitory GABAergic pathways (10 μM bicuculline) on information processing was studied.

In this analysis, reported in the graphs of Fig.7, all APs recorded at each electrode were averaged (multiunit recordings, see Methods). Therefore, given N electrodes, vector responses (of N dimensions) were computed as for single neurons (see Methods and fig. 1) but the number of evoked APs and the latency of the first evoked AP (τ) were measured in the pool of neurons recorded by each electrode. In this way t the variability of firing of each element is reduced. Fig. 7 A, B and C show the statistic of single-trial retrieval among 12 stimuli with different intensities and spatial locations in normal conditions, in the presence of 50μm APV and of 10μm bicuculline respectively. Stimuli were delivered at three spatial locations, (indicated by X1, X2 and X3 in the grid of fig. 3C) with four different intensities (see Methods). In all experimental conditions, as shown in the left panels of fig. 7, retrieval efficiency based on the distributed rate response

(distributed rate code, black line) was superior to the pooled rate response (population rate code, red line) (n=5, *t*-test $p<0.05$).

When the retrieval was based on the responses of 32 electrodes, the maximal average efficiency obtained with the two codes, compared to normal conditions, increased of about 10 % in the presence of 50μm APV (*t*-test $p<0.05$) and decreased of about 15% in the presence of 10μm bicuculline (*t*-test $p<0.05$). Therefore, blockage of excitatory pathways mediated by NMDA receptors improves information processing while the opposite effect is observed when inhibitory pathways mediated by GABAergic synapses were blocked. When the three distributed codes (rate, first evoked AP and binary) were compared, the maximal retrieval efficiency in normal conditions was not significantly different (n=5, *t*-test, $p>0.05$) (fig. 7 A second panel from the left) and similarly when NMDA receptors were blocked by 50μM APV (fig. 7 B second panel from the left).

(Fig. 7 near here)

Only in the presence of 10mM bicuculline, the rate code was slightly less efficient compared to the other two codes (n=5, t-test, $p<0.05$). None of the distributed codes outperformed the others. In fact all distributed codes were similarly influenced by synaptic blockers, and the correlation of the electrical activity played the same role for all.

A difference between the three distributed codes was observed varying the time window Δt where optimal response was measured. For the largest ensemble considered (32 electrodes, second panel from the right), the dependence of the average retrieval efficiency on Δt, was different for the three conditions and for the three codes. In normal conditions (fig. 7A second panel from the right), the efficiency reached its maximum for a Δt about 20ms and it remained constant at larger Δt for the first AP code. In fact, neurons with the largest latencies (τ) poorly contribute to the coding since the weight of their response is $1/\tau$. On the contrary, later APs do contribute to the binary and rate coding. Since APs evoked at later times are more variable (Bonifazi et al., in

press), their firing at larger Δt degrades the efficiency of these codes. When inhibitory synaptic pathways were blocked (fig. 7C second panel from the right) the late phase is prolonged, therefore there are more variable APs for longer values of Δt and more the rate and binary codes deteriorate. On the contrary, when the excitatory synaptic pathways were blocked (fig. 7B second panel from the right), no significant difference was observed between the three codes, as the late phase is either reduced or abolished in the presence of APV (Bonifazi et al., in press).

By increasing the ensemble size, the time needed to obtain the optimal response decreased similarly for the three distributed codes (right panels), in normal conditions (fig. 7 A right panels) and in the presence of 50μM APV (fig. 7 B right panels). When 10mM bicuculline was present (fig. 7 C right panels), the time needed to obtain the optimal response at larger ensemble size was lower for the rate code but, as discussed above, the rate code had a slight lower efficiency.

Discussion

The purpose of the present manuscript was to explore and compare coding mechanisms based on the response of a population of neurons. In the present investigation a dissociated neuronal culture of hippocampal neurons was grown over a MEA and stimuli were applied through the extracellular electrodes. Stimuli, consisting of a brief bipolar voltage pulse, differed for their intensity and their spatial location. The neural coding schemes explored were based alternatively either on the number of APs fired by a population of neurons in response to the stimulus or on the latency of the first evoked APs.

Our analysis provides two major conclusions. Firstly, distributed codes based on the firing rate and distributed coding based on the latency of first evoked APs or on a simplified form of it very often provides comparable results when APs on a bin width of about 10-20 ms were considered. Secondly, retrieval efficiency of all coding schemes depends critically on the balance between excitation and inhibition: inhibition of NMDA excitatory receptors decrease the correlation in the electrical activity of the network increasing successful retrieval and inhibition of GABAergic inhibitory receptors increase the correlation in the electrical activity of the network decreasing retrieval efficiency.

Decoding or retrieving the stimulus is really necessary?

Our investigation of the neural code is based on finding the best way to retrieve the stimulus and its characteristics from the evoked trains of APs. In this view, decoding the evoked trains of APs provides the key to understand the neural code. This paradigm cannot be taken as a general rule though: indeed, in simple avoiding reactions, animals and even humans have to escape very quickly from the obstacle or the noxious stimulation and it is not necessary to decode exactly the incoming train of APs (Arisi et al., 2001). On the contrary, when an animal or a human is exploring the environment, it may be very important to be able to retrieve properly the stimulus and its exact characteristics. In the present investigation, we aim at retrieving the intensity and

spatial location of stimuli, as often is the case in vision or in hearing, when it is useful and often necessary to retrieve the intensity of a stimulus and its location.

Pooled versus distributed responses

Considering the number of APs evoked in an ensemble of neurons, when APs are pooled and averaged (population rate code) the relevant information is reduced to a scalar quantity, when the activity of neurons is considered separately (distributed rate coding) a vector of numbers is obtained. It is evident that, whenever it is possible, pooling the activity is computationally economic and therefore advantageous. As shown in Figs. 5 and 6 and in agreement with Bonifazi et al. (in press), it is possible to use pooling to code and retrieve the intensity of a stimulus. In this case, increasing the ensemble size from few neurons to dozens of neurons, both the distributed and the pooled responses allow us to reach an efficiency close to 100 % (fig. 5 C left panel). As shown in Fig.5, the efficiency of pooling grows with a lower slope and requires a larger ensemble of neurons. The choice between pooled and distributed response is strictly linked to the tuning properties of the neurons to the different stimuli. It has already been shown that pooling is the right strategy to handle information from neurons with similar tuning characteristics, as in cortical columns where neurons in the sensory motor cortex respond to deflections of the same whisker (Panzeri et al., 2003) or in the visual cortex to visual stimuli with the same orientation and/or direction (Albright et al., 1984). In present investigation we showed that pooling can be used when neurons respond in a progressive-like way (see fig. 3 C) to the stimuli, as in the case of stimuli differing for their intensity. In this case the firing rate of neurons increases monotonically with the stimulus intensity. On the contrary, a distributed coding is the appropriate strategy for neurons with different tuning characteristics, such as those belonging to distinct cortical columns where neurons respond to deflections of the different whiskers (Panzeri et al., 2003) or in the visual cortex to visual stimuli, with the different orientation and/or direction (Albright et al., 1984). In our

investigation we showed that a distributed coding is advantageous with neurons tuned to different spatial stimuli (fig. 4D).

Comparison of distributed codes and retrieval of information

The comparison of the retrieval efficiency of differently distributed coding (see Fig. 6 and 7) shows that a rate code, based on the latency of the first APs and a binary code provide very similar results. All these distributed schemes seem to be equivalent, even in the presence of synaptic blockers such as APV and bicuculline (see Fig.7). The equivalence of a rate and of a temporal coding using bin width of 20 ms is not surprising: within 20 ms neurons respond to stimuli with one or at most two APs and a rate coding becomes very similar to a coding based on the first evoked AP. Indeed, as shown in Fig.7 the optimal bin width to retrieve correctly the stimulus from the population response is only about 20 ms, which appears to be the time required for one elementary computation. This was clearly shown by the code based on the first evoked AP, when the response of each neuron decayed as the inverse of the latency of the first AP. In this way, early responses contribute more to the retrieval of the stimulus. An integration time of about 20 ms is also suggested by several biophysical mechanisms occurring in that time scale, such as processing in dendrites (Koch, 1999) and timing-dependent synaptic plasticity rule required for hebbian-like learning (Song et al., 2000).

The short time needed for the retrieval of the stimulus prevents a significant role of NMDA receptors known to generate slow and long lasting synaptic potentials (Jimbo et al., 2000). Moreover, in the 20ms following the stimulus, the correlation present in the network activity is low (fig. 2B) while it seem to be more relevant at larger time windows when NMDA receptors are contributing to the network activity (compare open and closed circles of fig. 2B).

In agreement with our results, Bast et al. (2005) showed that in the hippocampus, retrieval depends on AMPA receptor and NMDA are required for storing. Analogously, we previously showed for hippocampal cultures how after LTP-induction - which requires the involvement of

NMDA receptors - pattern recognition, i.e. stimulus retrieval, was obtained by pooling APs in few tens of ms, the time domain of AMPA contribution.

An alternative view recently proposed and rather interesting is that the shape itself of the evoked AP is an essential component of the neural code (de Polavieja et al., 2005) which could code for the past history of the signal reaching the neuron under consideration.

The role of inhibition and excitation and the contribution of the correlation in stimulus retrieval

Inhibition and excitation greatly determine the efficiency of retrieval of all considered coding schemes (see Fig.7). Blockage of excitatory synaptic pathways mediated by NMDA-receptors in agreement with our previous investigation (Bonifazi et al., in press) substantially increased the retrieval capabilities of the neural coding mechanisms explored. An opposite effect was observed when inhibitory synaptic pathways mediated by GABA-receptors were blocked. The correlation of the electrical activity in the network, which is clearly present in the spontaneous activity in normal conditions (fig. 2 A), was highly affected by the balanced presence of inhibition and excitation and therefore played a fundamental role in the retrieval of the stimulus (Mariño et al., 2005). Nevertheless, in normal conditions, the spontaneous activity was clearly correlated even for short time windows of few dozens of ms, the presence of balanced inhibition and excitation allowed to maintain a low correlation in the evoked electrical activity and, as a consequence, it allowed the efficient retrieval of the stimuli. At a large bin width (>80 ms) when the excitatory synaptic pathways mediated by NMDA-receptors contributed to the evoked response, the correlation of the evoked response significantly increased and, as a consequence, the efficiency of rate and of the binary code decreased (fig. 6 central upper panel and fig. 7A second panel from the right). On the contrary, in absence of inhibition the evoked activity was highly correlated, analogously to the spontaneous activity.

Acknowledgements

This work was supported by the EU grant NEURO, by a FIRB grant from the Italian Ministers and by the CIPE grant (GRAND FVG). We thank Manuela Schipizza Lough for carefully reading the manuscript.

References

Abeles, M. (1991). *Corticonics*. Cambridge University Press.

Albright, T. D., Desimone, R., Gross, C. (1984). Columnar organization of directionally selective cells in visual area MT of the macaque. *J. Neurophysiol.* **51**: 16-31.

Arisi, I., D. Zoccolan, Torre V.. (2001). Distributed motor pattern underlying whole-body shortening in the medicinal leech. *J. Neurophysiol.* **86**: 2475-2488.

Arnold, F.J., Hofmann, F., Bengtson, C.P., Wittmann, M., Vanhoutte, P., Bading, H. (2005). Microelectrode array recordings of cultured hippocampal networks reveal a simple model for transcription and protein synthesis-dependent plasticity. *J Physiol.* **563**: 3-19.

Bast, T., da Silva, B.M., Morris, R.G. (2005). Distinct contributions of hippocampal NMDA and AMPA receptors to encoding and retrieval of one-trial place memory. *J Neurosci.* **25**: 5845-56.

Bialek, W., Rieke, F., de Ruyter van Steveninck, R.R., Warland, D. (1991). Reading a neural code. *Science* **252**: 1854–7.

Bonifazi, P., Ruaro, M.E., Torre, V. Statistical properties of information processing in neuronal networks. *Eur. J. Neurosci.* (in press)

DeCharms, R.C., Merzenich, M.M. (1996). Primary cortical representation of sounds by the coordination of action-potential timing. *Nature* **381**:610-613.

Delorme, A., Thorpe, S.J.. (2001). Face identification using one spike per neuron: resistance to image degradations. *Neural. Netw.* **14**:795-803.

Delorme, A. (2003). Early cortical orientation selectivity: how fast inhibition decodes the order of spike latencies. *J. Comput. Neurosci*. **15**: 357-365.

De Polavieja, G.G., Harsch, A., Kleppe, I., Robinson, H.P., Juusola, M. (2005) Stimulus history reliably shapes action potential waveforms of cortical neurons. *J Neurosci.* **25**: 5657-65.

De Ruyter van Steveninck, R.R., Lewen G.D., Strong S.P., Koberle R., Bialek W. (1997). Reproducibility and variability in neural spike trains. *Science* **275**:1805-1808.

Egert, U., Knott, Th., Schwarz, C., Nawrot, M., Brandt, A., Rotter, S., Diesmann, M. (2002). MEA-Tools: an open source toolbox for the analysis of multi-electrode data with MATLAB. *J. Neurosci. Meth.* **17**: 33-42.

Foffani, G., Moxon, K.A. (2004). PSTH-based classification of sensory stimuli using ensembles of single neurons. *J Neurosci Meth* **135**: 107–120.

Foffani, G., Tutunculer, B. Moxon, K.A. (2004). Role of Spike Timing in the Forelimb Somatosensory Cortex of the Rat. *J. Neurosci*. **24**: 7266 –7271.

Gawne, T.J., Richmond, B.J. (1993). How independent are the messages carried by adjacent inferior temporal cortical neurons? *J. Neurosci.* **13**:2758-2771.

Georgopoulos, A.P., Schwartz, A.B., Kettner, R.E. (1986). Neuronal population coding of movement direction. *Science* **233**:1416-1419.

Ghazanfar, A.A., Stambaugh, C.R., Nicolelis, M.A. (2000). Encoding of tactile stimulus location by somatosensory thalamocortical ensembles. *J Neurosci* **20**: 3761–75.

Gray, C.M., Konig, P., Engel, A.K., Singer, W. (1989) Oscillatory responses in cat visual cortex exhibit inter-columnar synchronization which reflects global stimulus properties. *Nature* **338**: 334-7.

Hopfield, J.J. (1995). Pattern recognition computation using action potential timing for stimulus representation. *Nature* **376**:33-36.

Jimbo, Y., Kawana, A., Parodi, P., Torre, V. (2000). The dynamics of a neuronal culture of dissociated cortical neurons of neonatal rats. *Biol Cybern.* **83**: 1-20.

Johansson, R.S., Birznieks, I.. (2004). First spikes in ensembles of human tactile afferents code. *Nat. Neurosci*. **6**: 750 – 757.

Koch, C. (1999) *Biophysics of computation*. Oxford University Press, New York.

Lewis, J.E., Kristan Jr, W.B.. (1998). A neuronal network for computing population vectors in the leech. *Nature* **391**:76-79.

Maeda, E., Robinson, H.P.C., Kawana, A.. (1995). The Mechanisms of Generation and Propagation of Synchronized Bursting in Developing Networks of Cortical Neurons. *J. Neurosci*. **75**: 6834-6845.

Mariño, J., Schummers, J., Lyon, D.C., Schwabe, L., Beck, O., Wiesing, P., Obermayer, K., Sur, M. (2005). Invariant computations in local cortical networks with balanced excitation and inhibition. *Nat Neurosci.* **8**:194-201.

McAlpine, D., Jiang, D., Palmer, A.R. (2001). A neural code for low-frequency sound localization in mammals. *Nat Neurosci* **4**:396–401.

Nicolelis, M.A., Ghazanfar, A.A., Stambaugh, C.R., Oliveira, L.M., Laubach, M., Chapin, J.K., Nelson, R.J., Kaas, J.H. (1998). Simultaneous encoding of tactile information by three primate cortical areas. *Nat. Neurosci*. **1**:621-630.

Nirenberg, S., Latham, P.E. (2003). Decoding neuronal spike trains: how important are correlations? *PNAS* **100**:7348–53.

O'Keefe, J., Recce, M. L. (1993) Phase relationship between hippocampal place units and the EEG theta rhythm. *Hippocampus* **3**:317-330.

Panzeri, S., Treves, A. (1996). Analytical estimates of limited sampling biases in different information measures. *Network Comput. Neural. Syst.* **7**: 87–107.

Panzeri, S., Petersen, R.S., Schultz, S.R., Lebedev, M., Diamond, M.E. (2001). The role of spike timing in the coding of stimulus location in rat somatosensory cortex. *Neuron* **29**:769-777.

Papoulis, A. (1984). *Probability, random variables and stochastic processes*. McGraw-Hill, New York.

Parker, A.J., Newsome, W.T.. (1998). Sense and the single neuron: probing the physiology of perception. *Annu. Rev. Neurosci*. **21**:227-277.

Petersen R.S., Panzeri, S., Diamond, M.E. (2001). Population coding of stimulus location in rat somatosensory cortex. *Neuron* **32**:503–14.

Ruaro, M. E, Bonifazi, P., Torre, V.. (2005). Towards the neurocomputer: image processing and pattern recognition with neuronal cultures. *IEEE Trans. Biomed. Eng.* **52**:371-383.

Schneidman, E., Bialek, W., Berry II, M.J. (2003). Synergy redundancy indipendence in population codes *J Neurosci* **23**: 11539-11553

Shannon, C.E., Weaver, W.. (1949). A mathematical theory of communication. In: *The mathematical theory of communication*. Urbana, IL: University of Illinois.

Shadlen, M.N., Newsome, W.T.. (1998). The variable discharge of cortical neurons: implications for connectivity, computation, and information coding. *J. Neurosci*. **18**:3870-3896, 1998.

Singer, W., Gray, C.M. (1995). Visual feature integration and the temporal correlation hypothesis. *Ann Rev Neurosci.* **18**: 555-86.

Song, S., Miller, K.D., Abbott, L.F. (2000) Competitive Hebbian learning through spike-timing-dependent synaptic plasticity. *Nature* **3**: 916-926.

Thorpe, S., Delorme, A., Van Rullen, R.. (2001). Spike-based strategies for rapid processing *Neural Network* **14**: 715-725.

Van Pelt, J., Wolters, P.S., Corner, M.A., Rutten, W.L., Ramakers, G.J. (2004). Long-term characterization of firing dynamics of spontaneous bursts in cultured neural networks. *IEEE Trans Biomed Eng.* **51**: 2051-62.

Van Rullen, R., Thorpe, S.J.. (2001). Rate coding versus temporal order coding: what the retinal ganglion cells tell the visual cortex. *Neural Comput*. **3**: 1255-1283.

Wagenaar, D.A., Potter, S.M.. (2002). Real-time multi-channel stimulus artifact suppression by local curve fitting. *J Neurosci. Methods* **120**: 113-120.

Wagenaar, D.A., Pine, J., Potter, S.M. (2004). Effective parameters for stimulation of dissociated cultures using multi-electrode arrays. *J Neurosci. Methods* **138**: 27-37.

Young, M.P., Yamane, S. (1999) Sparse population coding of faces in the inferotemporal cortex. *Science* **256**: 1327–31

Zoccolan, D., Pinato, G., Torre, V. (2002) Highly variable AP trains underlie reproducible sensory-motor responses in the medicinal leech. *J. Neurosci*. **22**: 10790-10800.

Figure legends:

Figure 1. Stimuli of different spatial location and vector responses. A Picture of the hippocampal neuronal culture grown on a grid of 10x6 electrodes after three weeks in culture. Electrodes are interspaced by 500μm. The white graph superimposed to the picture schematises the different spatial stimuli delivered through the electrodes. Four different patterns of electrodes were used to stimulate: three patterns composed of two electrodes, the forth composed by the all six electrodes. B Single-trial response of an ensemble of *n* neurons (or electrodes when multiunit recordings are considered, see Methods) to the stimulus. The delivery of the stimulation is indicated by the black vertical arrow. The population response was evaluated in the time window Δt of variable size. τ_i represents the latency of the first evoked AP in the neuron *i*. C Single-trial responses. For the three distributed neural codes examined (rate, first evoked AP and binary code) the response is represented by a vector. For the binary coding, the activity measured in Δt was converted to "0" when no APs were detected or to "1" when one or more APs were detected. For the first evoked AP code, the inverse of the latency τ_i was considered. When the latency was larger than the time window Δt, the latency was considered as infinite, i.e. the neuron was supposed not to fire. For the rate code, the number of APs fired within Δt are counted. For the population rate code, the APs fired within Δt in the all ensemble of neurons were pooled, i.e. summed.

Figure 2. Correlation in the electrical activity of the network. The results are averaged over 5 different preparations. For each dish, the average correlation was calculated between the firing rate of all possible pairs of electrodes. Closed circles, open circles and open squares correspond respectively to control conditions, 50μM APV and 10μM bicuculline. A. Average crosscorrelation of the spontaneous activity for different time bins. The electrical activity was binned into firing rate so to obtain a time series. The cross correlation between the time series of each pair of electrodes was calculated according to equation (1). B. Average crosscorrelation of the evoked

activity for different time bins Δt. For each single trial and each single electrode, the number of APs evoked in the bin Δt following the stimulus was calculated. The cross correlation between the trial time series of each pair of electrodes was calculated according to equation (1).

Figure 3. Tuning properties of the neurons for the distinct features of the stimuli. A Raster plots of three neurons (N1, N2 and N3) in response to stimuli (S1, S2 and S3) of different intensities (300, 450 and 900mV). The stimuli were delivered through the six electrodes indicated by X1, X2 and X3 in the grid of panel C. B: raster plots of neurons N1, N2 and N3, in response to the stimuli of different spatial location X1, X2 and X3. Stimuli of different spatial location were applied at the maximal intensity of 900mV. C. Upper plots: for each neuron, the average firing rate (AFR) in response to the higher (y-axis) and to the lower (x-axis) intensity of stimulation is plotted. The AFR is the average number of APs evoked in the 100ms following the stimulation. Lower Plots: analogous analysis but for stimuli of different spatial location.

Figure 4. Statistics of the mutual information encoded in the rate response of single neurons and of pairs of neurons. Analysis distinguishes stimuli of different intensity (S1, S2, S3) and of different spatial location (X1, X2 and X3) as described in fig. 3. The response of each neuron was represented by the number of APs fired in the time Δt following the stimulus. For pairs of neurons the response was pooled or considered as distributed (i.e. a vector). The maximal mutual information calculated varying Δt was plotted. A. Distributions of the mutual information for single neurons. Vertical arrows indicate the average values. B Mutual information of pairs of neurons for stimuli of variable intensity. The mutual information of the pooled response (I_{pool}) is plotted versus the mutual information of the distributed response (I_{dist}). C I_{dist} versus I_{pool} for stimuli of variable location. In B and C dotted lines represent $I_{pool}=I_{dist}$ and arrows indicate average values. D. For each pair of neurons, the relative variation of I_{dist} in respect to I_{pool} is plotted versus the relative specificity (RS, see Methods). RS is close to 1 when the two neurons have a similar tuning for the two stimuli and is close to 0 when the two neurons oppositely tuned (see fig. 4 B).

Figure 5. Efficiency of single-trial classification of stimuli, for different ensemble sizes. Analysis distinguishes stimuli of different intensity (S1, S2, S3) (left panels) and of different spatial location (X1, X2 and X3) (right panels) as described in fig. 3. Continuous and dotted lines refer respectively to the distributed rate code and to the population rate code. Data are averaged over 5 different preparations. The maximal efficiencies maximized varying the time window Δt of the response are considered. A. The twelve best predictors neurons (i.e. having the maximal mutual information) are one by one added to the ensemble, starting from the absolute best predictor. B. The twelve best predictors neurons (i.e. having the maximal mutual information) are one by one (from right to left in the x-axis) removed from the ensemble, starting from the absolute best predictor. C. Neurons are randomly added one by one to the ensemble. For each different ensemble size, the efficiency is calculated for a large number of possible random combinations and averaged.

Figure 6. Comparison between distributed codes: rate (red), first evoked APs (black) and binary (green) codes. Analysis distinguishes stimuli of different intensity (S1, S2, S3) (upper panels) and of different spatial location (X1, X2 and X3) (lower panels) as described in fig. 3. Data are averaged over 5 different preparations. Left panels: variation of maximal efficiencies of retrieval (maximized varying the time window Δt where the response is measured) when neurons are one by one added to the ensemble. Central panels: efficiency of retrieval for an ensemble of twelve neurons as function of Δt. Right panels. Minimal bin width of maximal efficiency of retrieval as function of the ensemble size. The minimal bin width was calculated considering the minimal Δt where the efficiency reached at least 95% of its maximal value.

Figure 7. Effect of bicuculline and APV on the distributed neural coding mechanisms. Population rate code (red) and distributed rate code (black) are compared in left column of panels. Rate (red), first evoked APs (black) and binary (green) codes are compared in the 2^{nd}, 3^{rd} and 4^{th} column of panels from the right. Twelve stimuli varying in intensity (300, 450, 600, 900mV) and spatial location (X1, X2, X3, see fig. 3) were used. Data are averaged over 5 different preparations. A, B and C correspond respectively to control conditions, 50μM APV and 10μM bicuculline. The

distributed response considered separately the APs recorded by each electrode (multiunit recordings, see Methods). 1st and 2nd column of panels form the left: variation of maximal efficiencies of retrieval (maximized varying the time window Δt where the response is measured) when electrodes are one by one added to the ensemble. For each different ensemble size, the efficiency is calculated for a large number of possible random combinations and averaged. 3rd column of panels form the left: efficiency of retrieval for an ensemble of 32 electrodes as function of Δt. 4th column of panels form the left: minimal bin width of maximal efficiency of retrieval as function of the ensemble size. The minimal bin width was calculated considering the minimal Δt where the efficiency reached at least 95% of its maximal value.

Figure 1

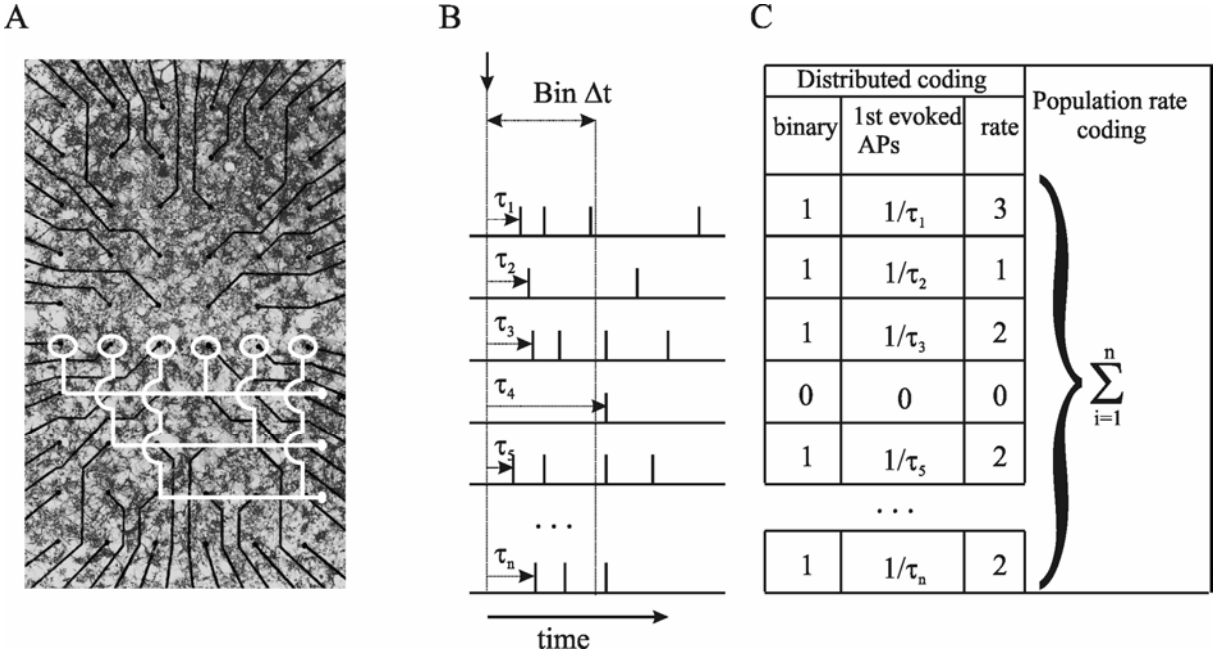
A
B
C
Bin Δt
τ1
τ2
τ3
τ4
τ5
τn
time
Distributed coding
binary
1st evoked APs
rate
Population rate coding
1 1/τ1 3
1 1/τ2 1
1 1/τ3 2
0 0 0
1 1/τ5 2
1 1/τn 2
Σ i=1 n

Figure 2

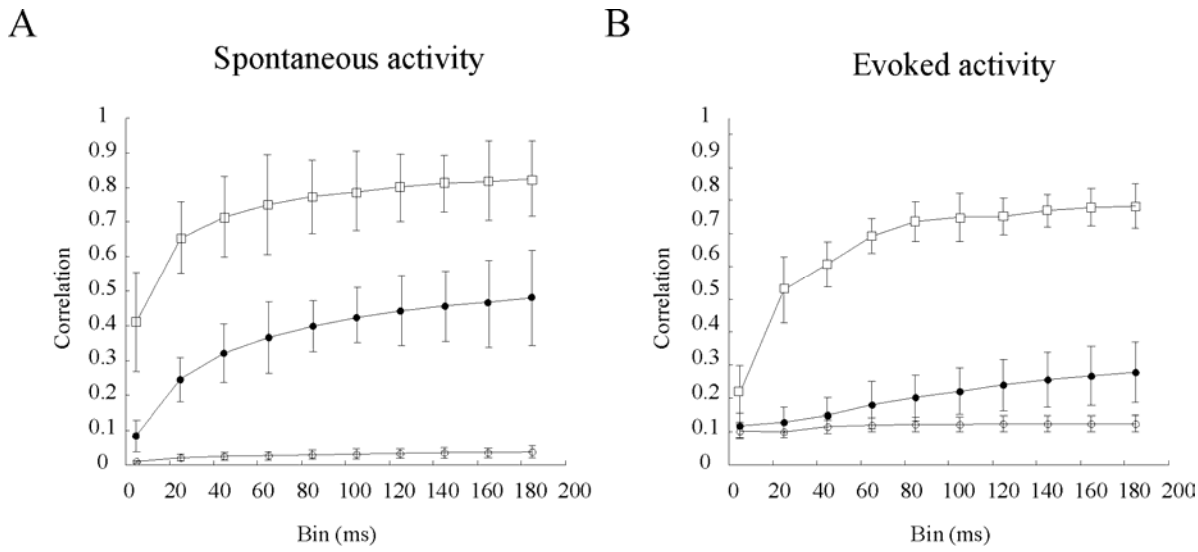
A
Spontaneous activity
Correlation
Bin (ms)
B
Evoked activity
Correlation
Bin (ms)

Figure 3

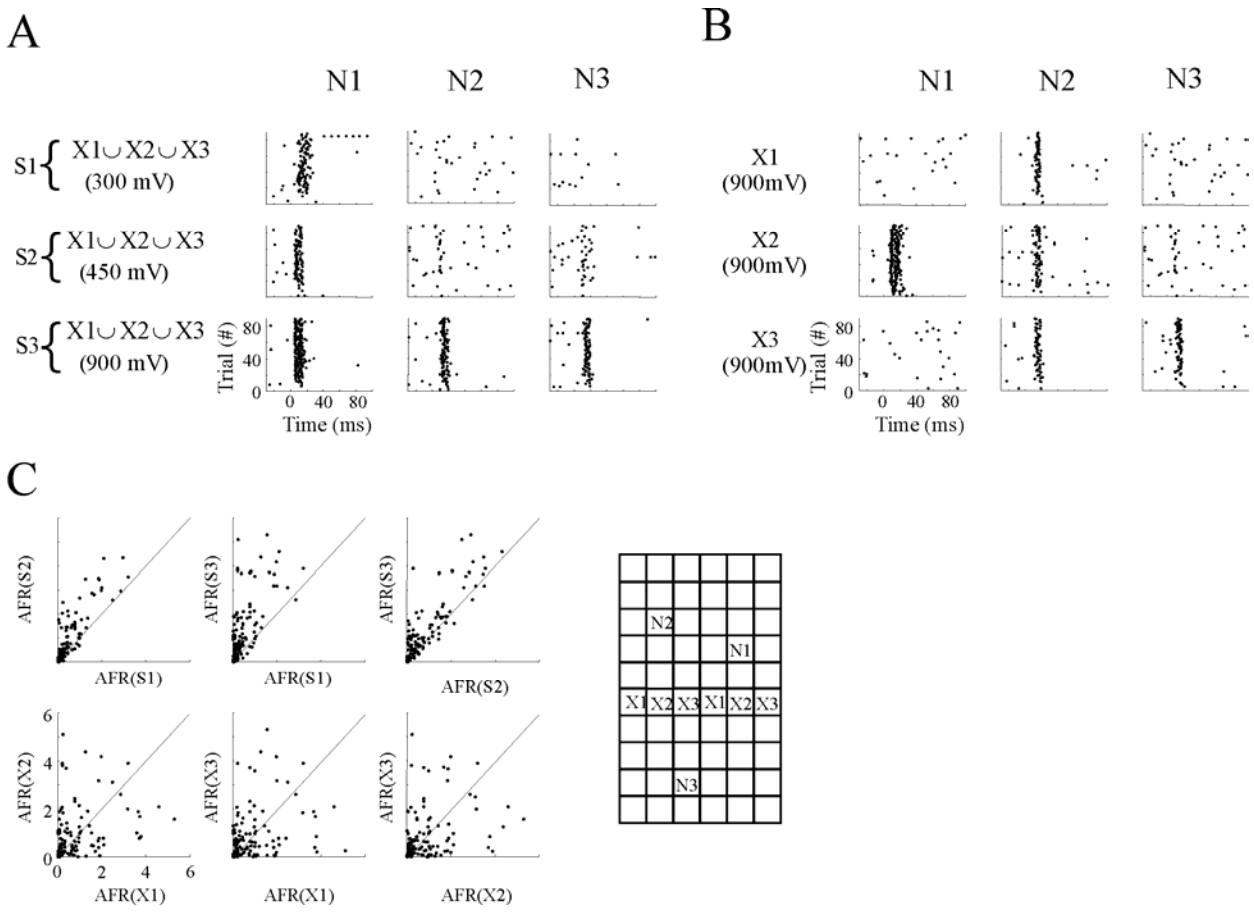
A
B
N1
N2
N3
S1 { X1∪X2∪X3 (300 mV)
S2 { X1∪X2∪X3 (450 mV)
S3 { X1∪X2∪X3 (900 mV)
X1 (900mV)
X2 (900mV)
X3 (900mV)
Trial (#)
80
40
0
0 40 80
Time (ms)
C
AFR(S2)
AFR(S1)
AFR(S3)
AFR(S1)
AFR(S3)
AFR(S2)
AFR(X2)
AFR(X1)
AFR(X3)
AFR(X1)
AFR(X3)
AFR(X2)
0 2 4 6
N2
N1
N3
X1 X2 X3 X1 X2 X3

Figure 4

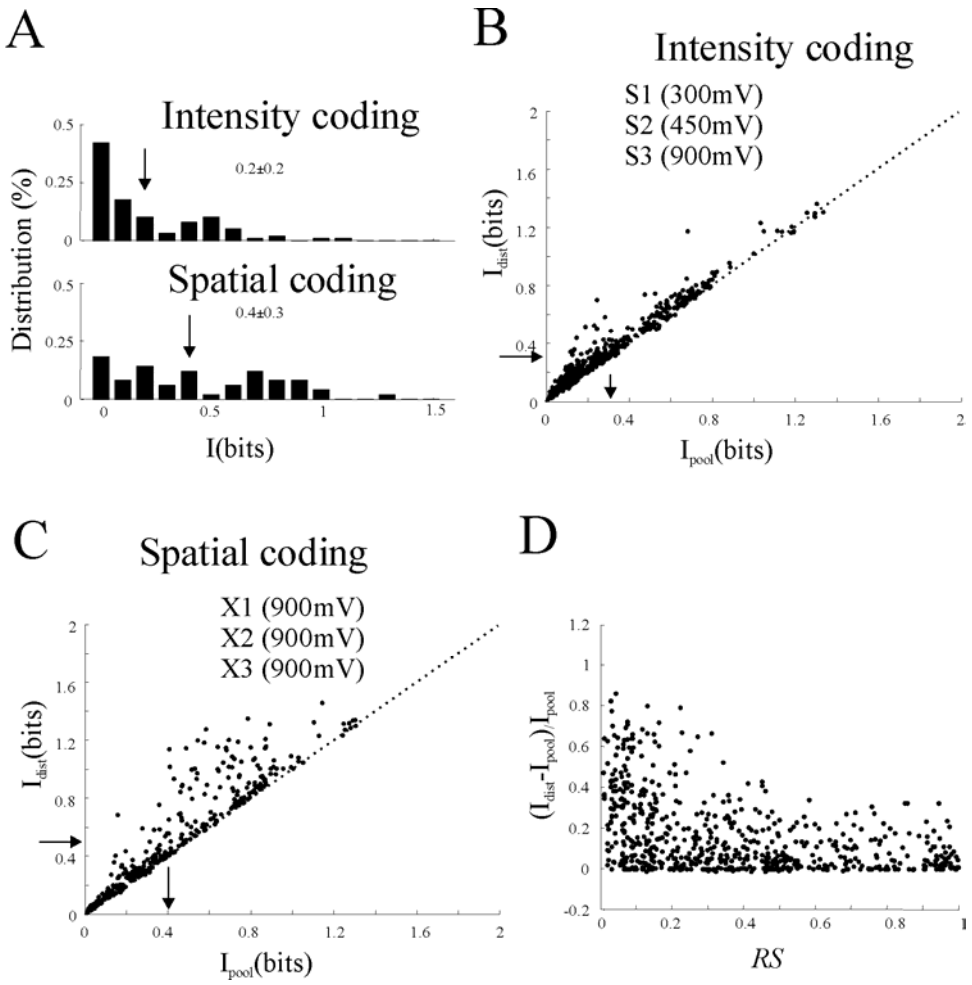
A
Intensity coding
0.2±0.2
Spatial coding
0.4±0.3
Distribution (%)
I(bits)
B
Intensity coding
S1 (300mV)
S2 (450mV)
S3 (900mV)
I_{dist}(bits)
I_{pool}(bits)
C
Spatial coding
X1 (900mV)
X2 (900mV)
X3 (900mV)
I_{dist}(bits)
I_{pool}(bits)
D
$(I_{dist}-I_{pool})/I_{pool}$
RS

Figure 5

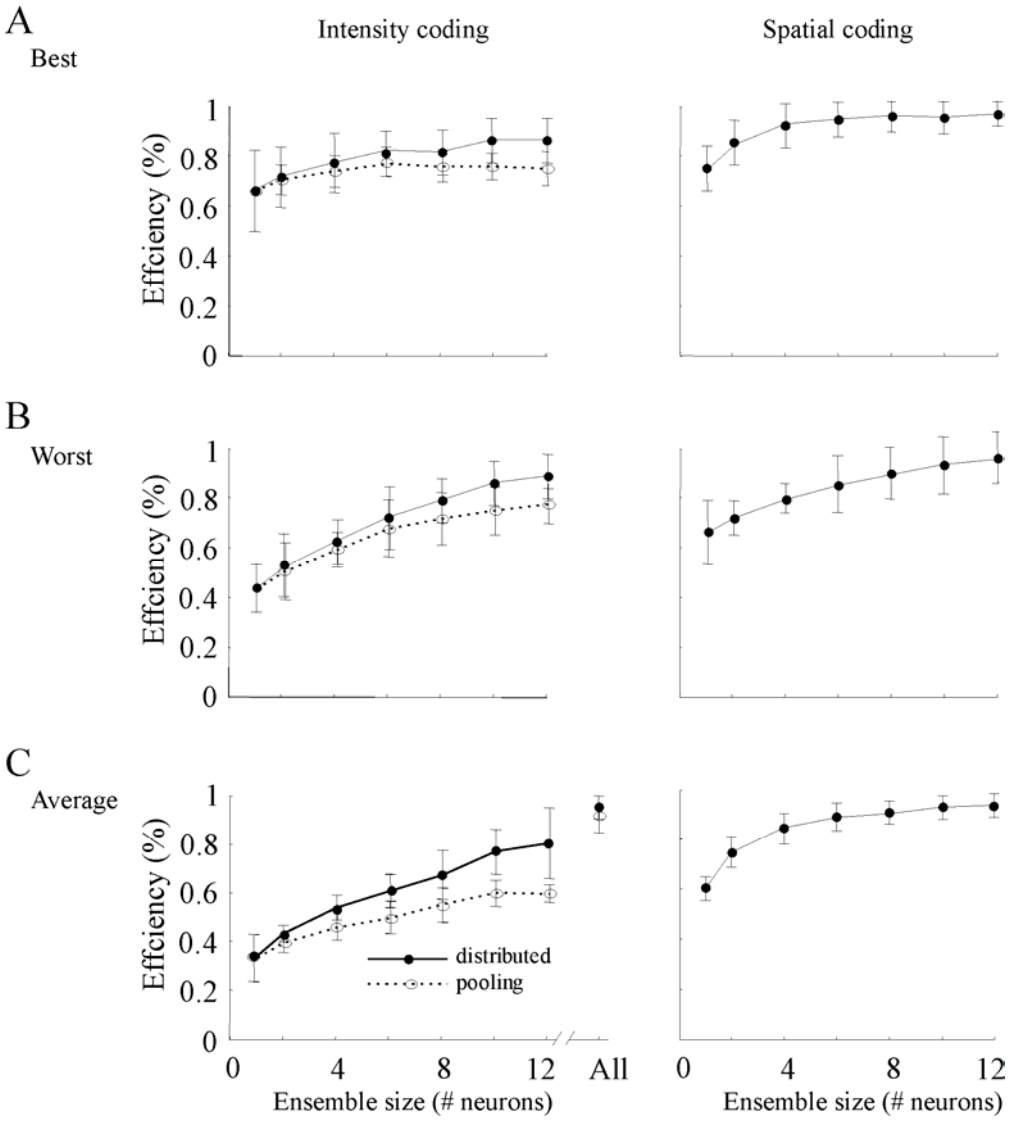
A
Best
Intensity coding
Spatial coding
Effciency (%)
1
0.8
0.6
0.4
0.2
0
B
Worst
C
Average
distributed
pooling
0
4
8
12
All
Ensemble size (# neurons)

Figure 6

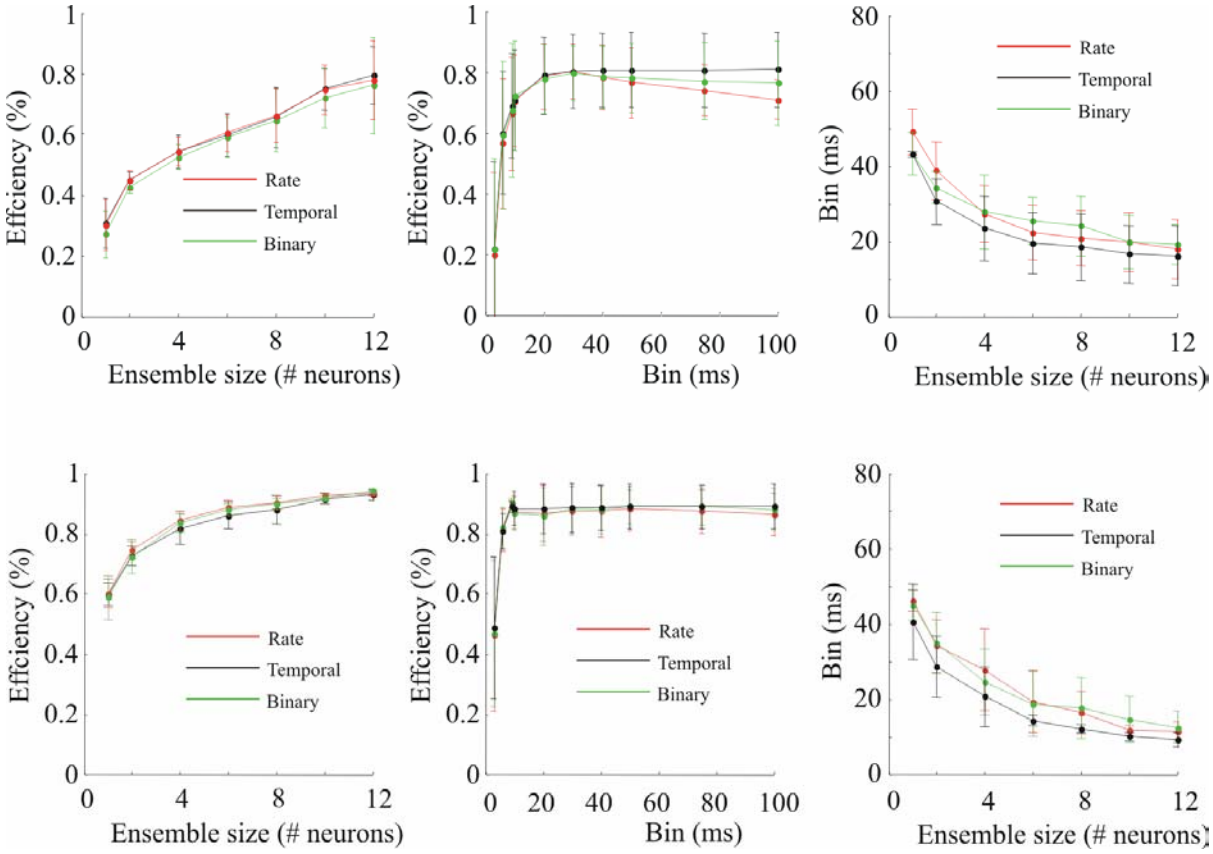
Effciency (%)
Ensemble size (# neurons)
Rate
Temporal
Binary
Effciency (%)
Bin (ms)
Bin (ms)
Ensemble size (# neurons)
Rate
Temporal
Binary
Effciency (%)
Ensemble size (# neurons)
Rate
Temporal
Binary
Effciency (%)
Bin (ms)
Rate
Temporal
Binary
Bin (ms)
Ensemble size (# neurons)
Rate
Temporal
Binary

Figure 7

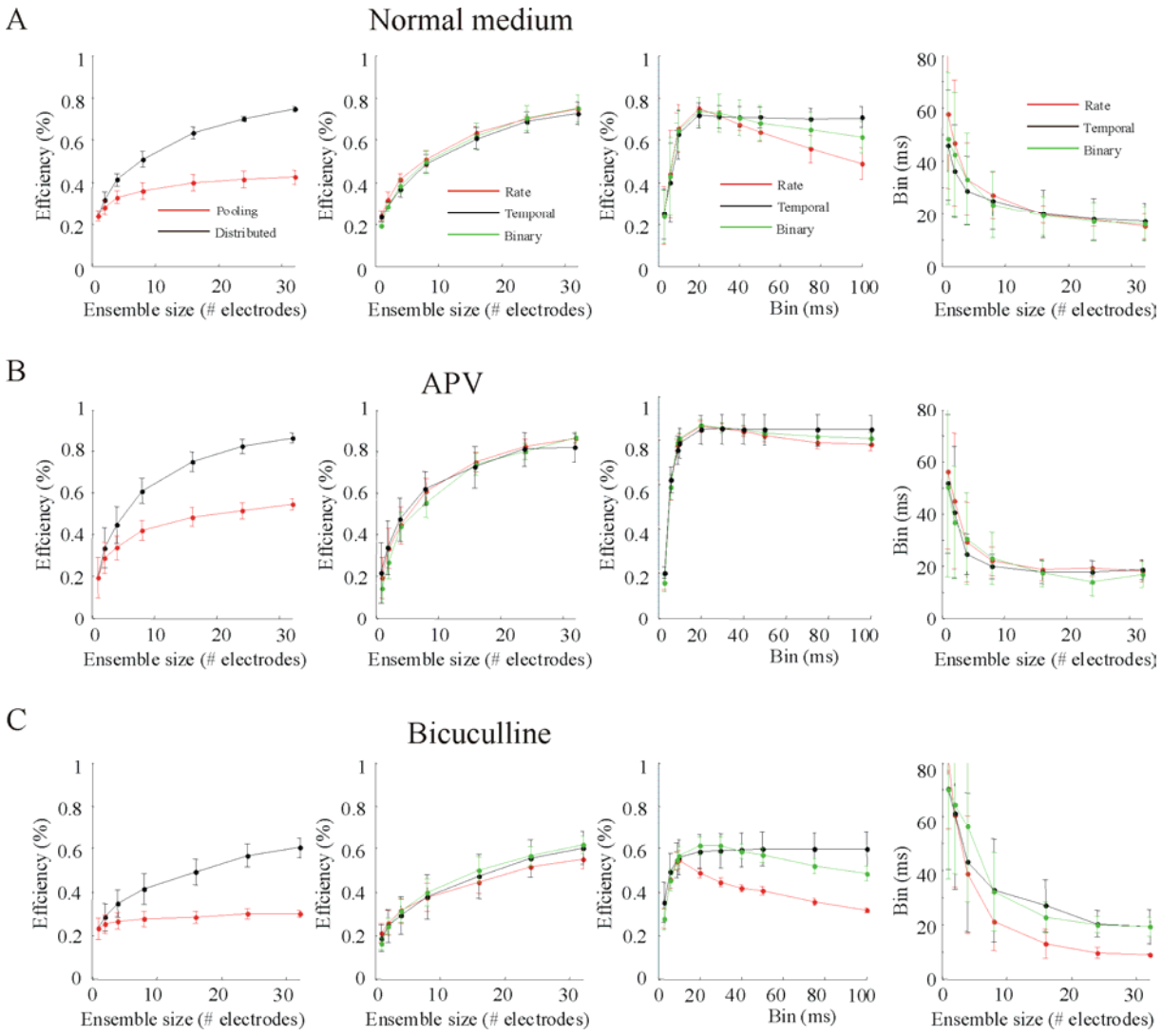
A
Normal medium
B
APV
C
Bicuculline
Efficiency (%)
Ensemble size (# electrodes)
Pooling
Distributed
Rate
Temporal
Binary
Bin (ms)

4. Conclusions and future perspectives

In my thesis I have studied information processing in neuronal networks. In particular I have analysed dissociated neuronal cultures of rat hippocampal neurons grown on MEAs. This system provided three major advantages for investigating the computational capabilities of neuronal networks. First, it was possible to record the activity of a large ensemble of neurons in the network (up to two hundreds), a fundamental requisite to investigate parallel processing in neural systems. Secondly, the use of extracellular electrodes allowed the delivery of controlled stimuli (i.e. INPUT) to the network. Stimuli could vary in amplitude, spatial location, spatial profile and frequency. In this way the network was processing well-known INPUT. Thirdly, varying the extracellular conditions, it was possible to block selectively the contribution of excitatory and inhibitory pathways during information processing.

My major research findings concern the role of single neurons, neuronal populations, inhibition and excitation in information processing and how optimal fast coding is obtained by distributed population codes.

When a neuron was post-synaptically excited by the stimulation, the evoked firing was composed of a first reliable AP followed by less reliable APs. The degree of correlation on short binwidths (i.e. few dozens of ms) between coactivated individual neurons was usually small, i.e. coactivated neurons fire almost independently on a short time scale. As a consequence of this statistical independence, when the electrical activity was pooled over a population of coactivated neurons (N), the variability of the pooled response (measured by the CV) decreased as $1/\sqrt{N}$. Since neurons had an average CV of 0.5, a good reproducibility - with a CV of less than 0.1 - was obtained by pooling the electrical activity of at least 25 neurons in a few dozens of ms following the stimulus. These conclusions are remarkably similar to those obtained in intact neuronal tissues or small nervous systems (Zoccolan et al., 2002; Shadlen & Newsome, 1998; Nicolelis et al., 1998). In terms of computation, it means that neurons are noisy and unreliable computing elements and a

good signal-to-noise ratio can be obtained by pooling the electrical activity over an ensemble of neurons. Therefore, neural ensembles composed of at least few dozens of neurons (column-like ensembles) can be considered reliable computing elements. In fact, when neurons were used as computing elements for pattern recognition (after LTP induction) or intensity discrimination, pooling the neuronal activity over a very large number of neurons (of the order of 100) enabled a successful discrimination over a single trial. In a different way, when neurons were used for image processing (a task commonly solved by conventional silicon devices which optimally require parallel computation), a low pass filtering was quickly and easily obtained in about 10 ms but the result of the computation was more noisy compared to pattern recognition. In fact pooling was restricted to neurons recorded by a single electrode, i.e. less than 6 neurons, a number which is too low to guarantee a very low noise signal. These results represent a proof of principle of the feasibility of neurocomputers, i.e. hybrid devices composed of biological neurons and artificial elements, ideal machines capable of massive parallel computation. In fact, I showed that using neuronal networks grown on MEAs, it was possible to process simple patterns using two fundamental properties of natural neuronal networks: parallelism and learning. The parallel processing performed by the neuronal networks allowed filtering of digital images in just a few milliseconds, independently from the dimension of the image processed. In standard digital computers performing serial computation, the time required for the same computation would diverge exponentially with the size of the images. Additionally, neuronal cultures could be trained to recognize a simple spatial pattern, due to a controlled induction of long-term potentiation. When filtering and learning were combined it was possible to extract features from processed images.

In my thesis I showed how optimal coding mechanisms depend on the tuning properties of the neurons. In fact pooling provides a nearly optimal coding when neurons are tuned to the same stimuli, as in the case of stimuli differing in their intensity. On the contrary, when neurons are specific for different stimuli, as in the case of stimuli of different spatial location, a distributed coding is required. My conclusions are very similar to what has been observed in *in-vivo* networks.

It has already been shown that pooling is the right strategy to handle information from neurons in the same cortical columns, where neurons share similar tuning characteristics (Panzeri et al., 2003; Albright et al., 1984). On the contrary, a distributed coding is the appropriate strategy for neurons belonging to distinct cortical columns where neurons have different tuning characteristics (Panzeri et al., 2003; Albright et al., 1984).

A further achievement of my thesis was to show how distributed codes based on the firing rate and distributed codes based on the latency of first evoked APs provide comparable results. These coding schemes allowed reliable retrieval of the stimulus in few dozens of ms. Information processing based on the first evoked APs over an ensemble of neurons is possibly the fastest computational scheme adopted by the nervous system. Several models and experiments in *in-vivo* networks demonstrated the feasibility of neural coding mechanisms based on the first evoked APs (Johansson & Birznieks, 2004; Thorpe et al., 2001). My results suggest that a few dozens of ms is the time required for one elementary computation. An integration time of about 20 ms was also suggested by several biophysical mechanisms occurring in that time scale, such as processing in dendrites (Koch, 1999) and a timing-dependent synaptic plasticity rule required for Hebbian-like learning (Song et al., 2000). I showed that the retrieval of the stimulus obtained in 20 ms prevented a significant role of NMDA receptors. In agreement with my results, Bast et al. (2005) showed that in the hippocampus, retrieval depends on AMPA receptors and NMDA receptors are required for storing. Analogously, I showed that after LTP-induction - which requires the involvement of NMDA receptors - stimulus retrieval was obtained in a few tens of ms, the time domain of AMPA contribution.

A major achievement of my thesis was to show that inhibition and excitation underlie variability and reliability of the evoked response and influence the network's potential to process information. Blockage of excitatory synaptic pathways mediated by NMDA-receptors substantially decreased the correlation of the electrical activity and increased the retrieval capabilities of the neural network. An opposite effect was observed when inhibitory synaptic pathways mediated by

GABA-receptors were blocked. This remarkable deterioration of information processing was caused by an increased variability of the early phase of the evoked response and by the occurrence of large spontaneous bursts of synchronized electrical activity. My results support the idea (Shadlen & Newsome, 1998; Mariño et al., 2005; Turrigiano & Nelson, 2004; Wehr & Zador, 2003; Zhang et al., 2003) that, in order to process information in a reliable way, neuronal networks require an appropriate balance of excitation and inhibition, so that a stimulus can generate a reliable neuronal response, distributed through the network.

The conclusions of my investigation concering the neural coding mechanisms of processing information are based on the study of brief transient stimuli, like that obtained by extracellular bipolar voltage pulses. Neural codes based on the first evoked APs allow reliable processing of this type of stimuli, as shown even in *in-vivo* networks. In order to process different types of stimuli like continuous, static or slow varying stimuli, the nervous system probably uses different neural coding mechanisms. Studies *in-vivo* (Gray et al., 1989; DeCharms & Merzenich, 1996) showed how neuronal networks could use synchrony or the relative timing of firing in a population of neurons to process information. Therefore, in the future, it could be interesting to investigate these neural coding mechanisms in *in-vitro* networks. For example, by applying high frequency stimuli of low amplitude the firing rate of the network might not vary significantly but a regime with correlated firing could be present.

In general, my results showed that *in-vitro* neuronal networks are valid and reliable systems for studying how information can be processed by the nervous system. Having described in detail how information processing is performed by dissociated hippocampal networks, my model could be used to compare different networks with different properties. For example it could be interesting to study how information is processed by neuronal networks derived from stem cells or by networks extracted from animals with genetic mutations.

5. References

Agmon-Snir H., Carr, C.E., Rinzel, J. (1998). The role of dendrites in auditory coincidence detection. *Nature* **393**: 268-72.

Arnold, F.J., Hofmann, F., Bengtson, C.P., Wittmann, M., Vanhoutte, P., Bading, H. (2005). Microelectrode array recordings of cultured hippocampal networks reveal a simple model for transcription and protein synthesis-dependent plasticity. *J Physiol.* **563**: 3-19.

Aziz, T., Yianni, J. (2003). Deep brain stimulation for unusual movement disorders. *ACNR*, **3**: 26-27.

Banker, G., Goslin, K. (1998). *Culturing Nerve Cells*. MIT Press, Cambridge, MA.

Barlow, H. (1972). Single units and sensation: a neuron doctrine for perception. *Perception* **1**: 371–-394.

Barlow, H.B., Hill, R.M., Levick, W.R. (1964). Retinal ganglion cells responding selectively to direction and speed of image motion in the rabbit. *J. Physiol.* **173**: 377–407

Barlow, H.B., Levick, W.R. (1965). The mechanism of directionally selective units in rabbit's retina. *J. Physiol.* **178**: 477–504

Basarsky, T.A., Purpura, V., Haydon, PG. (1994). Hippocampal synaptogenesis in cell-culture - developmental timecourse of synapse formation, calcium influx, and synaptic protein distribution. *J Neurosci.*, **14**: 6402-6411.

Bast, T., da Silva, B.M., Morris, R.G. (2005). Distinct contributions of hippocampal NMDA and AMPA receptors to encoding and retrieval of one-trial place memory. *J Neurosci.* **25**: 5845-56.

Ben-Ari, Y. (2001). Developing networks play a similar melody. *Trends Neurosci* **24**: 353–360.

Canepari, M., Bove, M., Maeda, E., Cappello, M., Kawana, A. (1997). Experimental analysis of neuronal dynamics in cultured cortical networks and transitions between different patterns of activity. *Biol Cybern.* **77**: 153-62

Chapin, J.K. (2004). Using multi-neuron population recordings for neural prosthetics. *Nat Neurosci.* **7**: 452-5.

Corner, M. A., Ramakers, G. J. (1991). Spontaneous bioelectric activity as both dependent and independent variable in cortical maturation. Chronic tetrodotoxin versus picrotoxin eåects on spike-train patterns in developing rat neocortex neurons during long-term culture. *Ann. N.Y. Acad. Sci.* **627**: 349-353.

Dan, Y., Poo M.M. (2004) Spike timing-dependent plasticity of neural circuits. *Neuron* 44: 23-30.

DeCharms, R.C., Merzenich, M.M. (1996). Primary cortical representation of sounds by the coordination of action-potential timing. *Nature* **381**:610-613.

De Polavieja, G.G., Harsch, A., Kleppe, I., Robinson, H.P., Juusola, M. (2005). Stimulus history reliably shapes action potential waveforms of cortical neurons. *J Neurosci.* 25: 5657-65.

Dobelle, W. H. (2000). Artificial Vision for the Blind by Connecting a Television Camera to the Visual Cortex. *ASAIO J.* **46**: 3-9.

Eytan, D., Brenner, N., Marom, S. (2003) Selective adaptation in networks of cortical neurons. *J. Neurosci.* **23**: 9349– 9356

Fetz, E.E., Gustafsson, B. (1983). Relation between shapes of post-synaptic potentials and changes in firing probability of cat motoneurones. *J Physiol.* **341**:387-410.

Foffani, G., Moxon, K.A. (2004). PSTH-based classification of sensory stimuli using ensembles of single neurons. *J Neurosci Meth* **135**: 107–120.

Fried, I., MacDonald, K. A., Wilson, C. (1997) Single neuron activity in human hippocampus and amygdale during recognition of faces and objects. *Neuron* **18**: 753-765.

Furukawa, S., Middlebrooks. J.C. (2002). Cortical representation of auditory space: information-bearing features of spike patterns. *J Neurophysiol* **87**:1749-1762.

Georgopoulos, A.P., A.B.. Schwartz, R.E., Kettner. (1986). Neuronal population coding of movement direction. *Science* **233**:1416-1419.

Gray, C.M., Konig, P., Engel, A.K., Singer, W. (1989). Oscillatory responses in cat visual cortex exhibit inter-columnar synchronization which reflects global stimulus properties. *Nature* **338**: 334-7.

Gross, C. G., Bender, D. B., Rocha-Miranda, C. E. (1969). Visual receptive fields of neurons in inferotemporal cortex of the monkey. *Science* **166**: 1303-1306.

Gross, C. G., Rocha-Miranda, C. E., Bender, D. B. (1972). Visual properties of neurons in inferotemporal cortex of the macaque. *J. Neurophysiol.* **35**: 96-111.

Habets, A.M., Van Dongen, A.M., Van Huizen, F., Corner, M. A. (1987). Spontaneous neuronal firing patterns in fetal rat cortical networks during development in vitro: a quantitative analysis. *Exp. Brain Res.* **69**, 43-52.

Henry, T. R. (2002) Therapeutic mechanisms of vagus nerve stimulation. *Neurology* **59**: 3-14.

Herz, J., Krogh, A., Palmer, R.G. (1991). Introduction to the Theory of Neural Computation. Santa Fe Institute Studies in the Sciences of Complexity. Lecture Notes, Vol. 1.

Hopfield, J.J. (1982). Neural networks and physical systems with emergent collective computational ability. Proc. Natl. Acad. Sci. USA 79:2554-2558.

Hopfield, J.J. (1995). Pattern recognition computation using action potential timing for stimulus representation. Nature 376:33-36.

Hubel, D.H., Wiesel, T.N. (1959) Receptive fields of single neurones in the cat's striate cortex. *J Physiol.* **148**: 574-91.

Huettner, J.E., Baughman, R.W. (1986). Primary culture of identified neurons from the visual cortex of postnatal rats. *J. Neurosci.* **6**, 3044-3060.

Jimbo, Y., Kawana, A. (1992). Electrical stimulation and recording from cultured neurons using a planar microelectrode array. *Bioelectrochem. Bioenerg.* **29**: 193–204.

Jimbo, Y., Kawana, A., Parodi, P., Torre, V. (2000). The dynamics of a neuronal culture of dissociated cortical neurons of neonatal rats. *Biol Cybern.* **83**: 1-20.

Jimbo, Y., Tateno, T., Robinson, H.P. (1999). Simultaneous induction of pathway-specific potentiation and depression in networks of cortical neurons. *Biophys. J.* **76**: 670-678.

Johansson, R.S., Birznieks, I. (2004). First spikes in ensembles of human tactile afferents code. *Nat. Neurosci.* **6**: 750 – 757.

Kamioka, H., Maeda, E., Jiibo, Y., Robinson, H.P., Kawana, A. (1996) Spontaneous periodic synchronized bursting during formation of mature patterns of connections in cortical cultures. *Neurosci. Lerr.*, **206**: 109-112.

Kennedy, P. R., Bakay, R. A. (1998) Restoration of neural output from a paralyzed patient by a direct brain connection. *Neuroreport*. **9**: 1707-1711.

Koch, C. (1999) *Biophysics of computation*. Oxford University Press, New York.

Koch, C., Segev, I. (2000). The role of single neurons in information processing. *Nat Neurosci.* **3**: 1171-7.

Koch, C., Poggio, T., Torre, V. (1982) Retinal ganglion cells: a functional interpretation of dendritic morphology. *Philos Trans R Soc Lond B Biol Sci.* **298**: 227-63.

Koch, C., Poggio, T., Torre, V. (1983). Nonlinear interactions in a dendritic tree: localization, timing, and role in information processing. *PNAS* **80**: 2799-802.

Koch, C., Poggio, T., Torre, V. (1986) Computations in the vertebrate retina: motion discrimination, gain enhancement and differentiation. *Trends Neurosci.* **9**: 204-11.

Konorski, J. (1967). *Integrative Activity of the Brain*. Univ. Chicago Press, Chicago.

Kreiman, G., Koch, C. Fried, I. (2000) Category-specific visual responses of single neurons in the human medial temporal lobe. *Nature Neurosci*. **3**: 946–-953

Le Masson G., Renaud-Le Masson S., Debay D., Bal, T. (2002) Feedback inhibition controls spike transfer in hybrid thalamic circuits. *Nature* **417**: 854–858.

Logothetis, N. K., Sheinberg, D. L. (1996). Visual object recognition. *Annu. Rev. Neurosci.* **19**: 577–-621.

London, M., Häusser, M. (2005) Dendritic Computation. *Annu. Rev. Neurosci.* **28**: 503–32

Maeda, E., Kuroda, Y., Robinson, H.P., Kawana A. (1998) Modification of parallel activity elicited by propagating bursts in developing networks of rat cortical neurones. *Eur J Neurosci.* **10**: 488-96.

Maeda, E., Robinson, H.P., Kawana, A. (1995) The mechanisms of generation and propagation of synchronized bursting in developing networks of cortical neurons. *J. Neurosci.*, **15**, 6834–45.

Mainen, Z.F., Sejnowski, T.J. (1995) Reliability of spike timing in neocortical neurons. *Science* **268**: 1503-6.

Marchiafava, P.L. (1979) The responses of retinal ganglion cells to stationary and moving visual stimuli. *Vision Res.* **19**: 1203-11.

Marom, S., Shahaf, G. (2002) Development, learning and memory in large random networks of cortical neurons: lessons beyond anatomy. *Q Rev Biophys.* **35**: 63-87.

Marr, D. (1982) *Vision: A Computational Investigation into the Human Representation and Processing of Visual Information*. San Francisco, CA: Freeman & Co.

Martinoia, S., Bove, M., Carlini, G., Ciccarelli, C., Grattarola, M., Storment, C., Kovacs, G. (1993) A general purpose system for long-term recording from a microelectrode array coupled to excitable cells. *J. Neurosci. Methods* **48**: 115–121.

McCulloch, W. S., Pitts, W. (1943) A logical calculus of the ideas immanent in nervous activity. *Bull. Math. Biophys.* **5**, 115–133

Meister, M., Wong, R.O.L., Baylor, D.A, Shatz, C.J. (1991) Synchronous bursts of action potentials in ganglion cells of the developing mammalian retina. *Science* **252**: 939 –943.

Minsky, M., Papert, S. (1988). *Perceptrons: An Introduction to Computational Geometry*. MIT Press, Cambridge MA.

Morin, F.O, Takamura, Y., Tamiya, E. (2005) Investigating neuronal activity with planar microelectrode arrays: achievements and new perspectives. *J Biosci Bioeng.* **100**:131-43

Nakanishi, K., Kukita, F. (2000). Intracellular [Cl(-)] modulates synchronous electrical activity in rat neocortical neurons in culture by way of GABAergic inputs. *Brain Res.* **863**: 192-204.

Neale, E. A., Oertel, W. H., Bowers, L. M., Weise, V. K. (1983). Glutamate decarboxylase immunoreactivity and gamma-[^{3}H] aminobutyric acid accumulation within the same neurons in dissociated cell cultures of cerebral cortex. *J. Neurosci.* **3**, 376-382.

Nicolelis, M.A., Ghazanfar, A.A., Faggin, B.M., Votaw, S., Oliveira, L.M. (1997) Reconstructing the engram: simultaneous, multisite, many single neuron recordings. *Neuron*. **18**: 529-37.

Nicolelis, M.A., Ghazanfar, A.A., Stambaugh, C.R., Oliveira, L.M., Laubach, M., Chapin, J.K. Nelson R.J., Kaas, J.H.. (1998). Simultaneous encoding of tactile information by three primate cortical areas. *Nat. Neurosci*. **1**:621-630.

Nicolelis, M. A. (2001) Actions from thoughts. *Nature* **409**: 403-407.

Nicolelis, M. A. (2003) Brain-machine interfaces to restore motor function and probe neural circuits. *Nat Rev Neurosci.*, **4**: 417-422.

Nisch, W., Bock, J., Egert, U., Hammerle, H., Mohr, A. (1994) A thin film microelectrode array for monitoring extracellular neuronal activity in vitro. *Biosens. Bioelectron.* **9**: 737–741.

Novak, J. Wheeler, B. (1986). Recording from the aplysia abdominal ganglion with a planar microelectrode array. *IEEE Trans. Biomed. Eng.* **33**: 196–202.

O'Keefe, J., Recce, M.L. (1993) Phase relationship between hippocampal place units and the EEG theta rhythm. *Hippocampus* **3**:317-330.

Panzeri, S., Petersen, R.S., Schultz, S.R., Lebedev, M., Diamond, M.E. (2001). The role of spike timing in the coding of stimulus location in rat somatosensory cortex. *Neuron* **29**: 769-777.

Petersen, R.S., Panzeri, S., Diamond, M.E. (2001). Population coding of stimulus location in rat somatosensory cortex. *Neuron* **32**:503–14.

Pfrieger, F.W., Barres, B.A. (1997) Synaptic efficacy enhanced by glial cells in vitro. *Science* **277**: 1684-1687.

Pine, J. (1980) Recording action potentials from cultured neurons with extracellular microcircuit electrodes. *J. Neurosci. Methods* **2:** 19–31.

Potter, S.M. (2001). Distributed processing in cultured neuronal networks. *Prog. Brain Res.* **130**:49-62.

Potter, S. M., DeMarse, T. B. (2001). A new approach to neural cell culture for long-term studies. *J Neurosci Methods.* **110**: 17–24.

Pouget, A., Dayan, P., Zemel, R. (2000) Information processing with population codes. *Nat Rev Neurosci.* **1**: 125-32.

Quiroga, R.Q., Reddy, L., Kreiman, G., Koch, C., Fried, I. (2005). Invariant visual representation by single neurons in the human brain. *Nature* **435**: 1102-7.

Regehr, W.G., Pine, J., Cohan, C. S., Mischke, M. D., Tank, D.W. (1989) Sealing cultured invertebrate neurons to embedded dish electrodes facilitates long-term stimulation and recording. *J. Neurosci. Methods* **30**: 91–106.

Robinson, H.P., Kawahara, M., Jiibo, Y., Torimitsu, K., Kuroda, Y., Kawana, A. (1993a) Periodic synchronized bursting and imracelhdar calcium transients elicited by low magnesium in cultured cortical neurons. *J Neuruphysiol.* **70**: 1606-1616.

Robinson, H.P., Torimitsu, K., Jimbo, Y., Kuroda, Y., Kawana, A. (1993b) Periodic bursting of cultured cortical neurons in low magnesium - cellular and network mechanisms. *Jpn. J. Physiol., Suppl*. **43**: l25-130.

Rolls E.T, Treves, A., Tovee, M.J. (1997). The representational capacity of the distributed encoding of information provided by populations of neuronsin primate temporal visual cortex. *Exp Brain Res* **114**:149–62.

Rousche, P.J., Normann, R.A. (1988) Chronic recording capability of the Utah Intracortical Electrode Array in cat sensory cortex. *J Neurosci Methods*. **82**: 1-15.

Rumelhart, D.E., McClelland, J.L. (1988) *Explorations in Parallel Distributed Processing*. MIT Press. Cambridge, Massachusetts.

Shadlen, M.N., Newsome, W.T. (1998). The variable discharge of cortical neurons: implications for connectivity, computation, and information coding. *J. Neurosci*. **18**: 3870-3896.

Shahaf, G., Marom, S. (2001) Learning in networks of cortical neurons. *J. Neurosci.*, **21**: 8782–8788.

Shannon, C.E., Weaver, W.. (1949). A mathematical theory of communication. In: *The mathematical theory of communication*. Urbana, IL: University of Illinois.

Siderowf, A., Stern, M. (2003) Update on Parkinson disease. *Ann Intern Med.* **138**: 651-658.

Singer, W., Gray, C.M. (1995). Visual feature integration and the temporal correlation hypothesis. *Ann Rev Neurosci.* **18**: 555-86.

Song, S., Miller, K.D., Abbott, L.F. (2000) Competitive Hebbian learning through spike-timing-dependent synaptic plasticity. *Nature* **3**: 916-926.

Streit, J., Tscherter, A., Heuschkel, M. O., Renaud, P. (2001) The generation of rhythmic activity in dissociated cultures of rat spinal cord. *Eur. J. Neurosci.* **14**, 191–202.

Tateno, T., Jimbo, Y. (1999) Activity-dependent enhancement in the reliability of correlated spike timings in cultured cortical neurons. *Biol Cybern.* **80**: 45-55.

Thorpe, S., Delorme, A., Van Rullen, R. (2001). Spike-based strategies for rapid processing *Neural Network* **14**: 715-725.

Torre, V., Poggio, T. (1978) A synaptic mechanism possibly underlying directional selectivity to motion. *Proc R Sot Lond [Biol]* **202**:409-416.

Vaadia, E., Haalman, I., Abeles, M., Bergman, H., Prut, Y., Slovin, H., Aertsen, A. (1995) Dynamics of neuronal interactions in monkey cortex in relation to behavioural events. *Nature* **373**: 515-8.

Wagenaar, D.A., Madhavan, R., Pine, J., Potter, S.M. (2005) Controlling bursting in cortical cultures with closed-loop multi-electrode stimulation. *J Neurosci.* **25**: 680-8.

Watanabe, S., Murakami, M. (1984). Synaptic mechanisms of directional selectivity in ganglion cells of frog retina as revealed by intracellular recordings. *Jpn J Physiol.* **34**: 497-511.

Wessberg, J., Stambaugh, C.R., Kralik, J.D., Beck, P.D., Laubach, M., Chapin, J.K., Kim, J., Biggs, S.J., Srinivasan, M.A., Nicolelis, M.A. (2000) Real-time prediction of hand trajectory by ensembles of cortical neurons in primates. *Nature* **408**: 361-5.

Wilson, B.S., Lawson, D.T., Müller, J.M., Tyler, R.S., Kiefer, J. (2003) Cochlear implants: Some Likely Next Steps. *Ann. Rev. Biomed. Eng.* **5**: 207-249.

Young, M.P., Yamane, S. (1992) Sparse population coding of faces in the inferior temporal cortex. *Science* **256**: 1327–-1331.

Zhang, L.I., Poo, M.M. (2001) Electrical activity and development of neural circuits. *Nat Neurosci* **4**: S1207–S1214.

Zrenner, E. (2002) Will Retinal Implants Restore Vision? *Science* **295**: 1022-1025.

Aknowledgements

.... and finally the acknowdelgements…
well, I would need so many pages and so extra space… anyway… let's try…
well, to Vincent first…Torre???… no I said Vincent… he never allowed me to use any formal approach with him … so he is Vincent… the one who day by day for nearly four years tried to guide my crazy anarchical approach to science …as to life but let's avoid it… so thanks for your help and your patience… try to imagine a long trip with someone who is boring… would you do it??? I would not… so well… with him it was not boring I can grant it!!!
And then???
Thanks to whom…
I will try to …
MiamadreMiofratelloMiopadreMianonnaIPantanaReiVittorioGrazianoMelottoGiorgioRexGermanoSimone MaraClemensMartinaGiulia...
...loro mi avevano garantito prima che arrivassi a Trieste che ovunque me ne fossi andato ci sarebbero stati sempre... ed e' vero...
…e then.... well I arrived in Trieste...it was crazy…
...LasgrecciaSimonaenicolaLamanuLamarcellaIlcarsoSimoneconvalentinalontanaLefesteOlaf...
…e quasi che non si era iniziato ancora.... perchè ...poi...
...PavelWolterFeliceSofijaElisabethDavideAndreaLalagoMOnicaCaterinaDylanElisabettaLamanuelepecorecheinciampanosullastaccionataesifanmaleecosìnontipuoipiùaddormentare...
...e ancora si faceva poco più che merenda...
...finchè... cambia casa... e where is the connection with the acknowledgements in english?!??!....
…well… crazy house… from those days I lived in a crazy house…
…he realized it would have been crazy… he was right…Dylan I mean…you can not imagine… sometimes I can not even believe it… just crazy… thank "bastardo"…many things started at those times… when my craziness became more grave and not reversible…
…that house grew with me… incredible evenings passed drinking wine playing guitars and with the melody of the violine of the bastard - i.e. Dylan but everyone knows it – … il violino " mi faceva drizzare i peli per l'emozione" … e questo come lo spieghi in inglese… maybe Felice Marcelo Walter Zonfrillo Simone Ras can forget it??!?… can we forget the music of those evenings?!?… I would not believe… …like the party in the beach… our neurons stored these emotions somewhere … and these emotions just wait to be retrieved at one point… this is the point… passing trough and leave a sign…
…. so that house… and then Dylan left…
…
… but Felice joined us… Felice… Felice… Feliceeeeeeeeee!!!!!!!!!!!…
… and Dennis the Russian passed thourgh the house too… and then …
… well in just one night many things had to change… somewhere it was written like that… accept or not … no time… it already happened… it's like this…
… … … …
….e poi giù di nuovo a correre come pazzi...
...thesiren... the birthday you would like to avoid and forget... and Frederic joint us … he smelled craziness and … he came in the house… and now it smell even more craziness…
the congress… that congress … piazza delle erbe… ilcostipatoconilm….enelc..o…lacamomilla… crazy months… Iporticati…
piazzasantostefano…lataranta…isilenzi…ibagniaottobre…nottifolli…ilcabernetfranc…RankenZagabriaandthecomunisticulicontrol... DavideIlciut…
…
…and now?!?!…well… I got lost in the acknowdelgements…
I would like to thank all the people of SISSA who shared with me spaces, computers, solutions, neurons… and EMOTIONS … during the all time I have spent here…
AnilKamil(andTheUnforgettableRussianWedding)SofijaElisabethJelenaWalterAlbertoJummyRadjesh(I get lost with exotic names…)… SilviaRezaAnnaGiuliettaJadaClaudioPaoloCosmaBellavistaglobalvillage…
…and still I would like to thank the neighbour "il vicino che ha rajjone"…

…I caffe' la mattina e La lago che mi ascolta in silenzio nei miei deliri...la Lago ve l'immaginate la Lago zitta ad ascoltare... bè ora diteglielo pure che è successo perchè credo che ancora non lo sappia...
…and … well… again in a months many things changed… you just go out for take some relax and look what it happens… crazymonth…GrisgnanaRovignoPiadineElefanticheattraversanolestradedellemarche…e vai a trovare un senso che un senso non ce l'ha… maybe it is all like this… when I was a child I was dreaming "what I will do in 2000"?… well in 2000 I arrived in Munich for cutting poor snails and looking for their neurons … questo ce l'ha un senso???… and then I was imaging "what I will do when I will be 30 years old?"… many people on a terrace were singing compleaño feliz for me… e questo ce l'ha un senso?… at the present moment I am speaking a language which is a mixture of marchigianoitalianoinglesespagnolo… "does it have any sense?"… this is the point…

… I have to thank all of you for helping me to avoid to give a sense to all… I prefer like this… I will have time to find the sense… and I hope that I helped you as well to avoid your sense…

… and finally ...
… a special thank for Manu who helped me with my poor English…
… Sergio for assisting the craziness of my computers …
… and to Elisabetta with whom it was a great pleasure to work dayByDay …
… thank to Felice Yolanda and Frederic … che mi hanno sopportato …
… thank to Simone&Valentina&Lalago…
… thank to Trieste and his poetry … and to the poets of Trieste Luca and Davide …

... e poi grazie alla mia famiglia Mara e Yolanda le persone che più di tutti mi hanno sopportato nei miei momenti di stanchezza e difficoltà e a dare un senso a questa tesi…

... finally I did it…